EFFECT OF SILVER COATING AND DOPING OF IRON AND COBALT ON THE OXYGEN PERMEABILITY OF La_2NiO_4

BY

ZEESHAN ALAM

A Thesis Presented to the

DEANSHIP OF GRADUATE STUDIES

KING FAHD UNIVERSITY OF PETROLEUM & MINERALS

DHAHRAN, SAUDI ARABIA

In Partial Fulfillment of the
Requirements for the Degree of

MASTER OF SCIENCE

In

MECHANICAL ENGINEERING

MAY 2013

KING FAHD UNIVERSITY OF PETROLEUM & MINERALS

DHAHRAN- 31261, SAUDI ARABIA

DEANSHIP OF GRADUATE STUDIES

This thesis, written by **Zeeshan Alam** under the direction his thesis advisor and approved by his thesis committee, has been presented and accepted by the Dean of Graduate Studies, in partial fulfillment of the requirements for the degree of **MASTER OF SCIENCE IN MECHANICAL ENGINEERING.**

Dr. Khaled Mezghani
(Advisor)

Dr. Khaled Saleh Al-Athel
Department Chairman

Mod Habib

Dr. Mohamed A. Habib
(Member)

Dr. Salam A. Zummo
Dean of Graduate Studies

Dr. Saheb Nouari
(Member)

16/6/13

Date

Dedicated to

My beloved parents, for all their efforts, duas and support throughout my life

ACKNOWLEDGMENTS

First and foremost I would thank the Almighty Allah (S.W.T.) for whatever I have achieved in my life and for all the blessings that He has bestowed upon me.

Secondly, I would like to take this opportunity to express my profound gratitude and deepest appreciation to my thesis advisor, Dr. Khaled Mezghani for his constant support and guidance throughout my thesis. His knowledge and vision towards research has inspired me a lot. He was always there for me whenever I needed him. The work was not that easy and without him it would have been really very difficult for me to accomplish this work. He is a complete package as an advisor and I consider myself very lucky that I got an opportunity to work under his supervision.

I would also like to thank my committee members Dr. Mohammad Habib and Dr. Saheb Nouari for their timely suggestions and guidance.

I would also like to acknowledge the financial support provided by the MIT-KFUPM collaboration and the National Science, Technology and Innovation Plan (NSTIP) for this project.

I am obliged for all the support provided by the technical staff during my experimental work. I also thank all my friends at KFUPM for their constant support.

Lastly, I thank my family members, especially my beloved parents for their constant support and duas and it is their effort and hardwork that I am able to reach to this level in my life.

TABLE OF CONTENTS

LIST OF TABLES

LIST OF FIGURES

ABSTRACT

Full Name : Zeeshan Alam

Thesis Title : Effect of Silver Coating and Doping of Iron and Cobalt on the Oxygen Permeability of La_2NiO_4

Major Field : Mechanical Engineering

Date of Degree : May, 2013

Ion transport membrane (ITM) based reactor is one of the developing technologies for carbon dioxide capture and sequestration which integrates air separation and fuel conversion. These ITM reactors use mixed conducting oxygen permeable ceramic membranes which can simultaneously transport both oxygen ions and electrons without the requirement of an external circuit. However, the oxygen permeability of these membranes is relatively low which still hinders their use in industrial applications. One of the potential materials for oxygen permeability is the La_2NiO_4 (LNO), which is known for its high temperature stability.

In this study, LNO powders were synthesized by sol-gel method from nitrate solutions. These powders were compacted to obtain LNO membranes and characterized using X-ray diffraction (XRD) and scanning electron microscopy (SEM). A gas permeation system was built for the oxygen flux measurement. This system was connected to a gas chromatograph for quantitative analysis. Thick membranes (1mm) were used for permeability measurements at temperature of 700°C.

The oxygen permeability of the LNO membrane was measured with different ratios of oxygen and nitrogen in the feed gas. The permeability increased with the increase in

oxygen concentration on the feed side. The oxygen permeability was also tested with respect to temperature and the flux was found to increase with increasing temperature. A maximum oxygen flux of 0.064 µmol $cm^{-2}s^{-1}$ (0.099ml min^{-1} cm^{-2}) was obtained at temperature of 800°C. The activation energy was calculated to be 0.67eV.

A long term stability test was performed on the LNO membrane and the flux was found to decrease sharply at the starting and then stabilize. In order to further enhance the permeability, the LNO membrane was coated with silver paste on the feed side. Results showed an enhancement of upto 40% in the flux values as compared to the pure LNO membrane suggesting that silver acts as a catalyst for the surface reactions on the feed side. However, for the membranes coated with silver by using an ion sputtering instrument a decrease in the flux value was observed as compared to the pure LNO membrane. The reason could be attributed to the disintegration of the dense silver coating into small particles of silver distributed all over the membrane which reduced the effective surface area of the membrane exposed for permeation.

The LNO membrane was also doped with iron and cobalt so as to increase the bulk diffusion in the membrane. The doping of the LNO membrane with 20% iron decreased the flux values by about 25%. However, doping the LNO with 20% cobalt increased the permeation flux by 25% as compared to the pure LNO membrane. A maximum flux of 0.1 µmol $cm^{-2}s^{-1}$ was obtained for the $La_2Ni_{0.75}Co_{0.25}O_4$ membrane and the $La_2Ni_{0.70}Co_{0.30}O_4$ membrane. Increasing the cobalt content further increased the amount of leakage in the system.

ملخص الرسالة

الاسم الكامل: زيشان عالم

عنوان الرسالة: تأثير طلاء الفضة وإضافة الحديد والكوبالت على نفاذية الأكسجين في La_2NiO_4

التخصص: الهندسة الميكانيكية

تاريخ الدرجة العلمية: مايو 2013

تعتبر الأغشية التي تعتمد على تفاعل انتقال الأيونات (ITM) أحد التقنيات المتطورة المستخدمة في الإمساك بثاني أكسيد الكربون وحجزه عن طريق فصل مكونات الهواء و تحويل الوقود. هذه المواد المتفاعلة تستخدم الأغشية الخزفية المختلطة النافذة للأكسجين والتي بدورها تمكن انتقال أيونات الأكسجين و الإلكترونات بدون الحاجة إلى دائرة كهربائية خارجية. غير أن نفاذية الأكسجين في مثل هذه الأغشية ضئيلة نسبيا والتي تحد من استخدام مثل هذه الأغشية في التطبيقات الصناعية. أحد هذه المواد المحتملة و المعروفة بنفاذيتها للأكسجين La_2NiO_4 (LNO) والمعروفة أيضا بثباتها عند درجات الحرارة المرتفعة.

في هذه الدراسة، تم تكوين بودرة LNO بطريقة sol – gel من محاليل النترات. بعد ذلك تم ضغط هذه البودرة لتكوين الأغشية المطلوبة . ثم تم تحديد خصائص هذه الأغشية باستخدام جهاز انحراف الأشعة السينية X-ray diffraction (XRD) وأيضا باستخدام مجهر إلكتروني scanning electron microscopy (SEM) . كما وأيضا تم بناء نظام لاختبار نفاذية الغاز لقياس تدفق الأكسجين . هذا النظام تم توصيله بجهاز لاختبار الكروماتوجرافيا للتحاليل الكمية. والأغشية المستخدمة في اختبارات النفاذية كانت بسماكة 1 مم عند درجة حرارة 700 درجة مئوية.

تم قياس نفاذية الأكسجين في هذه الأغشية بنسب مختلفة من الأكسجين و النيتروجين في الغاز المزود للنظام ،وأظهرت النتائج أن نفاذية الأكسجين كانت متناسبة بشكل خطي مع نسبة تركيز الأكسجين في الجهة التي تزود النظام بالغاز. بالإضافة إلى اختبار نفاذية الأكسجين عند درجات حرارة مختلفة وكان من الملاحظ أن التدفق يزداد بارتفاع درجة الحرارة. أقصى تدفق للأكسجين تم قياسه هو $0.064\ \mu mol\ cm^{-2}s^{-1}$ ($0.099ml\ min^{-1}\ cm^{-2}$) عند درجة حرارة 800 درجة مئوية .و طاقة التفعيل كانت 0.67eV.

تم اخضاع هذه الأغشية لاختبار استقرارها وثبوتها على المدى البعيد ، فوجد أن تدفق الأكسجين ينخفض بصورة حادة في البداية وبعد ذلك يستقر. لتحسين نفاذية الأكسجين في هذه الأغشية ، تم طلاء هذه الأغشية بمعجون الفضة على الجهة المعرضة للغاز المغذي للعملية، وأظهرت النتائج تحسن في تدفق الأكسجين بما نسبته 40 % مقارنة بأغشية LNO النقية مما يدفعنا بالتفكير بالفضة كعامل محفز للتفاعل على سطح الأغشية من الجهة المغذية. لكن في الأغشية المطلية بالفضة باستخدام جهاز لنشر أيونات الفضة على شكل رذاذ (ion sputtering machine) لوحظ انخفاض في تدفق الأكسجين مقارنة بالقيم للأغشية النقية. ويحتمل أن يكون السبب انحلال طلاء الفضة الكثيف وتكوين جزيئات من الفضة موزعة في جميع أنحاة الغشاء مسببا انخفاض المساحة السطحية الفعالة للغشاء المعرضة لنفاذية الأكسجين.

بإضافة الحديد و الكوبالت لهذه الأغشية لزيادة حجم الانتشار في الأغشية ، لوحظ أن إضافة الحديد بنسبة 20 % أخفض التدفق بما نسبته 25% . لكن عند إضافة الكوبالت بنسبة 20 % زاد التدفق بنسبة 25 % مقارنة بالأغشية النقية الخالية من الإضافات. أعلى تدفق تم تسجيله هو $0.1\ \mu mol\ cm^{-2}s^{-1}$ وتم الحصول علي من الغشاء $La_2Ni_{0.75}Co_{0.25}O_4$ $La_2Ni_{0.70}Co_{0.30}O_4$. ولكن بزيادة نسبة الكوبالت سيزيد من نسبة التسرب في النظام.

CHAPTER 1

INTRODUCTION

Global warming has emerged as a huge challenge to the mankind as this is the root cause of many environmental problems present nowadays like rising of sea levels and the melting of glaciers [1]. The emission of greenhouse gases is the main reason that is contributing to global warming as these gases absorb the infrared radiations that lead to the increase in the overall temperature of the earth. The gases in the Earth's atmosphere which contribute to the greenhouse effect are water vapor, carbon dioxide, methane, nitrous oxide, and ozone. The increasing greenhouse gas concentrations result from human activity such as fossil fuel burning and deforestation [1]. Carbon dioxide is generally held to be one of the most significant contributors to global warming. Fossil fuel-fired power plants are responsible for more than one third of the total global CO_2 emissions [2]. Therefore, efforts are increasingly directed towards a reduction of the CO_2 emission.

One option to burn fuels and at the same time not to release CO_2 into atmosphere is separation capture and sequestration. There are three possible technical solutions for CO_2 capture in fossil power plants: post-combustion, oxyfuel and pre-combustion [3]. The post combustion capture is required when the combustion takes place in air and CO_2 is separated from the flue gas after combustion. The other two solutions utilize air separation before combustion to obtain pure oxygen. The pre combustion process

involves partial combustion of fuel to produce syngas ($CO+H_2$). In the oxyfuel combustion coal is burnt in an oxygen-rich atmosphere which produces a flue gas having a high concentration of CO_2 and capture of CO_2 at higher concentration becomes easier. Now, considering the economic viability of the above processes, since normal combustion in a power plant results in the generation of flue gases with low concentration of CO_2, it has been observed that very high capital costs are involved in installing of a post combustion separation unit to process massive volumes of flue gases [3]. So, in order to reduce this cost there must be production of flue gases with high concentration of CO_2 which can be achieved through the pre-combustion or oxyfuel processes. Gas separation membranes are excellent candidates for this gas separation in coal fired plants because of their low energy consumption and their integration into membrane reactors is very promising. Dense ceramic membranes that exhibit high oxygen ionic and electronic conductivity are a great choice for producing oxygen by separation from air or other oxygen containing gas mixtures as the oxygen production by these membranes is quite economical, clean and efficient.

1.1 Oxygen Ion Transport Membranes

Oxygen Ion Transport Membranes (OTMs) are solid ceramic membranes which contain oxygen ion vacancies in the molecular lattice. When these membranes are activated by some external source like heat, oxygen ions can travel through the ceramic. O_2 molecules are adsorbed onto the surface and separate into O^{2-} ions, taking electrons from the ceramic to do so. The oxygen ions can travel equally well in both directions depending on

the partial pressure of oxygen. When the oxygen partial pressure is higher on one side of the membrane whereas lower on the other side, then the oxygen will be transported from the oxygen-rich side to the oxygen-lean side. The ions then reform as molecules as they reach the other side of the membrane, releasing their electrons back into the ceramic. The electrons are conducted back through the membrane in the opposite direction i.e. to the higher oxygen side. The overall effect is that oxygen and no other gas can travel through the membrane. The mobile species for these are anions and the movement of these ions is either under the effect of an electrical field or due to an oxygen pressure gradient. The application of electric field is necessary for the case when the membrane is not electronically conducting whereas if the transport is pressure driven the material must be a mixed ionic and electronic conducting (MIEC). The various membrane concepts which employ an oxygen ion conducting material are shown in Figure 1 below:

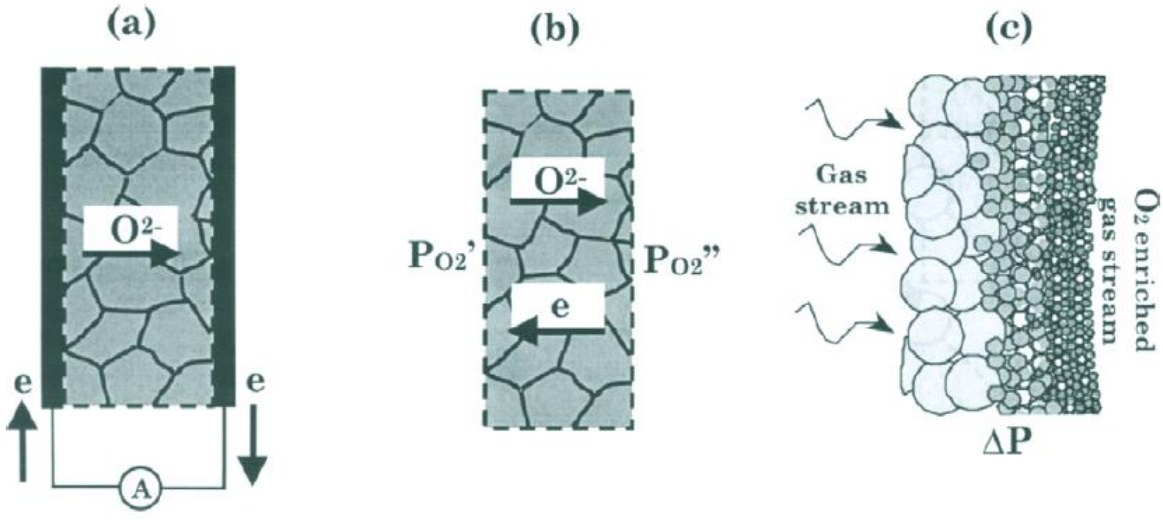

Figure 1: Different membrane concepts (a) solid electrolyte cell (oxygen pump), (b) mixed ionic-electronic conductor (MIEC), (c) asymmetric porous membrane with a graded porosity [4].

The first case shows the transport of oxygen ions under an externally supplied electric field. The second case shows a mixed ionic-electronic conducting (MIEC) membrane in which the driving force is the oxygen partial pressure. The third case shows a membrane with a porous support layer, an intermediate layer and a thin dense upper layer.

Temperature is also a very important factor as the oxygen permeation is feasible only at high temperatures. At elevated temperatures, typically above 700 °C, and oxygen chemical potential gradients across the membrane surface, determined by the local oxygen concentrations near the membrane surface, oxygen selectively permeates from the feed (air) side to the permeate (sweep gas) side. Oxygen undergoes gas phase mass transfer and surface exchange on both sides of the membrane, as well as bulk diffusion through the membrane itself. In the presence of a fuel on the permeate side, reaction with the permeated oxygen may lead to partial or full oxidation. This, besides enhancing the oxygen flux across the membrane, makes it possible to incorporate ITM reactors/combustor to perform oxy-fuel combustion without the need for a separate air separation unit, a combustion unit and an external heat exchanger. The integration of air separation and fuel conversion into a single unit could reduce the size and cost of this promising carbon-capture technology.

1.2 MIEC Materials for Oxygen Permeable Membranes

As discussed above the membranes made from the mixed ion electron conducting materials have the ability to transport oxygen ions through them along with the simultaneous transport of electrons in the opposite direction and as such an external

electrical circuit is not required to balance the electrical neutrality. The unique chemical structure of O-MIEC membranes results in theoretically 100% oxygen selectivity. This electronic conductivity without the requirement of an external electrical source is an important characteristic of these membranes as it eliminates the need of electrodes and therefore the fabrication and the installment of these membranes in the power plants or in other oxygen separation application is simplified to a great extent and also this leads to a considerable reduction in cost which makes these materials quite attractive for oxygen separation application. The structure and the composition of these materials govern the overall performance of these membranes.

1.2.1 The Perovskite Structure

The term perovskite is used to describe a mineral with the same crystal structure as calcium titanium oxide ($CaTiO_3$). This mineral was first discovered in 1839 in the Ural Mountains of Russia by Gustav Rose, who named it after Russian mineralogist Lev Aleksevich von Perovski (1792–1856). The silicate-based perovskite Al-(Mg, Fe) SiO_3 is the main component of the lower earth mantel (70% to 80%) and is considered the most abundant phase on earth. Perovskites have a wide range of attractive properties such as ferroelectricity, superconductivity and also electronic and ionic conductivity.

The general structure of the perovskite mineral is ABX_3, where A and B are cations and X, most commonly, oxygen anions. However, perovskites are not necessarily oxides as fluoride, chloride, carbide, nitride, hydride and sulphide perovskites are also found. In the ABO_3 structure, A is generally a large alkaline earth, alkali or rare earth cation and B is a transition metal or a rare earth metal. The ideal perovskite has a close-packed cubic structure. In the cubic unit cell, the larger A-site cation occupies the body centre of the

cube. The smaller B-site cations occupy the corner positions of the cube and are octahedrally coordinated to the oxygen anions in the mid-edge positions of the cube as shown in Figure 2. The A- and B-site cations have 12-fold and 6-fold anion coordination respectively. The total charge of A and B equals +6. A is usually of valence +2 and B of valence +4.

Although the cubic symmetry is the ideal structure, most perovskites have distorted structures due to rotation or tilting of the BO_6 octahedra caused by the relative radius difference between the A- and B-site cations. The most common distortion is the tilting of the BO_6 octahedra to accommodate the radius difference.

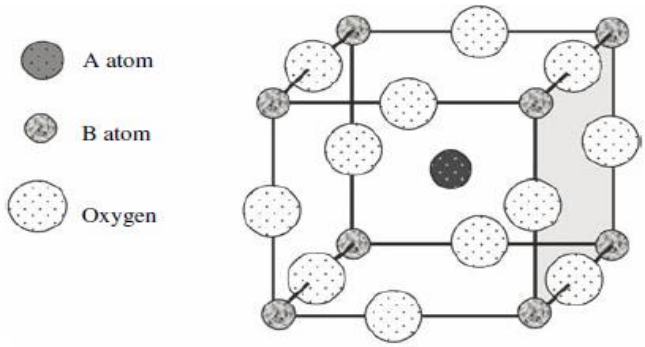

Figure 2: Representation of the ideal ABO_3 perovskite structure[5].

There is a tolerance factor (t) for perovskites to define the deformation from the cubic lattice which is given by:

$$t = \frac{(r_A + r_O)}{\sqrt{2}(r_B + r_O)}$$

where r_A, r_B and r_O are the ionic radii of the A-site cation, the B-site cation and the oxygen anion respectively.

When t equals unity, the perovskite is expected to adopt the ideal cubic structure while lower values of t correspond to lower symmetry. In the case of a tolerance factor higher than unity, the perovskite structure becomes hexagonal. Normally, when the tolerance factor (*t*) is between 0.8 and 1, the perovskite structure is preserved. The ionic radii for lanthanum (r_A), nickel (r_B) and oxygen (r_O) are 0.117 nm, 0.083 nm and 0.126 nm, respectively. The value t for LNO comes out to be 0.823.

1.2.1.1 Oxygen Migration through Perovskite Structure

Among MIEC membranes, perovskite-type ceramic membranes exhibit the highest oxygen permeability due to their high ionic and electronic conductivities. The ionic conductivity, which controls the oxygen permeation rate, is generated by the introduction of oxygen vacancies in the perovskite lattice which allows the vacancy hopping mechanism of oxygen ions to occur whereas the electronic conductivity is generated by the formation of electron holes which allows the electron hopping mechanism between metal cations of the lattice, counter-balancing the oxygen ion conduction.

Oxygen anion mobility requires crystal defects in the direct vicinity of the lattice site occupied by the ion considered. When no intrinsic defects are present in the perovskite structure, the material does not exhibit ionic conductivity. In order to use this material as a MIEC membrane material, it is therefore necessary to introduce defects in the lattice, most commonly vacancies. They can also be impurities, ions displaced in interstitial sites or lattice ions in valence states such that the total charge of A and B is different from +6 [6]. These crystal defects are usually present in low concentrations at low temperatures. However, high temperatures induce an increase in defect concentration and ion activity, which in turn increase the ionic conductivity of the perovskites.

The creation of oxygen vacancies (Vö), which provide a path for oxygen anion transport in the lattice of the perovskite material, is represented by the oxygen non-stoichiometry (3-δ) where (Vö= δ). The degree of non-stoichiometry ranges usually between 0 and 1 [6]. A high vacancy concentration is necessary but the presence of a too large number of vacancies will affect the structural stability of the perovskite.

The oxygen non-stoichiometry results either from the reduction of a mixed valence B-site cation or from the substitution of A- and B-site cations with other cations of lower oxidation state. The introduction of multivalent cations in the B-sites of perovskites leads to the formation of electron holes, while the decrease in total charge of A- and B-sites is compensated by the formation of oxygen vacancies. Charge defects must be counter-balanced by one of equal magnitude and opposite sign in order for the lattice to remain electronically neutral. Two charge compensation mechanisms are possible: the first one is the formation of oxygen vacancies; the second is the increase in valence state of the transition metal at the B-site. Temperature and oxygen partial pressure conditions will influence the charge defect compensation mechanism.

The valence of A-site cations is usually partially changed from 3+ to 2+ by doping of the perovskite material. If the A cation changes valence two compensation mechanisms are possible. In the first one, the surrounding oxygen anions counter-balance the valence charges by creating vacancies. If an oxygen vacancy is formed, the B-site cations will adjust their valence state and their coordination number. The second one involves, on the one hand, part of the B-site cations modifying their valence state from 3+ to 4+ to balance the local charge. The valence of the A-site cations will not be easily modified since they have a strong ionic bonding with adjacent oxygen anions. As a consequence,

the valence of the B-site cation generally depends on the oxidation state of A. On the other hand, as a result of some B-site cations being reduced, thus decreasing their valence state from 3+ to 2+, oxygen vacancies are created to compensate the excess negative charge.

Moreover, the size proportion of A and B is of importance in oxygen transport in the perovskite-type ABO_3 structure. The energy barrier for migration decreases with increasing size of B-site cations and decreasing size of A-site cations [7].

For fast oxide ion conductivity in perovskite materials, the following conditions are necessary [7]:

- High concentration of mobile charge carriers: O^{2-}
- Sufficient crystallographic sites for the charge carriers i.e. high oxygen vacancy concentration
- Low mean value of metal-oxygen bonding energy of the perovskite lattice,
- An open structure, i.e. a high lattice free volume, facilitating oxygen ion mobility,
- A critical cation saddle point for O^{2-} migration as large as possible.

1.2.1.2 Doping of Perovskite Structure

Perovskite properties are believed to derive from the non-stoichiometry of cations and anions, lattice distortion and cationic mixed valences, all of which can be tuned by appropriate cation doping. The perovskite structure has great chemical and geometrical flexibility. It can adapt easily to the relative sizes of the ions forming the compound. It can accommodate both high dopant concentrations, with a wide range of cation radii and also a high degree of oxygen non-stoichiometry.

Perovskite-type oxides can be doped by substituting a fraction of the A-site and/or B-site cations by cations with different atomic radii. This property is very interesting as it enables a tuning of the properties of these materials for a wide range of applications. Moreover, the fact that both A- and B-sites are available for substitutions provides a wide range of new possible perovskite materials with new interesting properties.

The increasing substitution of A-site cation for lower valence metal ions usually causes, on the one hand, an increase in the oxygen permeation flux due to the increase in oxygen vacancy concentration and, on the other hand, a decrease in the phase stability. A compromise between high electronic and ionic conductivity, i.e. high oxygen permeation, and stability of the membrane material is therefore necessary.

1.2.2 The Ruddlesden-Popper Phase, K_2NiF_4-type structure ($A_2BO_{4+\delta}$)

In recent years much attention has been drawn to a different class of mixed ionic-electronic conductors (MIEC) with the K_2NiF_4 perovskite-related structure for application as ceramic membranes for high purity oxygen separation.

The crystal lattice of the K_2NiF_4-type structure has the general composition $A_2BO_{4+\delta}$, where A is a rare earth cation and B a transition element. It can be described as a succession of perovskite layers ABO_3 alternating with rock salt AO layers in the c-direction as shown in Figure 3.

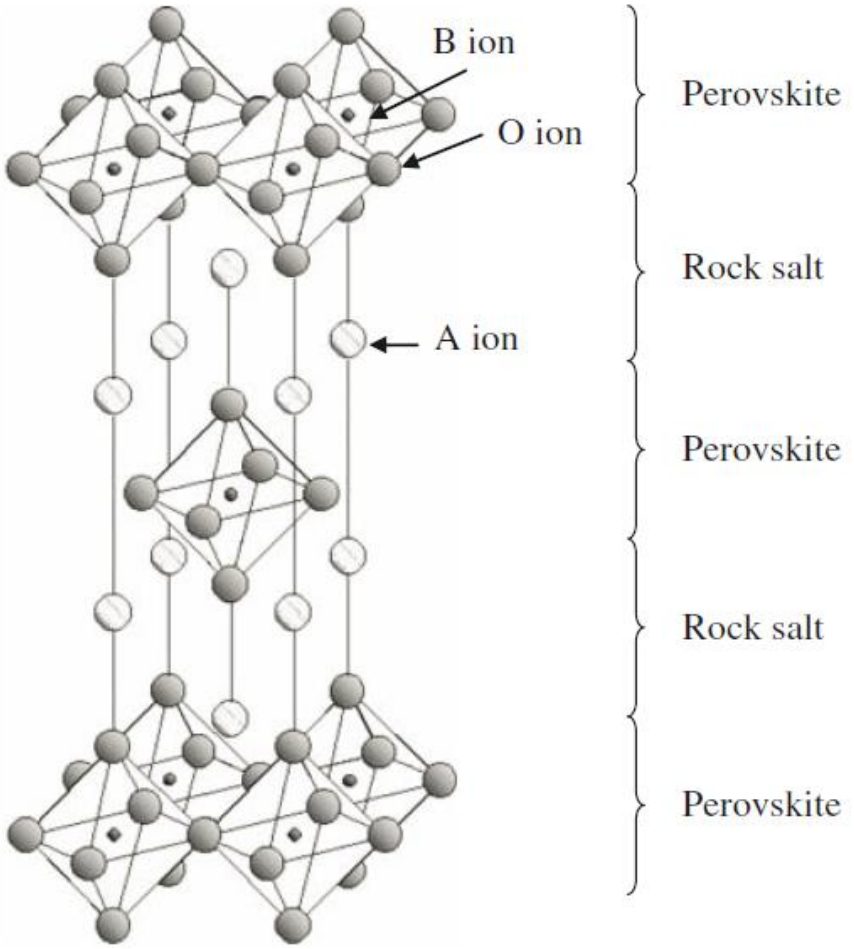

Figure 3: Representation of the perovskite-like $A_2BO_{4+\delta}$ structure [8].

Oxygen ionic conduction in K_2NiF_4-type materials is believed to occur via diffusion of oxygen interstitials in the rock-salt-type layers and also via a vacancy mechanism in the perovskite layers. In the K_2NiF_4- type structure, the interstitial oxygen atoms are in a tetrahedral environment of A-cations. One of the most promising K_2NiF_4-type compounds is lanthanum nickelate ($La_2NiO_{4+\delta}$) considered to have good permeation properties and high stability [9]. According to M. Al Daroukh et. al. [10], the thermodynamic stabilities, in terms of reversible oxygen desorption, for K_2NiF_4-type materials were higher than those of the corresponding perovskite-type oxides. When the

perovskite type oxides undergo oxidation they convert into K_2NiF_4 structure at high temperatures which can be assumed as a proof for higher stability of A_2MO_4 structure (M = Ni, Co, Fe, Cr) [10]. They compared the oxygen release of the perovskite oxides and the K_2NiF_4-type oxides with similar M cations and found that the values of oxygen deficiencies were always higher for the perovskite-type, indicating lower stabilities of this type of structure. They further found that the thermal expansion coefficients (TEC) of K_2NiF_4- type oxides were generally lower than that of the perovskite-type oxides. The value of TEC for LNO was about 11.9×10^{-6} K^{-1} whereas for LSCF it was about 17.5×10^{-6} K^{-1}.

1.3 Preparation of Oxygen Ion Transport Membranes

The preparation of these MIEC ceramic membranes generally consists of three steps:

- Preparation of the perovskite powder
- Compaction of the powder to prepare membranes of the desired shape
- Sintering of the compacted membranes

The structure and performance of these membranes depends very much on two of the above three steps: the preparation of perovskite powder and the sintering of the compacted membranes.

1.3.1 Preparation of the Perovskite Powder

There are different methods for the preparation of these MIEC perovskite powders, some of which are described below:

Solid state reaction method: The chemicals (oxides, carbonates or hydroxides) containing the desired metal ions are mixed, and then the mixture is fired for a given time (3-10 hours) in excess of 800 ºC to form the MIEC powders via the solid state reaction. The prominent advantages of solid-state reaction are easy-operation and low-cost. However, the size of the powder is controlled by laborious mechanical mixing of starting materials and grinding processes. The homogeneity and purity of the powder is relatively poor. Meanwhile, the powder commonly exhibits a very broad particle size distribution [11].

Co-precipitation method: The chemicals (carbonates, salts) containing the desired cations are dissolved into water, and then another solution acting as a precipitation agent is added. The precipitant resulting from the reaction of the precipitation agent and starting solution is filtered and dried. Finally, the dried materials are calcined in a high temperature furnace to form the MIEC powder [11]. The properties of powder can be adjusted using pH, mixing rate, and mixing temperature. The powder prepared by the co-precipitation method shows better homogeneity and higher purity than the powder prepared by the solid-state method. However, the appropriate precipitation agent is not easy to find. Meanwhile, the precipitation rate is not easily controlled and sometimes leads to the inhomogeneities of powders [12].

Sol-gel method (Citrate-EDTA method): In this method first an amorphous gel is produced, followed by dehydration at a low temperature. A common process in the sol-gel preparation family is the Citrate- ethylenediaminetetraacetic acid (EDTA) method. The Citrate-EDTA method contains three sequential steps: complexation of metal ions in EDTA and citric acid (both are the chelating agents), evaporation of water solvent, and

thermal decomposition of the complex to form the MIEC powders. Recently, employing the Citrate-EDTA method to produce the MIEC powders has received great attention due to its unique advantages, including: high purity of the product, excellent chemical homogeneity, and accurate composition control [13].

In the sol-gel method, the factors such as the pH, the evaporation of water in the sol, and the hydrolysis rate can remarkably influence the structures of the corresponding membranes. Great efforts have focused on revealing the relationship between these factors and the performance of the corresponding membranes. Among these factors, the pH has been studied intensively for some membrane compositions. It is generally acknowledged that the degree of complexation can be controlled by varying the pH of the precursor solution. A study on LSCF membranes demonstrated that the pH impacted the crystal structure, morphology, and oxygen permeability of the membranes significantly [14]. Compared with the powders and membranes derived from precursors with the pH higher than 5, the powders and membranes prepared with the lower pHs (pH =1, 3) exhibited remarkable differences in XRD patterns and microstructure images. Further analysis showed that these differences in XRD patterns and microstructure lead to a variation of the apparent activation energy for oxygen permeation. The membrane prepared using the precursors with the low pHs showed larger activation energies and low oxygen fluxes.

Figure 4 shows the difference in microstructure obtained in membranes of the same material prepared from different methods. The membrane prepared from citrate method does not show clear grain boundaries whereas the other three images show the presence of clear grains. The grain size is the largest for the membrane prepared by the solid state

method followed by the membranes prepared by co-precipitation method and spray pyrolysis method. The oxygen permeation flux for the membranes prepared by solid state method, citrate method and spray pyrolysis method was almost the same and higher than the co-precipitation membrane which is because of the considerable amount of difference in strontium ions. The membrane prepared by co-precipitation method has large Sr deficiency because of the involvement of filtration and washing steps in this method [12].

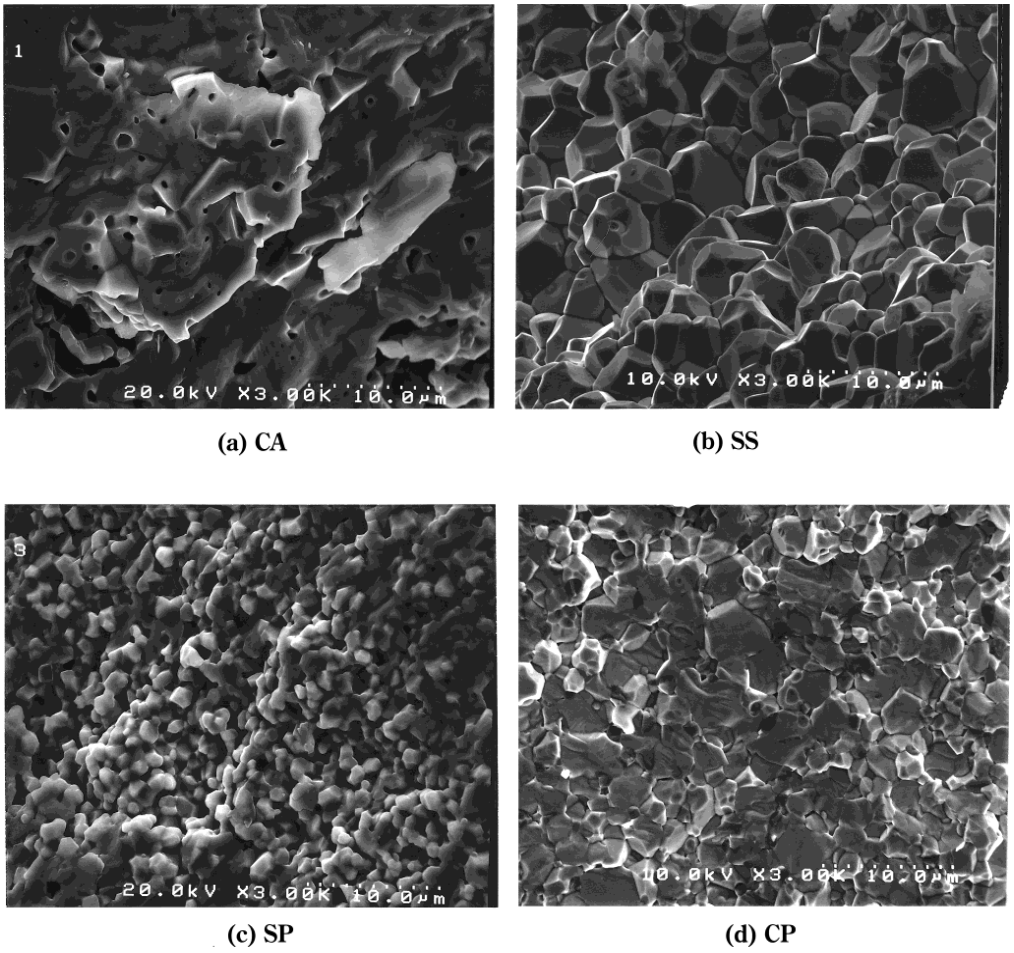

Figure 4: SEM microstructure of LSCF membranes prepared by different methods: (a) Citrate method (b) Solid state method (c) Spray pyrolysis method (d) co-precipitation method [12]

1.3.2 Sintering of the Compacted Membranes

Sintering is a thermally activated process which involves coarsening and densification of the powdered samples. In the first stage of sintering, a physical reaction takes place which results in the formation of necks between the grains which are in contact with each other. Small particles merge into larger ones, resulting in greater mean pore size. In the second stage of sintering, as the temperature increases, the necks broaden and shrinkage occurs which changes the microstructure of the packing. The driving force for sintering is a decrease of the surface energy of the system with solid state diffusion from areas with relatively large convex curvature (high Gibbs free energy) to areas with small concave curvature (low Gibbs free energy).

After the compaction, the membranes must be sintered for a certain time at elevated temperatures. The sintering results in the densification of the membranes and provides the membranes with the required mechanical properties, such as strength and hardness. Another important fact is that the sintering profile (sintering temperature and dwelling time) impacts the microstructures of the membranes prominently. The microstructures (especially the grain boundary) of the membrane were believed to be directly related to the oxygen permeability of the membrane. Therefore, the sintering step is a crucial step for the preparation of the membranes. One study on LSF membranes [15] showed that as the sintering temperature and the dwelling time increased, the grains grew larger and the grain boundary decreased. The oxygen permeation experiments showed that the membranes with larger grains exhibited lower oxygen fluxes. This suggests that grain boundary seemed to act as the pathway for the oxygen transportation through the membrane. In contradiction, another study on BSCF [16] showed that as the sintering

temperature and the dwelling time increased, the oxygen fluxes of the corresponding membranes increased significantly. In these cases, the grain boundary seemed to act as a barrier to the oxygen transportation through the membranes.

1.4 Oxygen Transport Theory

In the case of MIEC membranes, the driving force for oxygen transport is the differential oxygen partial pressure across the membrane. On the high oxygen partial pressure (PO_2) side, the feed side, molecular oxygen is reduced into oxygen anions O^{2-} which are incorporated in the lattice and released at the low PO_2 side, the permeate side, where they recombine to form oxygen molecules.

The permeation rate through dense oxygen permeable membranes is essentially controlled by two factors: one is the rate of solid state diffusion within the membrane material and the other is the rate of interfacial oxygen exchange on both sides of the membrane. A membrane is divided into a central bulk diffusion controlled zone and adjacent interfacial zones, between the gas phase and the oxide, where surface kinetics are predominant, as shown in Figure 5. Diffusion is rate determining if the membrane is above a certain thickness. When this thickness is reduced, the transfer of oxygen across the interfaces becomes the limiting factor for the oxygen flux.

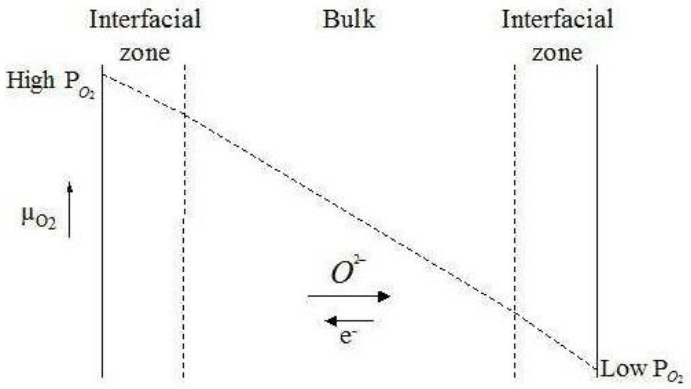

Figure 5: Diagram representing the chemical potential drop across an MIEC membrane[17].

The oxygen flux through a membrane can be increased by decreasing its thickness as long as the oxygen permeation is controlled by bulk transport. When the thickness of the membrane reaches a characteristic membrane thickness value, L_C, the permeation is controlled by both surface exchange and bulk diffusion kinetics. The characteristic membrane thickness L_C is determined by the ratio of the oxygen self diffusivity and surface exchange coefficient for predominant electronic conductors such as perovskites like LSCF. The value of L_C for LSCF (2828) was found to be 1.8mm at 850˚C [18] and for BSCF (5582) the value was 1.1mm at 900˚C [19]. Oxygen transport is also influenced by effects related to microstructure such as grain boundary diffusion and order-disorder phenomena, roughness or porosity of the membrane surface.

1.4.1 Bulk Transport

In the bulk transport theory it is assumed that the overall oxygen permeation is rate limited by diffusion of oxygen anions or transport of electronic charge carriers (electrons

and electron holes) through the bulk oxide. Oxygen diffusion through MIEC oxides is done via an oxygen vacancy transport mechanism as described previously.

1.4.2 Surface Processes

The oxygen exchange reaction between oxide surfaces and the gas phase involves a number of reaction steps, each step of which can be rate determining. These steps include molecular oxygen adsorption on the oxide surface, dissociation, charge transfer, surface diffusion of intermediate species (e.g. O_{ads}, O^-_{ads} and O^{2-}_{ads}) and incorporation into the lattice in the near-surface layer. It is generally assumed that these reactions apply to the re-oxidation of oxygen anions in the reverse direction.

The oxygen permeation flux is greatly influenced by the surface processes. The gradient in oxygen chemical potential will be consumed partially by the surface exchange kinetics at the interfacial zones of the membrane and partially by the bulk diffusion in the middle-zone. For sufficiently thick membranes, the permeation of oxygen flux depends very much on the diffusion in the bulk. A mixed control will occur when the membrane thickness is decreased. For very thin membranes, surface reactions will govern oxygen permeation through the membrane.

CHAPTER 2

LITERATURE REVIEW

2.1 Materials used for oxygen separation

There are various materials which are used nowadays for making gas separation membranes for oxygen permeation. To be a promising oxygen separation membrane material the material must fulfill some conditions. The material must exhibit good oxygen permeability as well as it should be thermally and chemically stable. A brief description of some of the commonly used materials is given below.

2.1.1 $Ba_{0.5}Sr_{0.5}Co_{0.8}Fe_{0.2}$ (BSCF-5582)

BSCF is one of the materials that is known for its high oxygen permeability. It has a perovskite structure. BSCF oxide is formed by substituting strontium with barium in the basic SCF oxide. Zongping Shao et. al. [20] compared the oxygen permeability and stability of $SrCo_{0.8}Fe_{0.2}O_{3-\delta}$ (SCF) and $Ba_{0.5}Sr_{0.5}Co_{0.8}Fe_{0.2}O_{3-\delta}$ (BSCF) oxides and thus analyzing the effect of doping barium on the SCF membranes. It was found that by incorporating barium in SCF the oxidation of Co^{3+} to Co^{4+} and the oxidation of Fe^{3+} to Fe^{4+} in the lattice was reduced to a great extent and thus the perovskite structure became quite stable under lower oxygen partial pressures. Now considering the effect of barium introduction on the oxygen permeability, they observed that the oxygen permeability was higher for BSCF as compared to that for SCF under air and He. For a 1.80mm thick BSCF membrane at 950°C the oxygen permeation flux was found to be 1.4 ml/cm^2 min.

The small amounts of CO_2 and water vapor that were present in the air did not have much effect on the oxygen permeation flux of BSCF as compared to that of SCF. The BSCF membrane showed a considerable amount of stability in terms of permeation flux and phase structure when it was continuously used for oxygen permeation testing for 1000h at 850°C. Due to a phase transition at temperatures below 825°C the oxygen permeation flux decreased slightly in an exponential manner. However, at higher temperatures this phase transition could be reversed, but the time taken by it to come to equilibrium was longer.

Jaap F. Vente et. al. [21] also studied the permeability properties of the perovskites SCF and BSCF, as well as their chemical and mechanical stability. They came to the conclusion that both these membrane materials show a considerable amount of oxygen flux which is quite suitable for practical applications. However BSCF is considered to more suitable material because of its phase stability. At low values of temperatures they observed a formation of brownmillerite phase in SCF which reduced the permeability at these temperatures. They also suggested that the membranes could also be doped with other elements like zirconium and tin to improve the chemical and mechanical stability. Although this improvement in stability might cause some reduction in the flux but this could be accepted in order to make the membrane stable. Zongping Shao et. al. [22] found that BSCF membrane was quite stable and efficient for partial oxidation of methane as they were able to operate the system at 875°C for about 500hours without any failure and with a good amount of oxygen permeability.

Further improvements in the permeation flux can be achieved by surface modifications of the membrane. Some common ways are fabrication of hollow fiber membranes or multi layer membranes. S. Liu et. al. [23] prepared some self-supported asymmetric hollow-

fiber membranes of BSCF 5582 in a single sintering step using phase inversion technique. An oxygen permeation flux of 0.031mol/m^2s was obtained at 950°C using helium as the sweep gas. This permeation flux was high as compared to that of the simple disc membranes. Studying the performance of these membranes both theoretically and experimentally they found that the oxygen permeation rate is controlled by slow oxygen surface exchange rates. Finally they concluded that in order to improve the oxygen permeability of these membranes researchers should focus on modifying the surface rather than just reducing the thickness of the membrane.

J. Caro et. al. [24] prepared some hollow fiber perovskite membranes of BCFZ as well as some disc membranes of BSCF, BSZF and SCF. Due to their thin walls the BCFZ hollow fiber membranes exhibited a high amount of oxygen permeability. The maximum amount of oxygen flux obtained was 6ml/cm^2 min at a temperature of 850°C using helium as the sweep gas. In addition to showing a good amount of oxygen permeability, it also showed good stability when tested for a long period. They also studied the effect of grain boundaries on the oxygen permeability and found that the oxygen permeability for the BSCF membrane with large size of the grains or with fewer amounts of grain boundaries is higher as compared to the BSCF membrane with a smaller size of grains. Thus, these grain boundaries might act as diffusion barriers for the migration of oxygen ions or vacancies. They observed that the thermal expansion coefficient for SCF was the highest followed by BSCF while BCFZ showed the lowest thermal expansion. This is mainly because of the large quantities of cobalt present in SCF and BSCF as compared to BCFZ. Cobalt has a large difference in the radius of its ions Co^{2+} and Co^{4+} which is the main reason of high TEC for Co-rich mixed conducting membranes. Thus they concluded that

if we dope the B-site of the perovskite with ions of stable oxidation state, the amount of thermal expansion will be lower while if the doping is with ions of variable oxidation state there will be large amount of thermal expansion.

S. Baumann et. al. [25] synthesized some BSCF membranes by tape casting and co-firing. These membranes consisted of two layers, one was the top gastight layer about 70µm thick, and the other was the porous substrate about 830µm thick on which this layer was deposited. A very thin layer of BSCF (about 17µm thick) was also deposited on the top gastight layer to act as an activation layer for oxygen permeation and thus measuring its effect on the overall oxygen permeability. They found that this activation layer increased the surface exchange rate and thus increased the permeability. An oxygen permeation flux of 12.2ml/cm^{2}min was obtained at 1000°C when air was used as the feed and argon as the sweep whereas a flux of 67.7ml/cm^{2}min was obtained at 1000°C when pure oxygen was used as the feed and argon was used as the sweep gas.

Another way to enhance the permeation is doping or substitution with different elements. P. Haworth et. al. [26] substituted some yttrium in place of iron in BSCF to form the perovskite type oxide $Ba_{0.5}Sr_{0.5}Co_{0.8}Fe_{0.2-x}Y_xO_{3-\delta}$ and optimized the concentration of yttrium by varying the value of x from 0to 0.2. It was observed that there was an improvement in the oxygen permeability for the values x=0 to x=0.15. At x=0.20 i.e. when yttrium was fully substituted for iron, the XRD showed the disappearance of the cubic phase which is not suitable for oxygen permeability as it becomes a non-perovskite structure. The cubic crystal phase is an important parameter for the oxygen permeability of the perovskite material which present for the values of x less than or equal to 0.15. However the best result for oxygen permeability was observed for x=0.025 and a flux of

2.05ml/cm^{2}min was obtained for a BSCFY membrane of 1.2mm thickness at a temperature of 900°C showing an enhancement of more than 1.5 times as compared to the pure BSCF membrane which gave a flux of about 0.79ml/cm^{2}min. There were two main reasons attributed to this increase in the oxygen permeability with yttrium substitution: one was the increase in the concentration of oxygen vacancies with yttrium substitution and the other was the increase in the mobility of oxygen ions due to the expansion of the crystal lattice.

Although these membranes give high amount of permeation flux but it is observed that they are not stable under reducing environments especially when the membrane is exposed to CO_2. Mirko Arnold et. al. [27] investigated the effect of carbon dioxide on the oxygen permeability and the microstructure of the BSCF membranes by testing the BSCF membranes under different environments of CO_2. They found that there was an immediate stoppage of the oxygen permeation when these membranes were tested using pure CO_2 as the sweep gas but this oxygen permeability and the microstructure could easily be recovered by using helium as the sweep gas. Microstructure examinations of these BSCF membranes exposed to CO_2 for a period of 72 hours indicated that the perovskite structure was damaged only upto a depth of 50µm which led to the formation of two different phases. They also examined the effect of concentration of CO_2 on the oxygen permeability of these membranes and found that BSCF membranes can successfully work only upto a 10% CO_2 concentration applied in the feed air. Jung Hoon Park et. al. [28] also observed that with the introduction of CO_2 as the feed gas there was a decrease in the oxygen permeability of about 43%. This low value of oxygen

permeability was obtained because of the formation of carbonates on reaction between Ba/Sr metal and carbon dioxide.

Jianxin Yi et. al. [29] studied the microstructure degradation and phase composition of perovskite material BSCF 5582 membrane when it was exposed to CO_2 containing atmospheres at temperatures around 800 to 900°C. There was the formation of a carbonate layer on the surface of the treated membrane. Along with this carbonate layer there was another decomposed zone consisting of CoO, a complex oxide of Ba–Sr–Co–Fe, and the (Ba, Sr) CO_3 carbonate phase. They observed the formation of three different carbonate phases, formed at different annealing conditions. The growth of the top carbonate layer was observed to be diffusion controlled as it was showing a parabolic behavior. The growth of this carbonate layer was not much affected by the change in partial pressure of oxygen and carbon dioxide. The cobalt in BSCF was completely substituted by iron to monitor the degradation of the membrane and it was observed that there was a reduction in degradation for this material under an environment of carbon dioxide. The adverse effect of CO_2 was found to be more pronounced at the grain boundaries of the membrane.

Kirsten Foy et. al. [30] conducted a review on the recent development in ion transport membranes and did a comparison between various membranes. They found that the best permeability was obtained for BSCF 5582 particularly for the tube BSCF. The maximum flux obtained was 1.86µmol/cm^{2}s. Figure 6 shows the permeability of different membranes. They also studied these materials in hydrogen containing environments and found that for BSCF the structure was destroyed. For the case of synthetic gas production

also it was observed that highest flux is given by BSCF. So, it can be seen that although BSCF has the highest flux, but it is not stable under reducing environments.

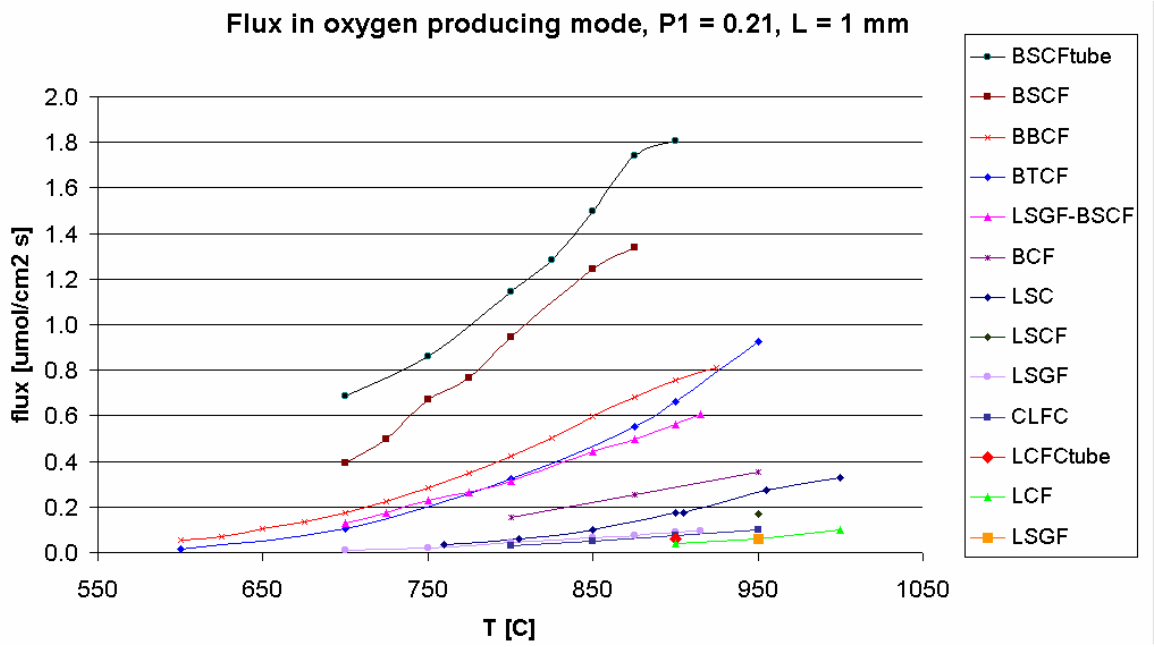

Figure 6: Flux of different membranes as a function of temperature [30].

2.1.2 $La_{1-x}Sr_xCo_{1-y}Fe_y$ (LSCF)

The $La_{1-x}Sr_xCo_{1-y}Fe_y$ perovskite-type oxides are one of the most extensively studied materials for application as membranes for oxygen separation. Although these materials have high conductivity but they may show a rise in thermal expansion and low stability at certain compositions [31]. $La_{0.6}Sr_{0.4}Co_{0.2}Fe_{0.8}$ (LSCF-6428) is a common member of this family. Anthony Petric et. al. [31] investigated different compositions of LSCF to determine an optimum value and for this they studied the following compositions: $La_{1-x}Sr_xCo_{1-y}Fe_yO_{3-\delta}$ (a) x=0.1-0.9 & y=0; (b) x=0.7 & y=0.1-1.0; (c) x=0.2-0.4 & 0.7 with y=0.8. The investigation was done based on electrical conductivity. They compared the

potential use of LSCF perovskite materials for solid oxide fuel cells (SOFC) or gas separation membranes. They found that the compositions for which good conductivity was obtained showed large thermal expansions with increasing strontium and cobalt content and as such these compositions were not suitable for SOFC. In case of membranes that are used for gas separation the compositions which showed good conductivity were $0.2<x<0.4$ & $y<0.5$ and so these materials could be more efficiently used in case of these membranes.

The performance of these membranes is also affected by process parameters like powder preparation techniques and sintering conditions. Y. Zeng et. al. [32] prepared the LSCF-6428 powder with different methods such as hydrothermal synthesis, co-precipitation and calcination, spray-pyrolysis, and conventional ball milling and calcination and compared these different techniques on the basis of obtaining dense membranes. They found that the densest membranes were obtained when LSCF powder was prepared using co-precipitation method while the membranes were least dense with the powder prepared through spray-pyrolysis. They obtained an oxygen permeation flux of 1×10^{-7} mol/cm^2 at a temperature of 950°C for a 1.85mm thick LSCF membrane.

Jung Hoon Park et. al. [33] prepared LSCF 6428 ($La_{0.6}Sr_{0.4}Co_{0.2}Fe_{0.8}O_{3-\delta}$) perovskite powders using citrate method and hydrothermal method. They found that the oxides prepared by citrate method were fully perovskite whereas the oxides prepared from hydrothermal method showed some amount of secondary phase also. However, the hydrothermal method gave better powder morphology and particle size distribution. They also investigated different sealing materials like Pyrex glass, silver melting seal and a commercial ceramic binder. Both the glass and silver melting seal provided good gas

tight sealing at elevated temperatures but this gas tightness was not achieved with the ceramic binder which may be due to different thermal expansion of sealant and membrane. Glass gave the maximum amount of gas tightness but because of the spreading of glass on the surface there was a reaction between it and the membrane. An oxygen permeation flux of 0.33ml/cm^{2}min was obtained for a LSCF membrane of 1mm thickness at a temperature of 950°C under air and helium.

Pingying Zeng et. al. [34] studied the effects of sintering temperature on the performance of LSCF 6428 membrane. The sintering temperature had a significant effect on the microstructure of the membrane and thus on the oxygen permeability. As the sintering temperature increased grain size also increased with a value of 0.3 μm at 1000°C to 3.5μm at 1300°C and thus the electrical conductivity also increased. The phase structure and oxygen nonstoichiometry were not much affected by the sintering temperature. However, an increase in oxygen permeability was observed as the sintering temperature increased. The oxygen permeability increased upto 10 times with an increase of sintering temperature from 1000°C to 1300°C indicating that the grain boundaries act as a hindrance for the movement or the conduction of oxygen ions.

As far as the stability of these membranes is concerned, Shiguang Li et. al. [35] compared the oxygen permeability and stability of three perovskites membranes $La_{0.2}Sr_{0.8}Co_{0.2}Fe_{0.8}O_{3-\delta}$ (LSCF), $La_{0.2}Ba_{0.8}Co_{0.2}Fe_{0.8}O_{3-\delta}$ (LBCF) and $La_{0.2}Ca_{0.8}Co_{0.2}Fe_{0.8}O_{3-\delta}$ (LCCF). They noticed that the oxygen permeability was the highest for LSCF membrane followed by LBCF and LCCF membranes and as obvious the activation energy for oxygen permeability was the highest for LCCF followed by LBCF and LSCF. The data of oxygen permeability based on temperature dependence is

shown in Figure 7. LSCF was found to have the maximum oxygen permeability mainly because of three reasons: the average bond energy for LSCF is lower; the free volume is the highest in this case thus providing activation volume for the transport if ions and it also has the largest critical radius. However, regarding the stability it was found that the perovskites phase in LSCF was not stable when the temperature went higher than 923K. Beyond this temperature there was dissociation of the perovskites phase and the XRD analysis showed that some other phases started forming like the oxides of La, Sr and Co. So, it was concluded that LSCF membrane is not stable at high temperatures and low oxygen partial pressure whereas on the other hand there was no phase change in LBCF membranes indicating that they are quite stable under these conditions. Similar results were obtained by Jung Hoon Park et. al. [33] as they also observed the formation of lanthanum oxide and some other compounds on the membrane surface after a continuous testing of the membrane for 160 hours.

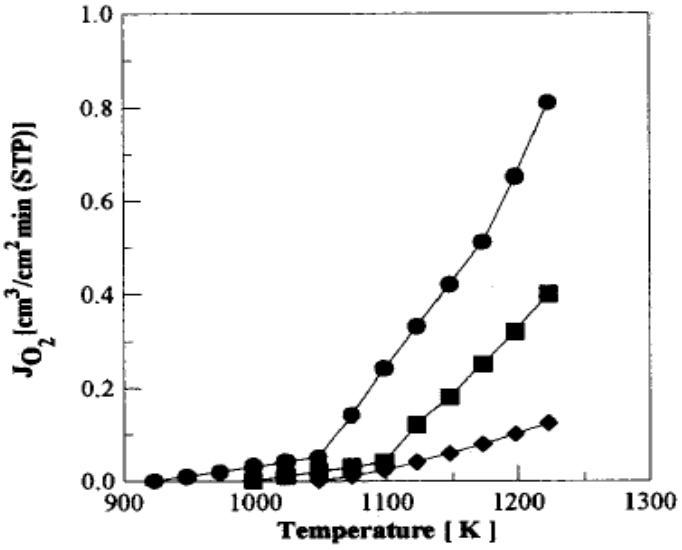

Figure 7: Oxygen permeability as function of temperature for LSCF (●), LBCF (■) and LCCF (♦) membranes [35]

As discussed previously modifying the surface of the membranes is an important criteria for improving the oxygen permeation flux. Xiaoyao Tan et. al. [36] prepared LSCF 6428 hollow fiber membranes using the combined phase inversion and sintering technique. They modified the surface of these hollow fibers by coating a porous layer of silver or LSCF perovskite on the outer surface in an effort to improve the surface exchange. It was observed that modifying the surface improved the oxygen permeability of the membranes. The oxygen permeation flux increased to a value of 0.08–1.85mL/cm^2min for silver coated hollow fibers and to a value of 0.05–1.48mL/cm^2min for the fibers coated with LSCF perovskite as compared to the original values of 0.01–0.81mL/cm^2min for the uncoated fibers. The permeability was tested in a temperature range of 700-1000°C. There was a maximum improvement of about 18 times for the silver coated membranes and an improvement of about 9.3 times for the LSCF perovskite coated hollow fibers. The operating temperature at which a considerable amount of permeability could be achieved was also reduced.

2.1.3 La_2NiO_4 (LNO) for Oxygen Permeation

La_2NiO_4 (LNO) is one of the materials that can be used for oxygen permeation. LNO has certain advantages compared to other perovskite materials. It includes higher chemical stability, stable thermal expansion, and lower chemical expansion [9] [10]. The LNO material has a K_2NiF_4- type structure. Oxygen ionic conduction in K_2NiF_4-type materials is believed to occur via diffusion of oxygen interstitials in the rock-salt-type layers and also via a vacancy mechanism in the perovskite layers. S.-Y. Jeon et. al. [37] studied the effects of the applied oxygen chemical potential gradient and temperature on the oxygen permeability of LNO at various thicknesses. They observed an increase in flux with

increasing temperature and partial pressure of oxygen. They found a maximum flux of 0.097µmol $cm^{-2}s^{-1}$ (0.15ml min^{-1} cm^{-2}) under air/N2 conditions for the 0.95 mm-thick LNO specimen at 900°C. D.C. Zhu et. al. [38] prepared some tubular LNO membranes by mixing the La and Ni oxides to form the calcined powder followed by extrusion to form the tubes. They studied this LNO tubular membrane for the conversion of methane to syngas and observed an oxygen flux of 0.863µmol $cm^{-2}s^{-1}$ (1.33ml min^{-1} cm^{-2}). Cheng Li etal [39] prepared some supported dense oxygen permeating membranes of mixed conductor $La_2Ni_{0.8}Fe_{0.2}O_{4-\delta}$ by sol-gel method. They coated the sol of $La_2Ni_{0.8}Fe_{0.2}O_{4-\delta}$ on a porous α-Al_2O_3 substrate and followed by heat treatment to prepare the dense supported membrane. They observed an increase of about 5 to 10 times in the oxygen permeation flux of these dense membranes as compared to the supported membranes made from pure LNO. They got a value of more than 0.649µmol $cm^{-2}s^{-1}$ (1.00ml min^{-1} cm^{-2}) for the Fe doped supported membranes. V.V. Vashook et. al. [40]studied the oxygen permeation of various $La_{2-x}Sr_xNiO_{4-\delta}$ type materials and observed a maximum permeability of about 0.7µmol $cm^{-2}s^{-1}$ (1.08ml min^{-1} cm^{-2}) for the pure La_2NiO_4 as compared to the Sr doped materials. J.M. Bassat [41] compared the ionic conductivities of K_2NiF_4- type structures (LNO, PNO) and the perovskite structures (LSCF, LSFN) and observed that the K_2NiF_4-type structures gave better results especially at lower temperatures, so these materials were found to be more suitable for applications in Solid Oxide Fuel Cell (SOFC). The results are shown in Figure 8. V.V. Vashook et. al. [42] compared the oxygen permeability of pure La_2NiO_4, La_2NiO_4 + 40% Ag composite and $LaSrNiO_{4-\delta}$ + 40% Ag composite. They found that the oxygen permeability of La_2NiO_4 was not much improved by the introduction of silver and for both the cases they found a maximum permeability

of about 0.087µmol $cm^{-2}s^{-1}$ (0.134ml min^{-1} cm^{-2}) at a temperature of 927°C. The permeability for $LaSrNiO_{4-\delta}$ + 40% Ag composite was about 100 times lower than that of La_2NiO_4. Cheng Li et. al. [43] prepared some supported dense oxygen permeating membranes of mixed conductor LNO by coating the sol of LNO on the α-Al_2O_3 substrate. They found a maximum oxygen permeability of about 0.285µmol $cm^{-2}s^{-1}$ (0.44ml min^{-1} cm^{-2}) at a temperature of 627°C.

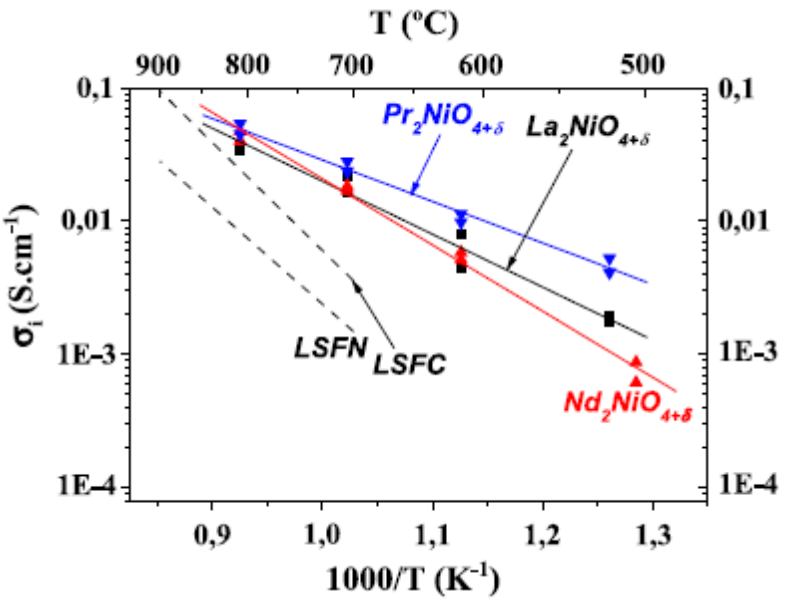

Figure 8: Comparison of the ionic conductivites of K2NiF4 type structure and perovskite type structure [41].

K. Wiik et. al. [44] studied the effect of cobalt substitution with respect to oxygen flux in strontium ferrate-based materials and found that there was an enhancement in the permeation owing to the increasing concentration of oxygen vacancies with cobalt content. As explained in their work, Co^{3+} ion has a comparatively smaller ionic radius as well as smaller bonding energy to oxide ions which facilitates the diffusion of oxygen.

2.2 Stability of the LNO Membrane as Compared to Other Materials

P. Odier et. al. [45] studied the influence of temperature on the stability of the various phases in the La-Ni-O system. They performed high temperature X-ray structure studies and found that La_2NiO_4 was stable in air up to more than 1300°C based on the X-ray spectra obtained at high temperatures. M. Al Daroukh et. al. [10] conducted a thorough study on the thermal and chemical stabilities of the perovskite type oxides (ABO_3) and the K_2NiF_4 (A_2BO_4) type oxides. According to them that at higher temperatures and lower oxygen partial pressures, the ABO_3 phase becomes unstable and transform into A_2BO_4 phase and thus it can be said that the A_2BO_4 compounds have higher thermodynamic stability as compared with the ABO_3 type compounds. Comparable compositions of the perovskite and the K_2NiF_4 type oxides showed higher O/M stoichiometries at low oxygen partial pressures for the K_2NiF_4 structure, demonstrating higher thermodynamic stability as shown in Figure 9. The initial state of the oxygen-to-metal stoichiometry was determined using chemical analysis and total reduction of the compounds. The chemical analysis was done using cerimetric titration in H_2SO_4 solution. The reduction was performed by heating in Ar/5% H_2 mixture at 900-1000°C. The titration was done after the total reduction of the compounds. They also compared the oxygen release of the two types of oxides showing that the oxygen deficiency of perovskite oxides is higher, indicating their lower stability.

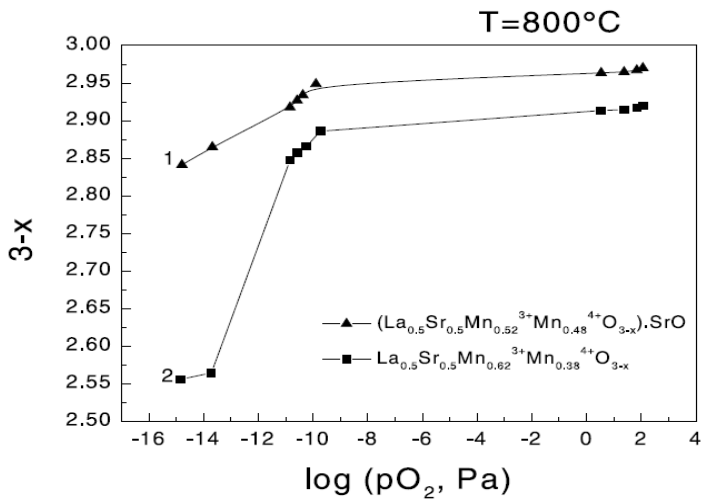

Figure 9: O/M stoichiometries of the perovskite oxide and the K_2NiF_4 type oxide [10].

Skinner et. al. [46] studied the transport properties of La_2NiO_4 as compared to LSC and LSCF and found that the LNO showed good transport properties with an added advantage that it was thermodynamically more stable at elevated temperatures. Yaremchenko et. al. [47] introduced cobalt in La_2NiO_4 by replacing 10% of the nickel with cobalt ($La_2Ni_{0.9}Co_{0.1}O_{4+\delta}$). They studied the permeability and the stability of these membranes under a reducing environment of hydrogen and observed that membranes were quite stable with time at 973K, however at high temperatures degradation in the flux values was observed as shown in Figure 10.

Tobias Klande et. al. [48] compared the stability of the LSCF and the LNO under a reducing environment using CO_2 as the sweep gas. They observed that LSCF was not stable under CO_2 environment whereas LNO showed excellent long term stability with even 100% CO_2 in the sweep as shown in Figure 11.

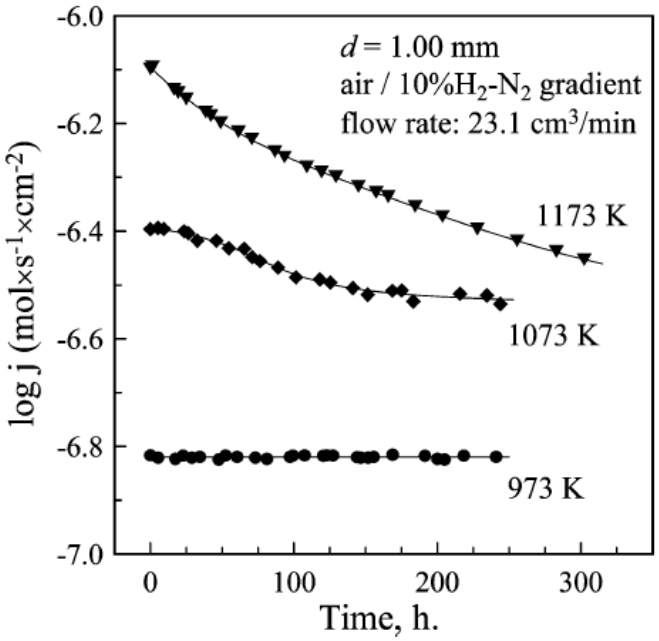

Figure 10: Time dependence of the oxygen permeation fluxes through $La_2Ni_{0.9}Co_{0.1}O_4$ ceramic membranes under an air/10% H_2–90% N_2 gradient. Porous Pt layers were applied onto the permeate-side surface. [47]

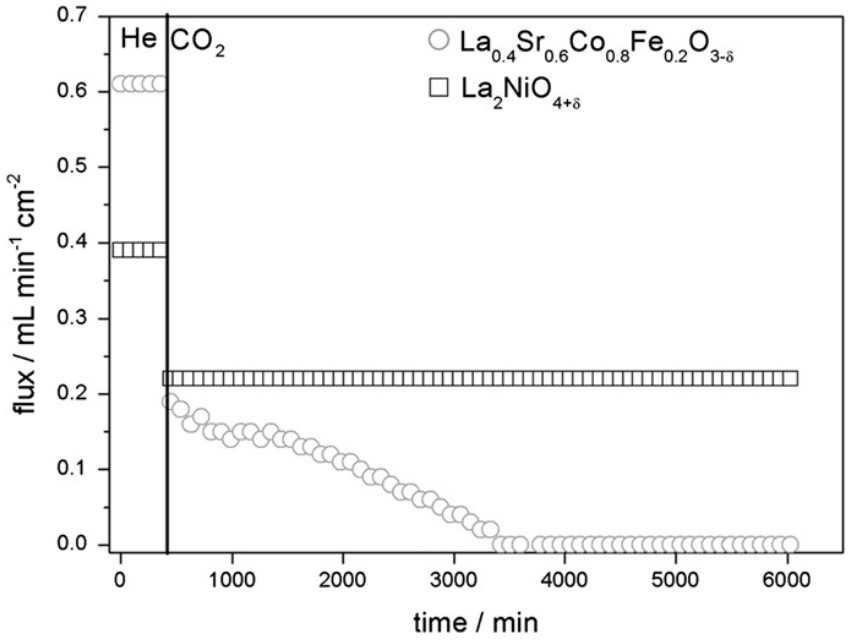

Figure 11: Oxygen flux rate of La_2NiO_4 and $(La_{0.4}Sr_{0.6})(Co_{0.8}Fe_{0.2})O_{3-\delta}$ membranes at 1173K with a thickness of 1mm,feed side:150mL/min synthetic air,sweep side: 29mL/min He orCO_2 and 1mL/min Ne. [48]

Nebojsa Cebasek et. al. [49] conducted a study on the decomposition of a $La_2NiO_{4+\delta}$ membrane under an oxygen potential gradient. They exposed the LNO membrane to an oxygen gradient between O_2 and argon for 800 h at 1000◦C. They observed that the flux dropped for some time and then a steady state was achieved as shown in .The reason they attributed to this behavior was the formation of a thin blocking layer of La_2O_3. The membrane side that was exposed to high oxygen partial pressure showed the formation of nickel oxide. The side where the partial pressure of oxygen was low, pores were created.

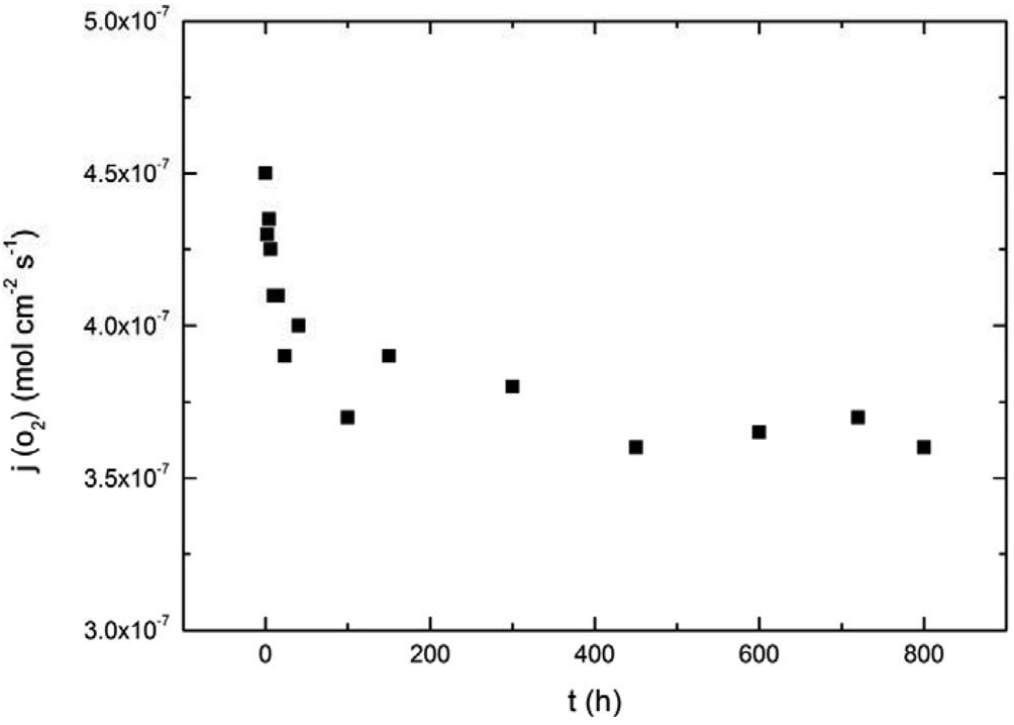

Figure 12: Oxygen flux of the LNO membrane versus time when exposed to an oxygen gradient between O_2 and Ar at 1000°C [49].

H. Kruidhof et. al. [50] studied the variation of oxygen permeability with time for perovskite oxides like $SrCo_{0.8}Fe_{0.2}0_3$ (SCF) and $La_{0.6}Sr_{0.4}CoO_3$ (LSC) and observed that this behavior depended very much on the order-disorder transitions or the processes that occur during the ordering of oxygen vacancies in these oxides. They found that at temperatures around 650°C to 750°C the oxygen permeability decreases with time and takes about 30-40 hours for the SCF membrane to attain steady state conditions whereas for the LSC membrane the oxygen permeability keeps on decreasing with time as shown in Figure 13.

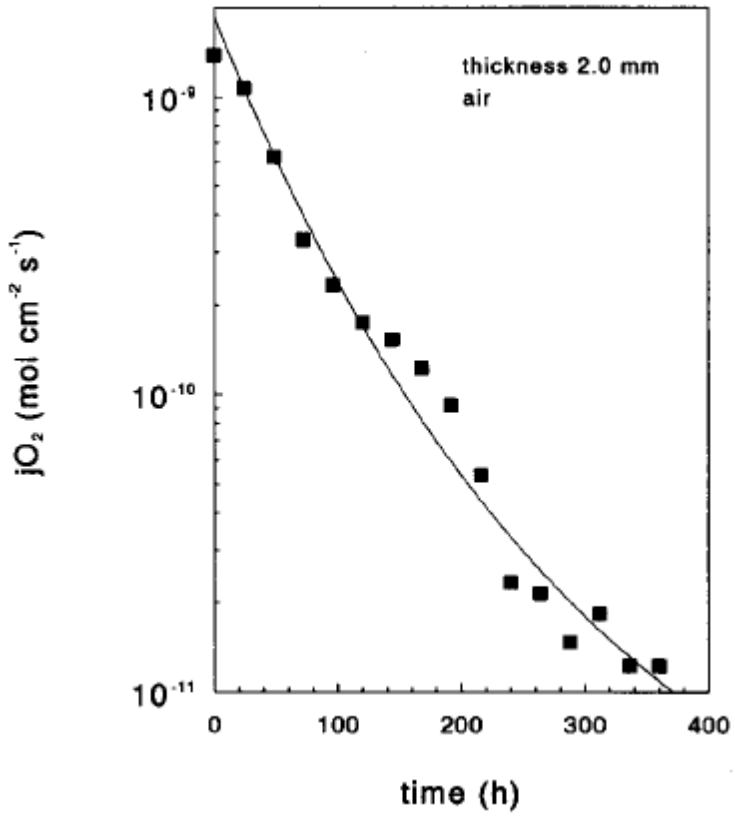

Figure 13: Oxygen permeation with time observed for LSC at 750 °C [50]

LNO is therefore much more stable than the other corresponding perovskite materials. A summarized comparison of the stability of LNO with some other perovskite materials is shown in Table 1.

Table 1: Stability of LNO compared to other materials

Material	**Group of Researchers**	**Comments**
La_2NiO_4	P. ODIER et. al. [45]	X-Ray spectra at high temperatures show that La_2NiO_4 is stable in air up to more than 1300°C.
	Skinner et. al. [46]	La_2NiO_4 more stable than LSC and LSCF in terms of expansion behaviour at high temperatures.
	Tobias Klande et. al. [48]	LNO showed excellent long term stability with even 100% CO_2 in the sweep.
$La_2Ni_{0.9}Co_{0.1}O_{4+\delta}$	Yaremchenko et. al. [47]	Membrane quite stable with time at 973K. At high temperatures there is degradation in flux.
LSCF (6428)	Sherman J. Xu et. al. [51]	Initially flux increases and then becomes constant with time under air/N_2. This flux further increased with the introduction of methane on the lean side.

	Shiwoo Lee et. al. [52]	The methane conversion with LSCF membrane was extremely low and unstable.
LSCF (6482)	E.D. Wachsman [53]	High flux initially, then degrades rapidly. LSCF membrane coated with SDC showed better stability.
	Xiaoyao Tan et. al. [54]	Membrane not stable with CO_2 as the sweep gas, significant decrease in oxygen permeation flux.
LSCF (4682)	Tobias Klande et. al. [48]	Membrane not stable under CO_2 environment.
BSCF (5582)	Mirko Arnold et. al. [27]	Perovskite structure damaged under CO_2 environment.
BSCF (5582)	Kirsten foy et. al. [30]	Membrane structure destroyed under hydrogen containing environment.

2.3 Spark Plasma Sintering (SPS) of the MIEC Materials

Spark plasma sintering is a technique used to produce highly dense materials. In spark plasma sintering a pulsed DC current is used to generate the heat which causes the sintering of the membrane. SPS is a very fast process as very high heating and cooling rates can be achieved. SPS is not very common for the synthesis of these oxygen

permeable membranes. Yuan-Hua Lin et. al. [55] prepared La_2CuO_4 ceramics using the SPS technique. They were able to obtain dense samples for the sintering temperature of 875°C; however with increase in temperature they observed an increase in the grain size. C.L. Song et. al. [56] compared the electrical properties of the $La_{1.75}Ba_{0.25}NiO_4$ ceramics prepared by spark plasma sintering process and the solid state sintering process. The XRD analysis showed the presence of secondary phases in the $La_{1.75}Ba_{0.25}NiO_4$ ceramics prepared by spark plasma sintering. The electrical conductivity of the sample prepared by SPS was also much lower as compared to the one prepared by solid state sintering. The reason attributed to the decrease in the conductivity of the SPS sample was that during the SPS there was extraction of the interstitial oxygen from the sample which decreased the conductivity. SPS has also been used to prepare BSCF as cathode material for solid oxide fuel cells [57].

CHAPTER 3

EXPERIMENTAL PROCEDURE

3.1 Preparation of the Perovskite Membranes

The La_2NiO_4 (LNO) perovskite powders were prepared via modified sol gel method similar to the Pechini's method [M.P. Pechini, Patent 3,330,697, 11th July 1967]. Lanthanum nitrate, $La(NO_3)_3.6H_2O$ and nickel nitrate, $Ni(NO_3)_2.6H_2O$ were used as the starting salts. The stoichiometric amounts of these nitrates were mixed in 10% nitric acid (HNO_3) solution prepared in deionized water. Citric acid ($C_6H_8O_7$) and ethylene glycol ($C_2H_6O_2$) were added to obtain an organic-polymeric complex containing the metal cations. Citric acid was added as a chelating agent while ethylene glycol was added to this solution to promote polymerization of the mixed citrate. The solution was stirred for some hours on a magnetic stirrer until we obtain a clear green solution. This solution is dehydrated by heating slowly onto the stirrer to obtain a green viscous gel. The gel was then calcined at a temperature of 250°C for about half an hour to obtain a creamy calcined lump of powder. This lump of the powder was crushed and was kept for heat treatment at a temperature of 1000°C to obtain the final black colored La_2NiO_4 perovskite powder. The LNO powder obtained was mixed with few drops of ethylene glycol (added as a binder). After mixing the binder thoroughly the powder was sieved through a fine mesh in order to ensure a homogeneous distribution of particles. This sieved powder was then compacted in a mould of 1″ diameter at a force of about 10000lb for 10 minutes

using a Carver Auto Pellet Press shown in Figure 14. The compacted membrane was sintered at a temperature of 1500°C for 10 hours. The membrane was heated and cooled slowly at a rate of 2°C/min in order to prevent cracking. The sintered membrane was polished using silicon carbide (SiC) papers with different grits (120, 180, 240, 320, 400 and 600). The final thickness of the membrane was about 1mm. Figure 15 shows the conversion from the pre-heat treated cream powder to the black LNO powder and finally to the LNO disc.

Figure 14: Carver Auto Pellet Press

Figure 15: LNO disc prepared from the powder

Different sets of perovskite powders were prepared by introducing different percentages of cobalt or iron in place of nickel in an effort to further increase the permeation flux of LNO. Cobalt nitrate, $Co(NO_3)_2.6H_2O$ was used as the source of cobalt whereas iron nitrate, $Fe(NO_3)_3.9H_2O$ was used as the source of iron. The same procedure was used to prepare each set of powders. The powders that were prepared are as follows: $La_2Ni_{0.8}Fe_{0.2}$, $La_2Ni_{0.95}Co_{0.05}$, $La_2Ni_{0.9}Co_{0.1}$, $La_2Ni_{0.8}Co_{0.2}$, $La_2Ni_{0.75}Co_{0.25}$, $La_2Ni_{0.7}Co_{0.3}$, $La_2Ni_{0.5}Co_{0.5}$ and $La_2Ni_{0.2}Co_{0.8}$. Membranes were prepared from all of these powders and tested for oxygen permeability.

LNO membranes were also coated with silver in order to enhance the surface activity so as to increase the permeation. The silver coating was done in two ways. In the first case porous silver in the form of silver paste (Alfa Aesar) was coated on the membrane whereas for the second case an ion sputtering instrument with a silver target was used.

LNO membranes were also prepared using the spark plasma sintering process. The spark plasma sintering for the LNO membrane was carried out in the following steps: pressing the powder under a pressure of 50MPa in vacuum; heating upto 1200°C at a rate of

100°C/min; holding at 1200°C for 5minutes; and then cooling to room temperature at 100°C/min.

3.2 Characterization Techniques

3.2.1 X-Ray Diffraction Technique (XRD)

The XRD analysis of the powders as well as the discs was done to examine the phase developments occurring in the samples. The XRD data was recorded at room temperature in the angular range of $20° \leq 2\theta \leq 60°$ with a step size of 0.02°/min.

3.2.2 Scanning electron microscopy (SEM) and Energy dispersive x-ray spectroscopy (EDS)

JEOL® 6400 Scanning Electron Microscope shown in Figure 16 was used to study the morphology of the surface and the cross-section of the membranes. Samples were coated with gold using a sputtering instrument to make them conductive. EDS was used to find the composition of the different elements or phases that were present.

3.2.3 Density Measurements

The density of the samples was determined by the Buoyancy method based on the Archimedean Principle. The apparent weight of the sample, i.e. the weight reduced by the buoyancy force, in a reference liquid was measured by a precision balance. The value of the weight of the sample in air combined with the weight of the sample in the reference liquid was used to calculate the density of the sample.

Figure 16: Scanning Electron Microscope (SEM)

3.3 Oxygen Permeability Measurement

Figure 17 shows the schematic of the experimental setup for the measurement of oxygen permeation flux. The experimental setup mainly consisted of a vertical gas permeation system connected to the gas cylinders and a gas chromatograph. The gas permeation system consisted of two aligned sets of alumina tubes separated with the ITM inside a split furnace. Each alumina set was considered as a chamber composed of two coaxial ceramic tubes. In each ceramic chamber, the gas flew from the inner tube towards the membrane and exited through the outer tube. The membrane was placed inside a glass

ring between the two alumina chambers. A thermocouple was placed in the upstream chamber and used to measure the actual temperature near the membrane's surface. The top set of alumina tubes was free to move vertically so that it will seal the membrane during the heating of the system using the gravitational force to squeeze the glass sealant between the membrane and the alumina tubes. The detailed description of the apparatus is shown in Figure 18.

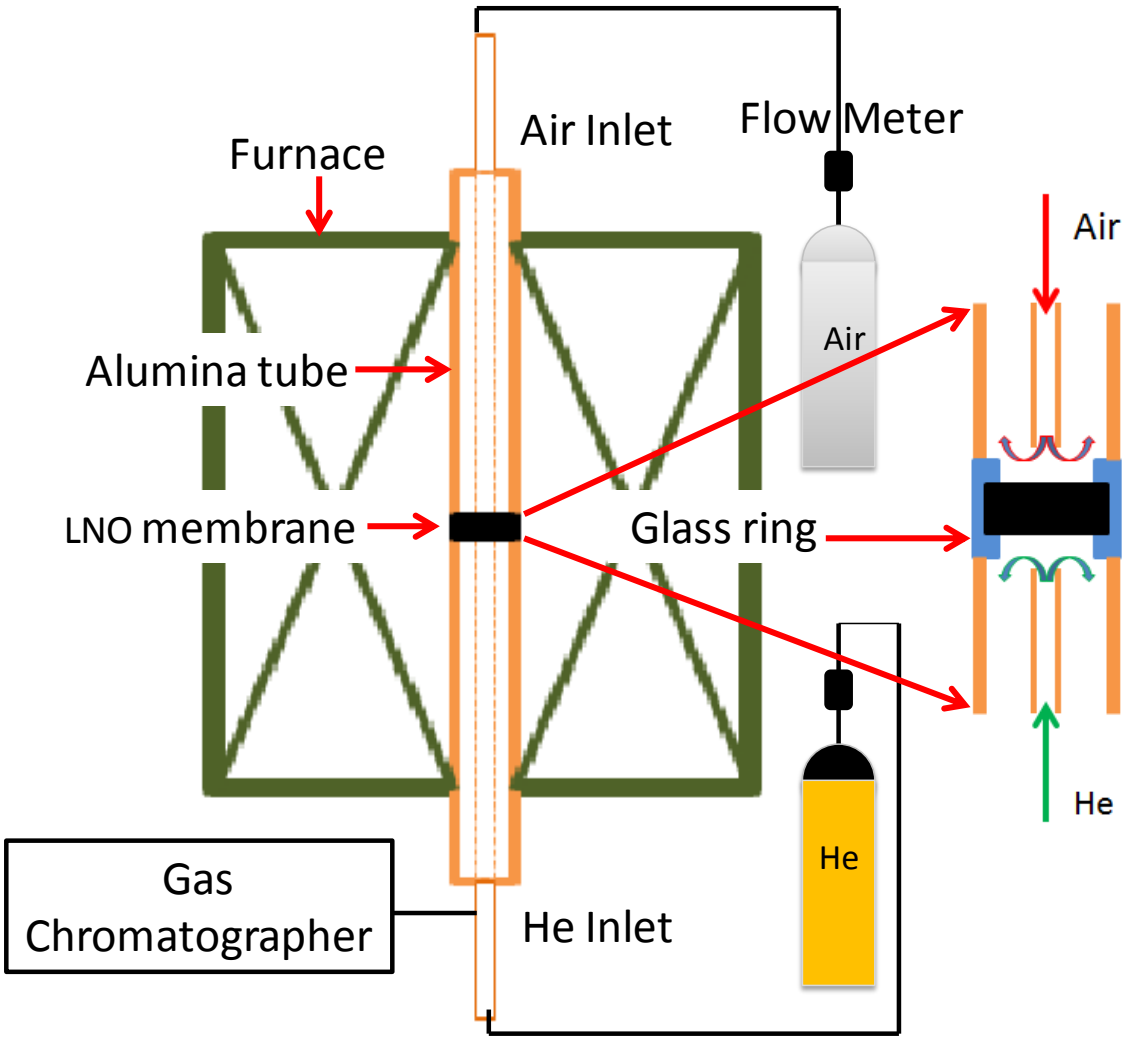

Figure 17: Schematic of the experimental setup

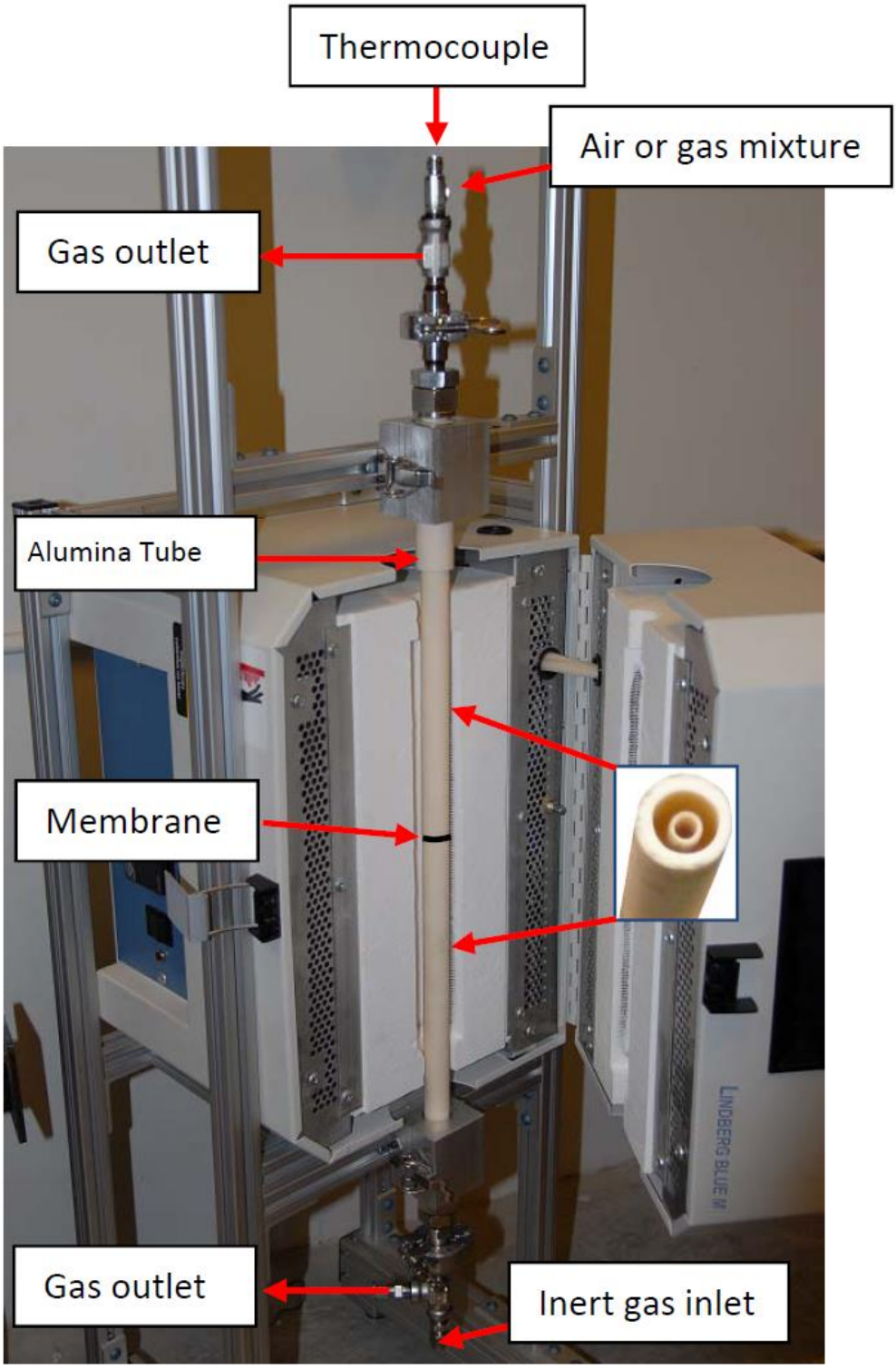

Figure 18: Vertical high temperature gas permeation system.

Glass rings of appropriate thickness were cut with the help of a diamond cutter and the membrane was kept inside a casing of these glass rings. The glass rings were used in order to seal the membranes between the two alumina tubes. Silver paste was painted on the area where the membrane was in contact with the glass rings and was cured at 300°C for 1 hour. The silver paste was used so as to prevent the membrane material from reacting with the glass rings at high temperatures. The membrane was heated in the split furnace to a temperature of 700°C at a heating rate of 2°C/min for the measurement of oxygen flux. A gas stream of pure oxygen or oxygen/nitrogen mixture or pure air was introduced in the upstream chamber (feed side) using mass flow controllers. Helium was used as the sweep gas in the downstream chamber (permeate side) which was connected to a gas chromatograph (Bruker GC) shown in Figure 19.The GC was used to analyze the concentration of oxygen and/or nitrogen in the sweep gas stream. The flow rate of air at the feed side was fixed at 20ml/min whereas the flow rate of helium on the permeate side was 30ml/min. The leakage in the whole system was negligible as the concentration of nitrogen in the permeate gas was very small.

Three sets of experiments were performed on the LNO membrane. In the first case a mixture of oxygen and nitrogen gases was supplied on the feed side and the concentration of these gases in the mixture was varied. The temperature was fixed at 700°C in this case. In the second case the temperature of the split furnace was raised from 700°C to 850°C in steps of 50°C to analyze the effect of temperature on the oxygen permeation of LNO membrane. The feed gas used in this case was air. For the third case the feed gas introduced was air and the temperature of the furnace was kept constant at 700°C. In this

case the stability of the oxygen permeation flux of the LNO membrane was monitored with respect to time.

Figure 19: Gas chromatograph

CHAPTER 4

RESULTS AND DISCUSSION

4.1 Pure La_2NiO_4 (LNO) Membrane

4.1.1 Characterization of the Membrane (XRD, SEM, EDS, Density measurements)

The XRD of the powder heat treated at 1000°C is shown in Figure 20 which shows some development of the K_2NiF_4 structure. However, the XRD of the LNO disc shows a fully developed K_2NiF_4 structure (Figure 21) as reported in the literature [48] [58]. No other phases were observed in the structure.

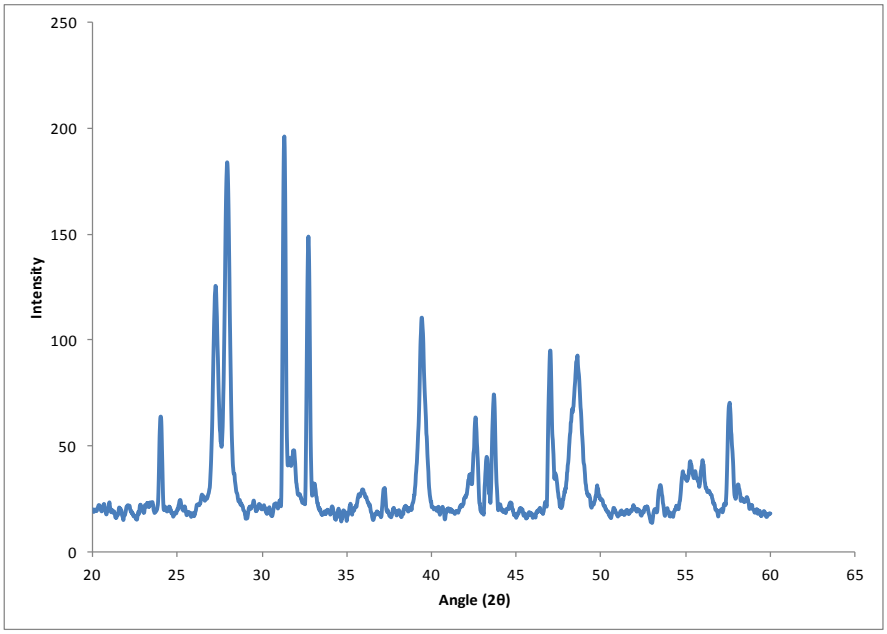

Figure 20: XRD of the LNO powder

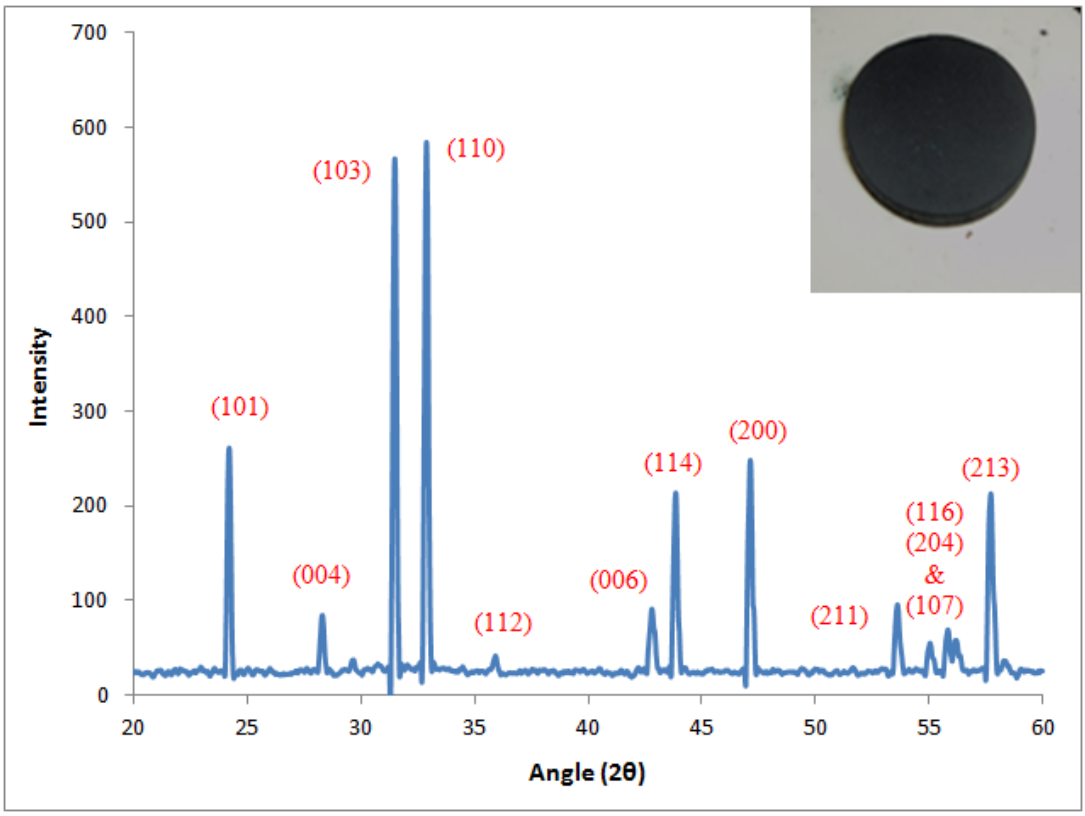

Figure 21: XRD of the LNO membrane.

The EDS analysis of the LNO powder (Figure 22) showed that the elements were in stoichiometric proportions. The microstructure of the membrane was studied by scanning electron microscopy (SEM). The SEM images of the LNO membrane are shown in Figure 23. It can be seen from the images that there are pores distributed across the membrane cross-section. The density of the LNO membrane was calculated using the Archimedes principle. The value of density was found to be around 6.5g/cm^3 which is about 92% of the theoretical density and a membrane with relative density more than 90% is usually considered to be suitable for permeation measurements.

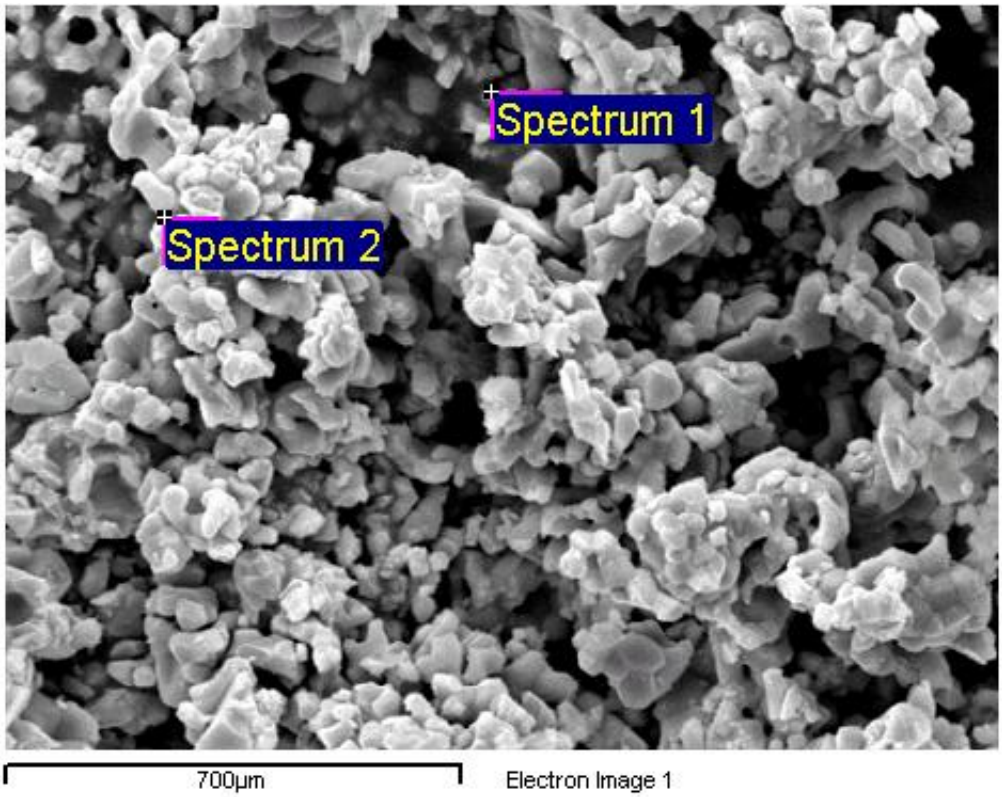

Processing option : All elements analyzed (Normalised)

Spectrum	O	Ni	La	Total
Spectrum 1	42.37	18.69	38.94	100.00
Spectrum 2	41.97	18.09	39.94	100.00
Mean	42.17	18.39	39.44	100.00
Std. deviation	0.28	0.42	0.70	
Max.	42.37	18.69	39.94	
Min.	41.97	18.09	38.94	

Figure 22: EDX analysis of the LNO powder

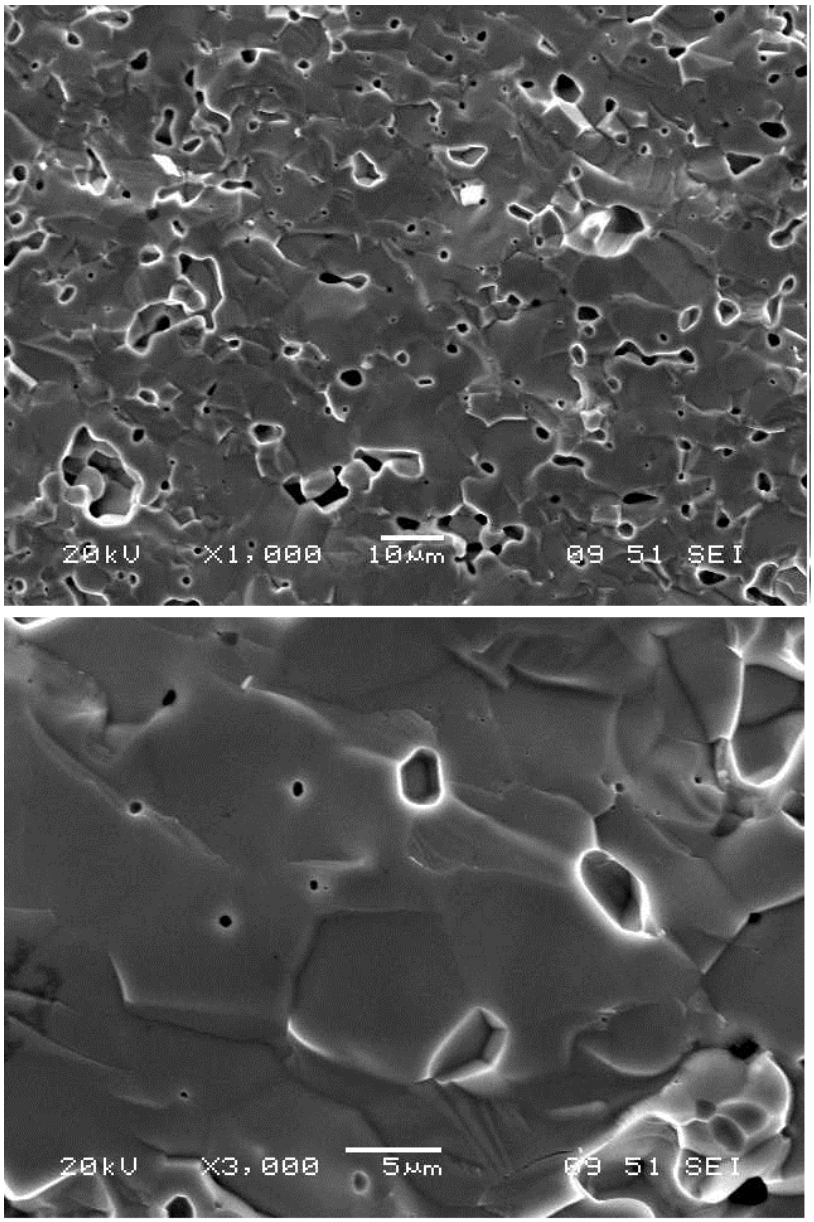

Figure 23: SEM images of the LNO membrane.

4.1.2 Oxygen Permeability Measurement

The oxygen permeability was measured for various ratios of oxygen and nitrogen. The concentration of both the gases was controlled by flow meters and measured by the GC. Helium was used as the sweep gas. A flow rate of 30ml/min was used for helium. The GC produces peaks for oxygen and nitrogen and the area under these peaks is a measure of the oxygen and nitrogen concentrations in the permeate gas. A gas chromatogram is shown as an example in Figure 24. The oxygen permeability of the LNO membrane was measured with different ratios of oxygen and nitrogen in the feed gas. The results are shown in Figure 25. The temperature of the furnace throughout this experiment was 700°C.

It can be seen from Figure 25 that the oxygen permeation flux increased with the concentration of oxygen on the feed side. With 100% oxygen concentration an oxygen permeation flux of 0.151 µmol $cm^{-2}s^{-1}$ (0.23ml min^{-1} cm^{-2}) was obtained. This is the maximum value of flux that could be achieved through this LNO membrane at 700°C. At this stage the oxygen permeation flux was limited by bulk diffusion because the surface was exposed to the maximum amount of oxygen possible. For the cases where the oxygen concentration was lower than 100%, the permeation flux was surface limited as the surface was not fully exposed to oxygen. The interfacial oxygen exchange was the rate determining factor. This is the reason that we obtained an increase in the oxygen flux with the increase in the oxygen concentration at the surface.

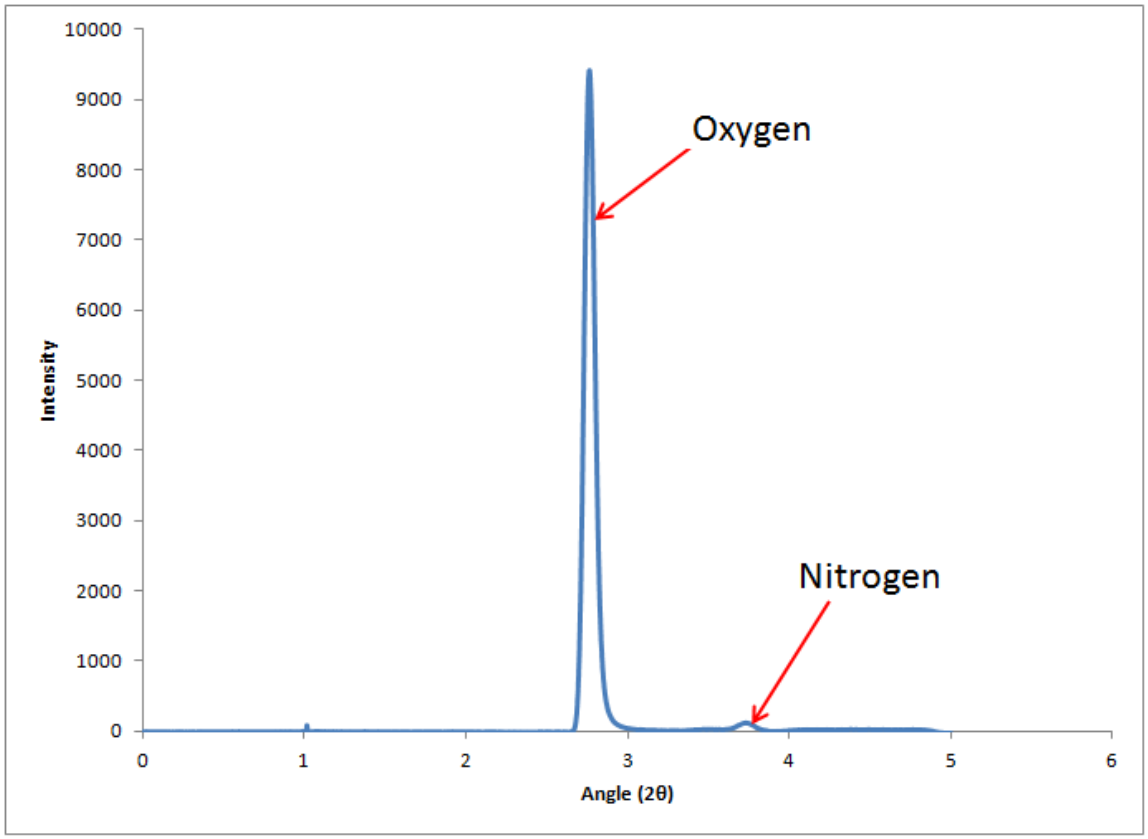

Peak results :

Index	Name	Time [Min]	Quantity [%]	Height [µV]	Area [µV.Min]	Area % [%]
4	Oxygen	2.76	97.74	9414.9	808.6	96.566
6	Nitrogen	3.73	2.26	125.3	18.2	2.178
Total			100.00	9640.6	837.3	100.000

Figure 24: Gas chromatogram obtained for the LNO membrane

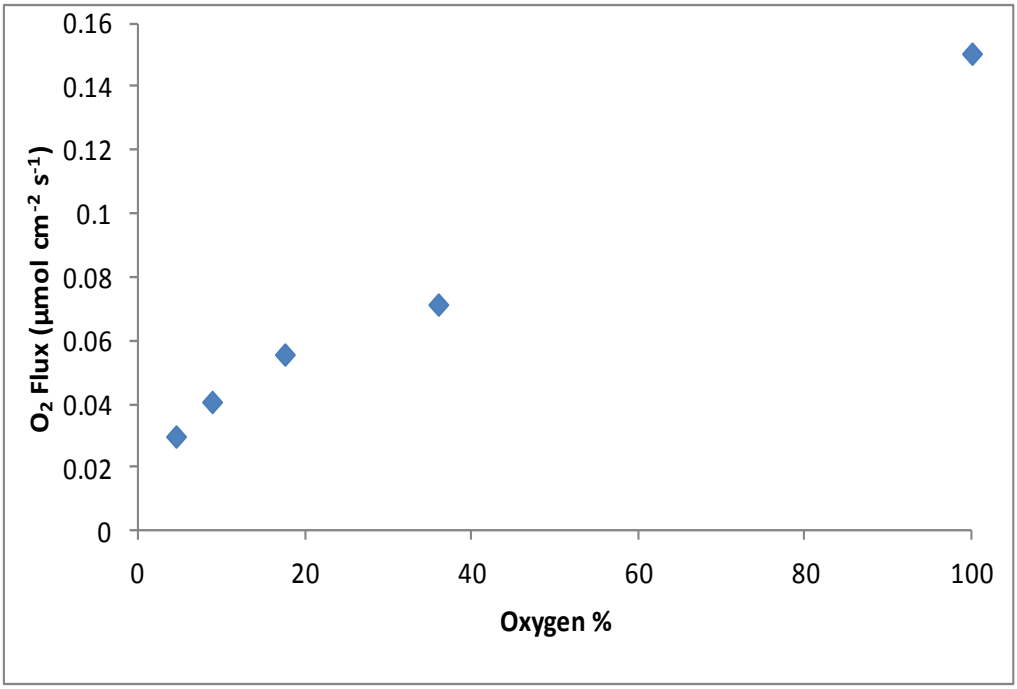

Figure 25: Oxygen permeation flux through a 1mm thick LNO membrane for different oxygen nitrogen mixtures

Another study that was conducted was to measure the oxygen permeability of the LNO membrane with respect to temperature. The temperature test was carried out after keeping the membrane at 700°C for 21 hours so as to stabilize the membrane. The oxygen permeation flux values for different values of temperature are reported in Table 2. Figure 26 shows a logarithmic plot of the permeation flux with respect to temperature.

Table 2: Flux values at different temperatures.

Temperature (°C)	O_2 Flux (ml/min)	O_2 Flux (µmol $cm^{-2}s^{-1}$)
700	0.024	0.031
750	0.037	0.048
800	0.050	0.064

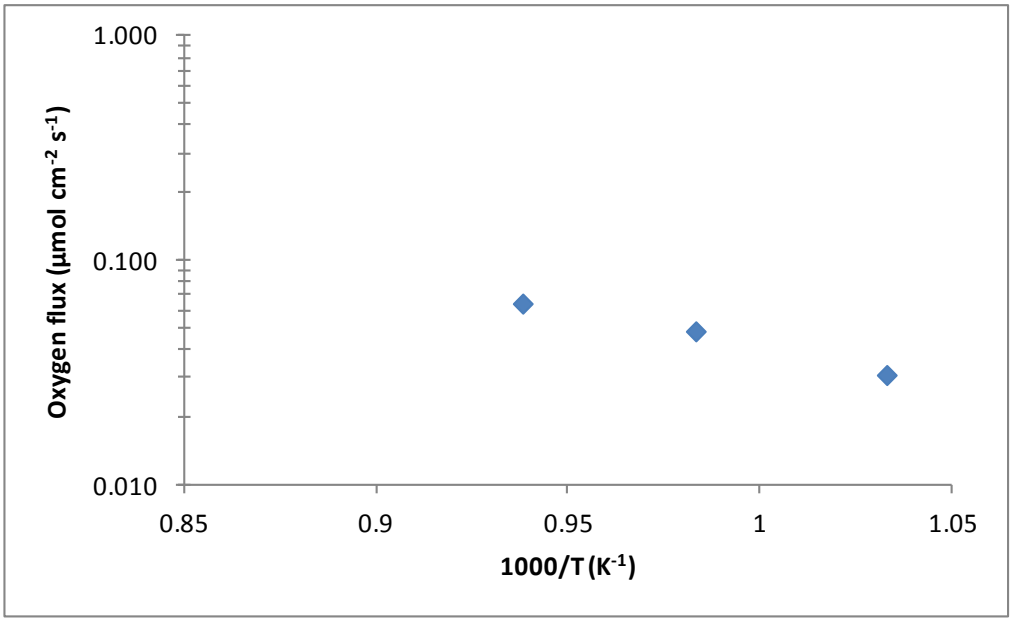

Figure 26: Oxygen permeation flux through a 1mm thick LNO membrane as a function of temperature.

This graph illustrates that with the increase in the temperature of the furnace there is an increase in the oxygen permeation flux. A maximum oxygen flux of 0.064 µmol $cm^{-2}s^{-1}$ (0.099ml min^{-1} cm^{-2}) was obtained at temperature of 800°C. The flux value increased by more than 2 times for a temperature increase of 100°C i.e. from 700°C to 800°C. S.Y. Jeon et. al. [37] observed that the thermally activated oxygen permeation flux increased monotonically with increasing oxygen chemical potential gradient, yielding a maximum of 0.097 µmol $cm^{-2}s^{-1}$ (0.15ml min^{-1} cm^{-2}) for the 0.95mm-thick La_2NiO_4 specimen at 900°C V.V. Vashook et. al.[40] observed a permeability of about 0.7 µmol $cm^{-2}s^{-1}$ (1.08ml min^{-1} cm^{-2}) for an LNO membrane thickness of 1.3mm. S.J. Skinner et. al.[46] concluded that in La_2NiO_4 the oxygen permeation is due to the formation of oxygen interstitials rather than cation vacancies and as such the oxygen diffusivity is higher.

The activation energy was calculated from Figure 12. The approximate value of activation energy was found to be 0.67eV. Jeon et. al. [37] calculated the activation energy for a 0.95mm thick LNO membrane to be 1.2eV. The relatively smaller activation energies were noticed compared to perovskite mixed conductors due to the interstitial mechanism rather than a vacancy mechanism. D.C. Zhu et. al. [38] calculated the activation energy for LNO tubular membranes to be 0.45eV. S.J. Skinner et. al. [46] found this activation energy to be 0.85eV.

4.1.3 Flux Stability with Time

A long term stability test was also performed on the LNO membrane at 700°C so as to analyze the stability of the permeation flux with time. The oxygen permeability of the LNO membrane was measured after every few hours to see the effect of time on the value of the permeation flux of the membrane. The flow rate of air was kept constant at 20ml/min on the feed side whereas the flow rate of helium was kept to be 30ml/min on the permeate side. The complete experiment was carried out for about three days and the temperature of the membrane was maintained at 700°C throughout the experiment. It was observed that there was a sharp decrease in flux at the starting whereas after sometime the value of flux tends to stabilize as shown in Figure 27. The value of flux at the starting was about 0.062 µmol $cm^{-2}s^{-1}$ which decreased to a value of 0.049 µmol $cm^{-2}s^{-1}$ within two hours, thus decreasing by more than 20% in the first two hours of the experiment. However, at the end of the experiment i.e. after almost 70 hours this value decreased by almost 70% to 0.019 µmol $cm^{-2}s^{-1}$.

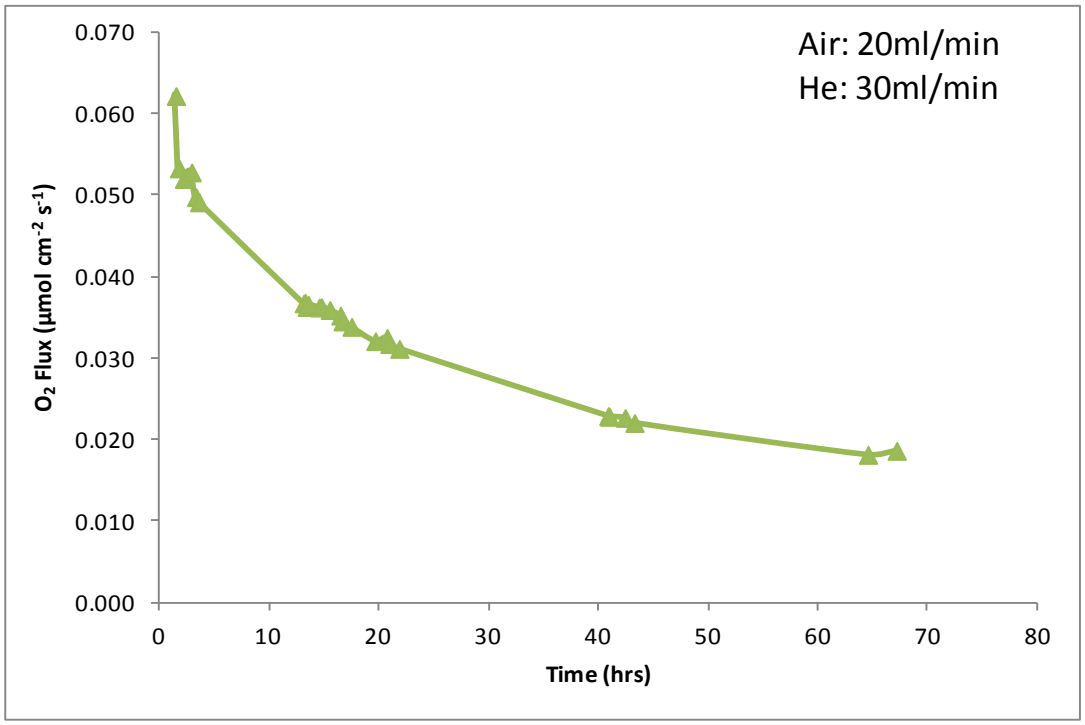

Figure 27: Oxygen Permeability of the LNO membrane with respect to time.

One probable reason could be the wetting or reacting of the membrane surface with glass sealing. With time this glass flows and spreads on the membrane surface and thus it reduces the effective membrane surface area exposed for permeation. This is shown in Figure 28. Hence, we observe a decrease in the permeation as a good portion of the membrane becomes ineffective. Moreover, it is also possible that glass might react with the membrane to form secondary phases. This phenomenon was also observed by other researchers where they observed the formation of these secondary phases [33].

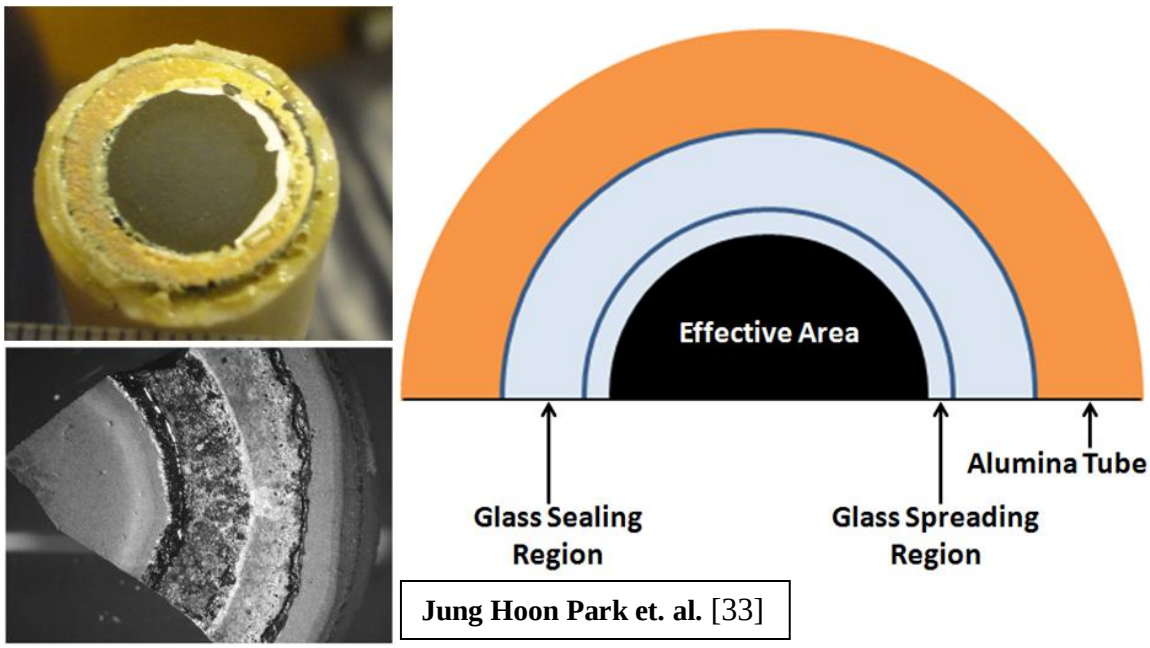

Figure 28: Spreading of glass on the membrane surface.

To further investigate the phenomenon, we did the XRD and EDX analysis of the membrane after the completion of permeation test. The XRD of the membrane (Figure 29) showed that the perovskite structure started disintegrating and also there was development of some secondary phases. The profile EDX analysis of the membrane surface is shown in Figure 30. The analysis was done starting from the edge of the membrane and moving towards the centre of the membrane. It can be clearly seen that the concentration of silicon at the edge of the membrane was quite high. Almost about 40% silicon (glass) concentrations were observed at the edge of the membrane. Silicon was quite abundant on the membrane surface upto about 3 to 3.5mm of the membrane length. Around 3.5mm from the membrane edge the concentration of silicon dropped to about 2 to 3% and then it was found to be constant throughout the membrane surface.

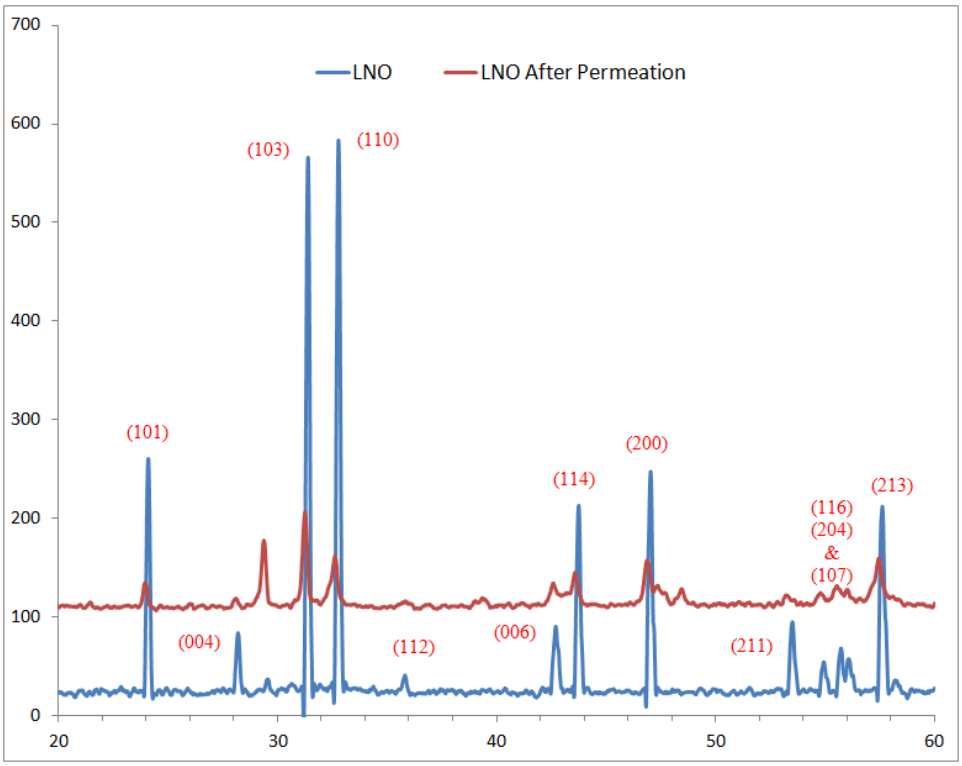

Figure 29: XRD of the LNO membrane after permeation test.

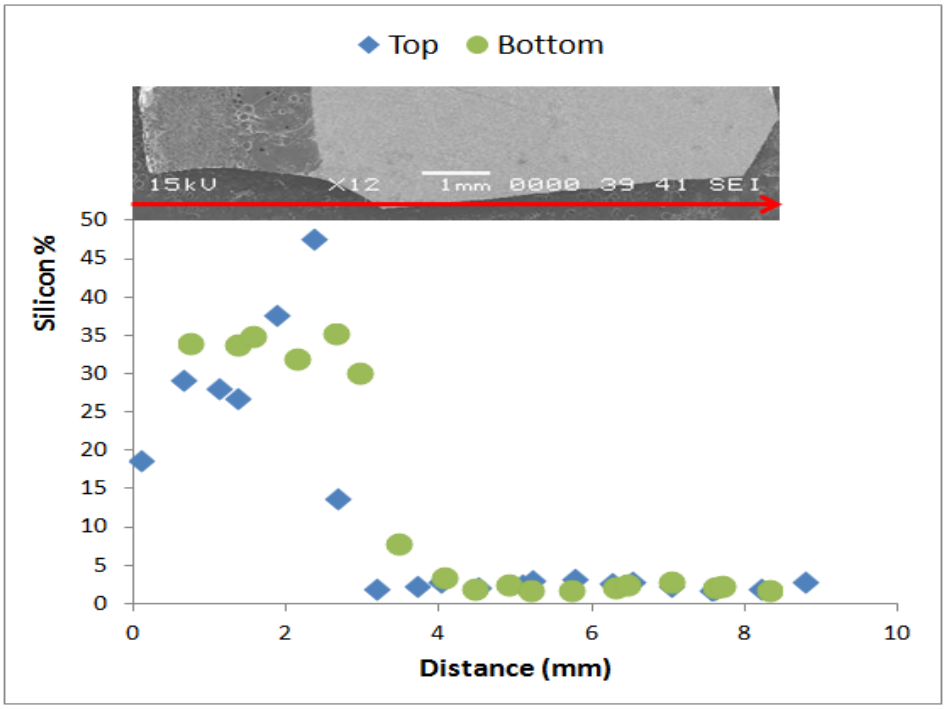

Figure 30: Profile EDX analysis of the surface of LNO membrane after permeation.

So, it is quite evident from the above analysis that the glass sealing is inducing a negative effect on the permeation flux with time. The glass is spreading on the membrane surface with time which can be seen from the presence of silicon throughout the membrane surface. This silicon or glass thus blocks the membrane surface and hence the permeation flux decreases. There is also a possibility of this glass reacting with the membrane and this could be the reason that we observed the formation of secondary phases in the membrane structure.

Another reason that could be attributed to this decrease in the flux can be the fact that the membrane was not completely dense. Although it was dense enough to carry out the permeation test which was confirmed from the fact that we observed very little or almost negligible amount of nitrogen during the oxygen permeability experiment. As far as the reason for this decrease in flux is concerned it could be visualized from Figure 31. The figure shows a diagrammatic representation of the phenomenon that is taking place during the permeation. There is a good amount of possibility that the pores that are present in the membrane are connected to a certain distance through the membrane.

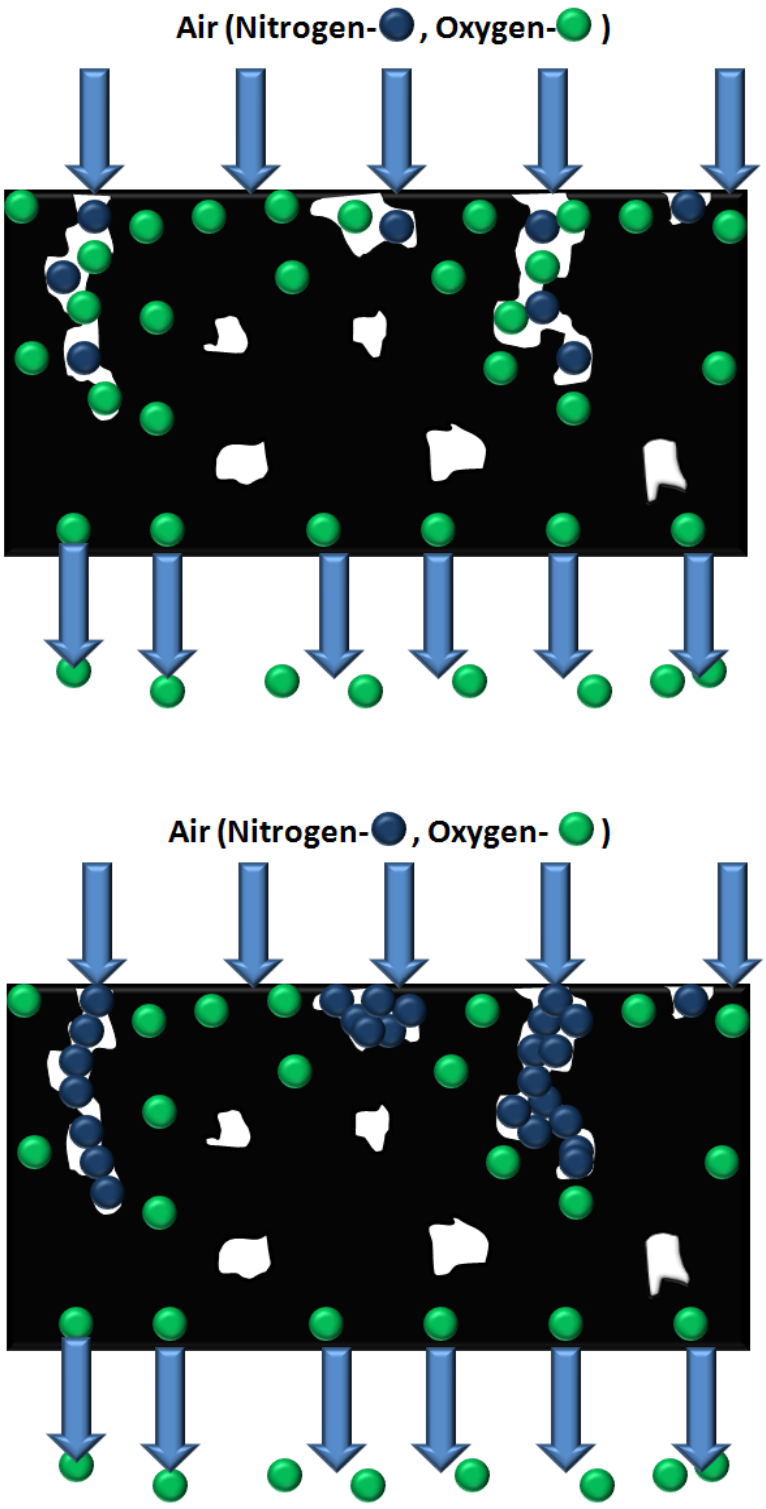

Figure 31: Diagrammatic representation of the phenomenon related to the flux variation with time.

When the air was feed to the membrane both the major constituents of air (oxygen and nitrogen) come in contact with the membrane surface. The area where the membrane is dense it allows only oxygen ions to pass through it. However, if there are some pores on the membrane both the oxygen and nitrogen ions enter that area. The nitrogen ions move until the depth to which the pores are connected and beyond that only oxygen ions move through and finally get to the other side of the membrane (permeate side), whereas the nitrogen ions are trapped inside the pores. This phenomenon keeps on repeating itself until all the pores get filled with the nitrogen ions and there is no place for oxygen ions to enter. So, initially when the pores were not filled completely with nitrogen ions, the oxygen ions can move through the pores and thus have to travel less distance to reach the other side of the membrane i.e. it can be said that the effective thickness of the membrane decreases and this is the reason that we observe a high value of permeation flux at the starting. However, after some time when these pores get accumulated with nitrogen ions, the oxygen ions cannot pass through and thus there is a decrease in the value of flux.

The decrease in the flux with time has also been observed by other researchers. Nebojsa Cebasek et. al. [49] observed a similar behavior of the oxygen flux with time for the LNO membrane as shown in Figure 12. The reason they attributed to this behavior was the formation of a thin blocking layer of La_2O_3 and it is the blocking effect of this layer due to which the oxygen flux decreases initially and then stabilizes. Membranes of other materials like LSCF and SCFZ also showed the same behavior however their stabilizing time was much lower [59].

H. Kruidhof et. al. [50] studied the variation of oxygen permeability with time for perovskite oxides like $SrCo_{0.8}Fe_{0.2}0_3$ (SCF) and $La_{0.6}Sr_{0.4}CoO_3$ (LSC) and observed that this behavior depended very much on the order-disorder transitions or the processes that occur during the ordering of oxygen vacancies in these oxides. They found that at temperatures around 650°C to 750°C the oxygen permeability decreases with time and takes about 30-40 hours for the SCF membrane to attain steady state conditions whereas for the LSC membrane the oxygen permeability keeps on decreasing with time as shown in Figure 13.

4.1.4 Spark Plasma Sintering (SPS) of LNO

We have already observed that the conventional sintering process was not able to give us completely dense membranes. So in order to further increase the density of the membrane we tried with the spark plasma sintering technique. The XRD and SEM of the LNO membrane prepared by SPS are shown in Figure 32 and Figure 33 respectively. The XRD shows that the required K_2NiF_4 structure was not fully developed. The SEM image shows that there are still good amount of pores in the membrane. The permeability of this LNO membrane prepared by SPS is shown in Figure 34. It can be seen that the permeability of the LNO membrane prepared by SPS was quite low as compared to the LNO membrane prepared by conventional sintering method. Also, we observed a large amount of leakage in the system for the LNO SPS membrane.

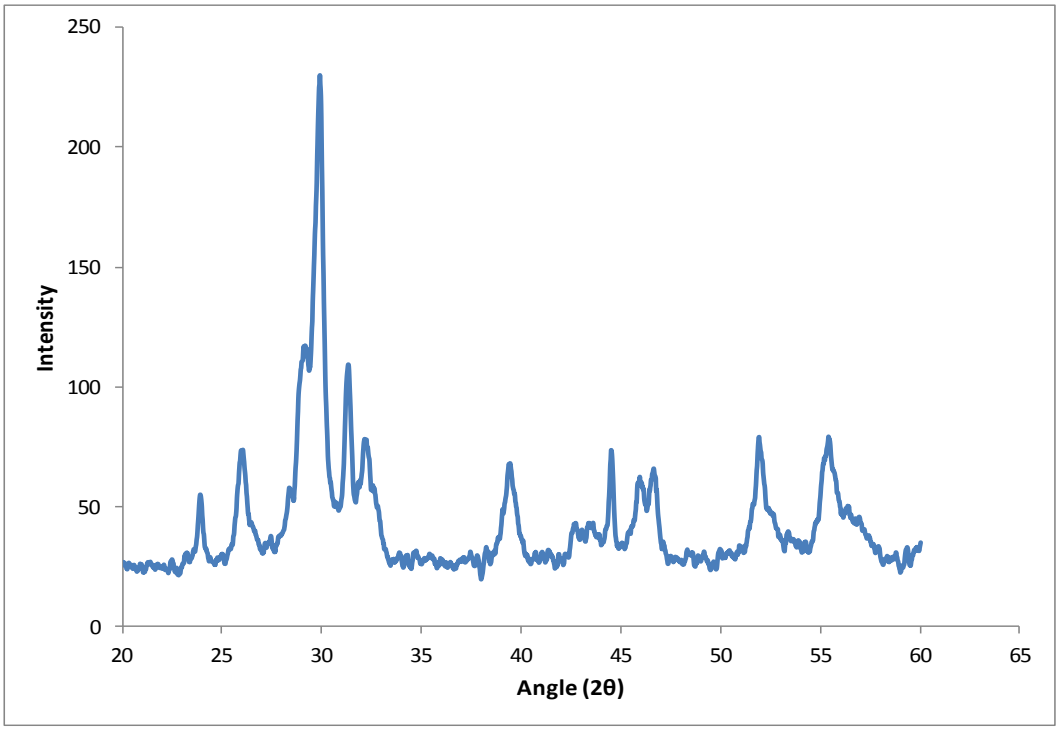

Figure 32: XRD of the LNO membrane prepared by SPS.

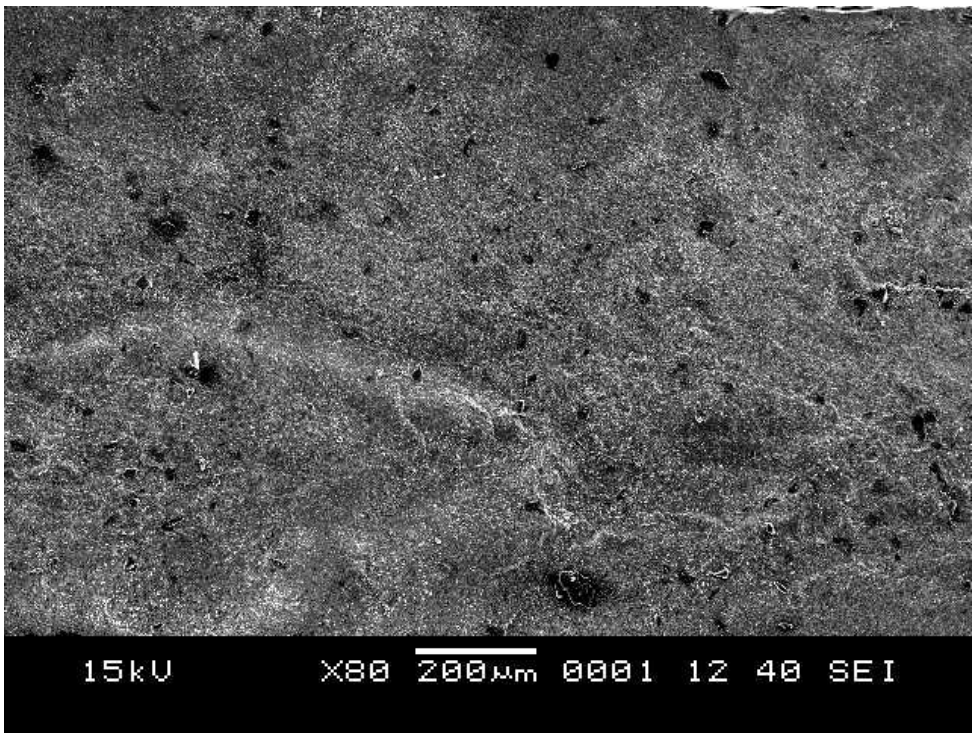

Figure 33: SEM of the LNO membrane prepared by SPS

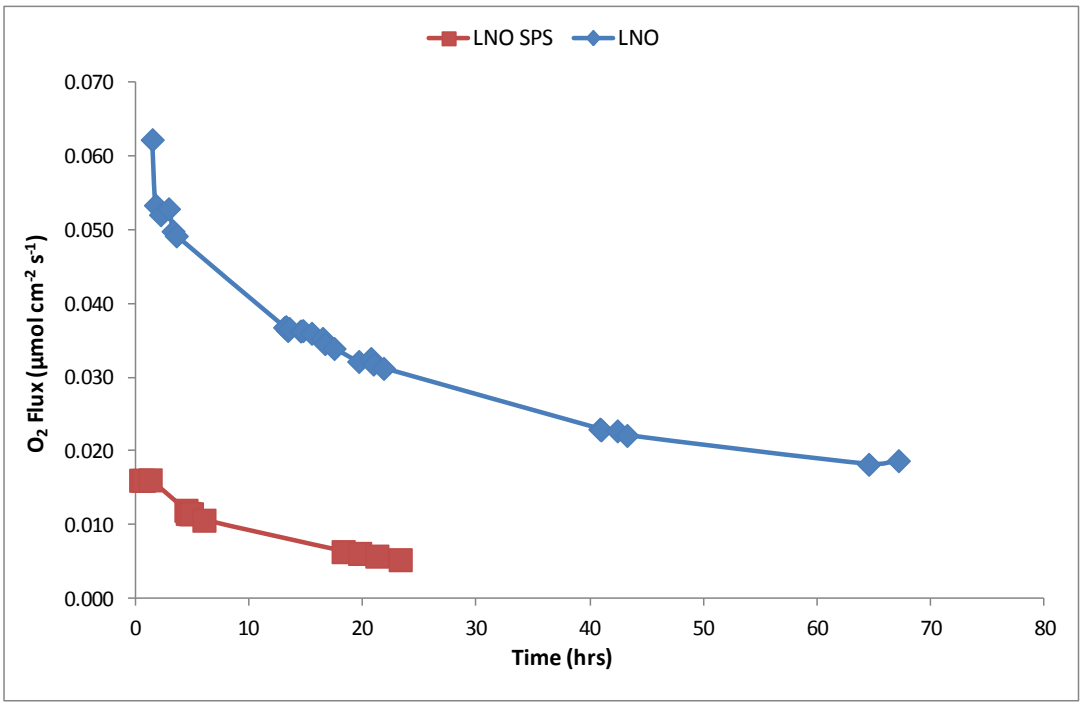

Figure 34: Permeability of the LNO membrane prepared by SPS.

The reason for this type behavior was that the LNO membrane that was prepared by SPS did not have a fully developed K_2NiF_4 structure which can be seen from the XRD analysis. The SPS process is very fast and it does not give enough time for the structure to develop. We know that the structure plays a very important role in these types of membranes, so it is the deficiency of this structure that caused the permeation flux to decrease. C.L. Song et. al. [56] also observed the presence of secondary phases for the $La_{1.75}Ba_{0.25}NiO_4$ ceramics prepared using SPS. They also observed a decrease in the electrical conductivity.

4.2 La_2NiO_4 (LNO) Membrane coated with silver

4.2.1 Oxygen Permeation of the LNO Membrane Coated with Silver Paste

The top surface (the feed side of the membrane) was coated with silver paste in order to enhance the surface activity of the membrane. After coating, the membrane was heated to 300°C to cure the silver paste. The membrane was then tested in the oxygen permeability setup to see the effect of this silver coating on the oxygen permeability of the LNO membrane. The permeation flux of the membrane was measured with respect to time for about 50 hours. The flow rate of air was kept constant at 20ml/min on the feed side whereas the flow rate of helium was kept to be 30ml/min on the permeate side. The temperature was maintained at 700°C. The results are shown in Figure 35. The maximum flux obtained for the LNO membrane was 0.06 µmol $cm^{-2}s^{-1}$ whereas for the LNO membrane coated with silver the maximum flux obtained was around 0.08 µmol $cm^{-2}s^{-1}$, thus showing an increase of about 35% in the flux value. In the region where the flux was relatively stable the value of flux for LNO membrane coated with silver was about 40% higher as compared to the pure LNO membrane.

Hence it could be clearly seen that there was a good amount of improvement in the flux when the LNO membrane was coated with sliver. This increase in flux was due to the reason that the silver coating acted as a catalyst for the reactions occurring on the membrane surface and thus it improved the rate of interfacial oxygen exchange on the feed side. We have already seen from the previous analysis (Figure 25) that the rate of oxygen permeation was surface limited for the LNO membrane for oxygen concentration below 100% on the feed side. So, this porous silver metal layer accelerated the

dissociation of the oxygen molecules into oxygen ions and electrons and thus a larger concentration of the oxygen ions was permeated through the membrane resulting in high values of flux as compared to the uncoated membrane.

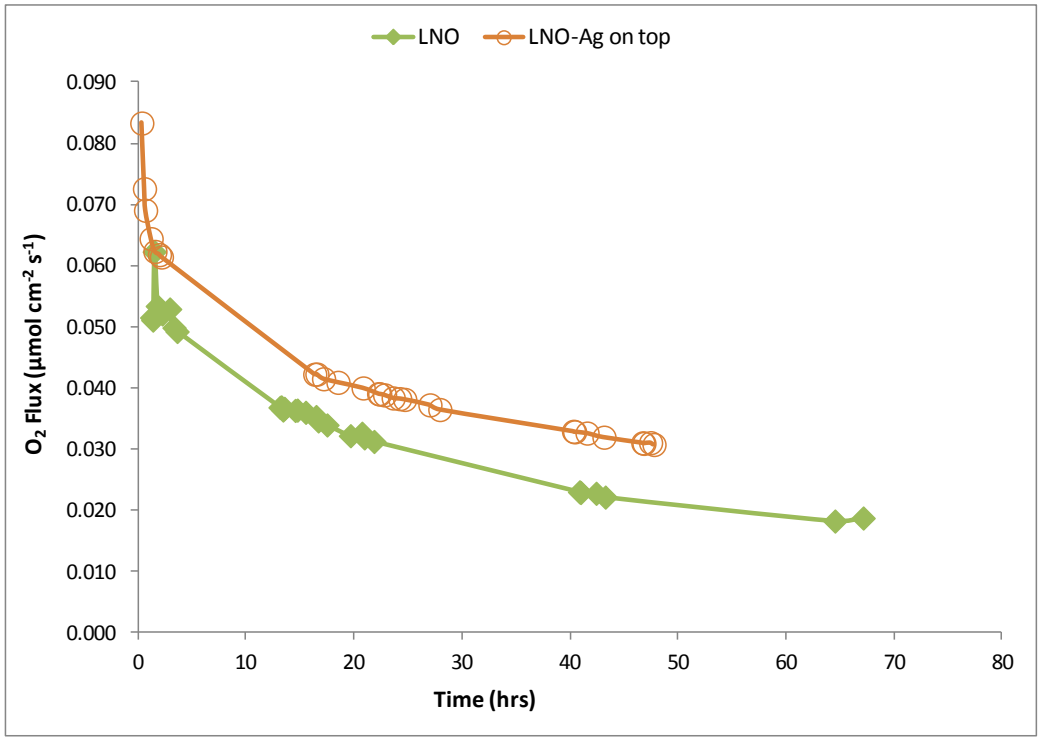

Figure 35: Oxygen permeability of the pure LNO membrane and LNO membrane coated with silver on top [Air: 20ml/min, He: 30ml/min].

Cheng Li et. al. [39] [43] also observed a good amount of increase in the flux when they just coated a thin layer of LNO or $La_2Ni_{0.8}Fe_{0.2}O_{4-\delta}$ on porous alumna substrate. Hashim et. al. [60] made some surface modifications on the LSCF membrane and observed that the oxygen flux of the surface modified LSCF membrane improved by 30 to 60%. Wanqin Jin et. al. [61] also found that the surface modified LSCF membrane exhibited about three to four times as high an oxygen flux as compared to the dense sintered

membrane. So, it can be said that the surface reactions play a vital role in the permeation through these oxygen permeable membranes and thus modifications made to the surface of the membrane contribute significantly to the oxygen permeation flux.

As already discussed in the previous section that there are two types of surface reactions that occur on the feed side and the permeate side of the oxygen permeable membranes. Oxygen dissociation i.e. the dissociation of oxygen molecules into oxygen ions and electrons occurs at the feed side whereas oxygen association i.e. the combination of these oxygen ions and electrons to form oxygen molecules occurs at the permeate side. We have already seen from the above results that the coating of silver on the feed side favored the oxygen dissociation reaction and thus increased permeation. So, in an effort to further enhance the permeation we coated the membrane with silver paste on both sides. The membrane was then tested for oxygen permeability. The experimental conditions were kept the same as in the previous experiment. The oxygen permeability of the LNO membrane coated with silver paste on both sides is shown in Figure 36.

It was observed that there was no change in the oxygen permeation flux of the membrane coated with silver paste on both sides as compared to the membrane coated with silver on the feed side only. The curve for this membrane followed the same path as the curve for the membrane coated with silver on the top. The reason for this kind of behavior could be that although the porous silver layer favored the oxygen dissociation reaction on the feed side, it did not have any effect on the oxygen association reaction occurring on the permeate side.

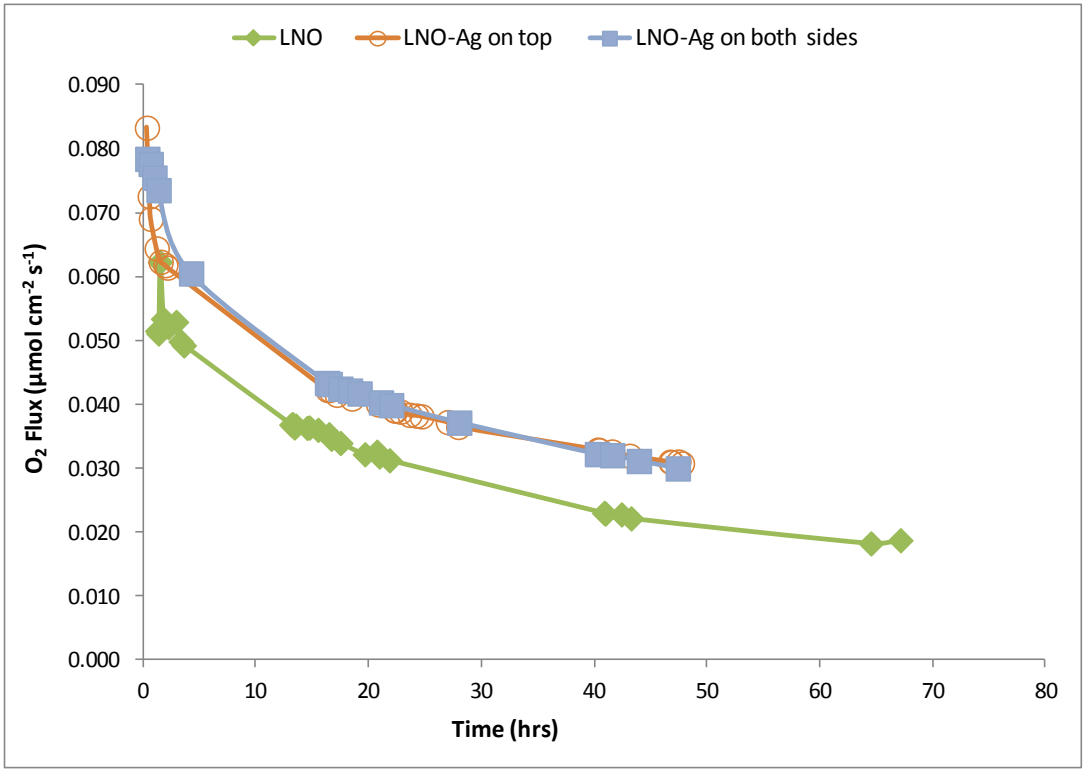

Figure 36: Oxygen permeability of the pure LNO membrane, LNO membrane coated with silver on top and LNO membrane coated with silver on both sides [Air: 20ml/min, He: 30ml/min].

4.2.2 Oxygen Permeation of the LNO Membrane Coated with Silver using an Ion Sputtering Machine

In the previous section silver layer on the LNO membrane was produced by coating the membrane with the silver paste whereas in this case an ion sputtering machine with a silver target was used to coat the membrane with silver. The advantage here was that we could obtain a dense, more uniform layer through this process and also the thickness of the coating could be easily controlled. A silver layer of different thicknesses like 10nm,

20nm and 200nm were coated on the feed side of the LNO membrane. These membranes were then tested for oxygen permeability with respect to time.

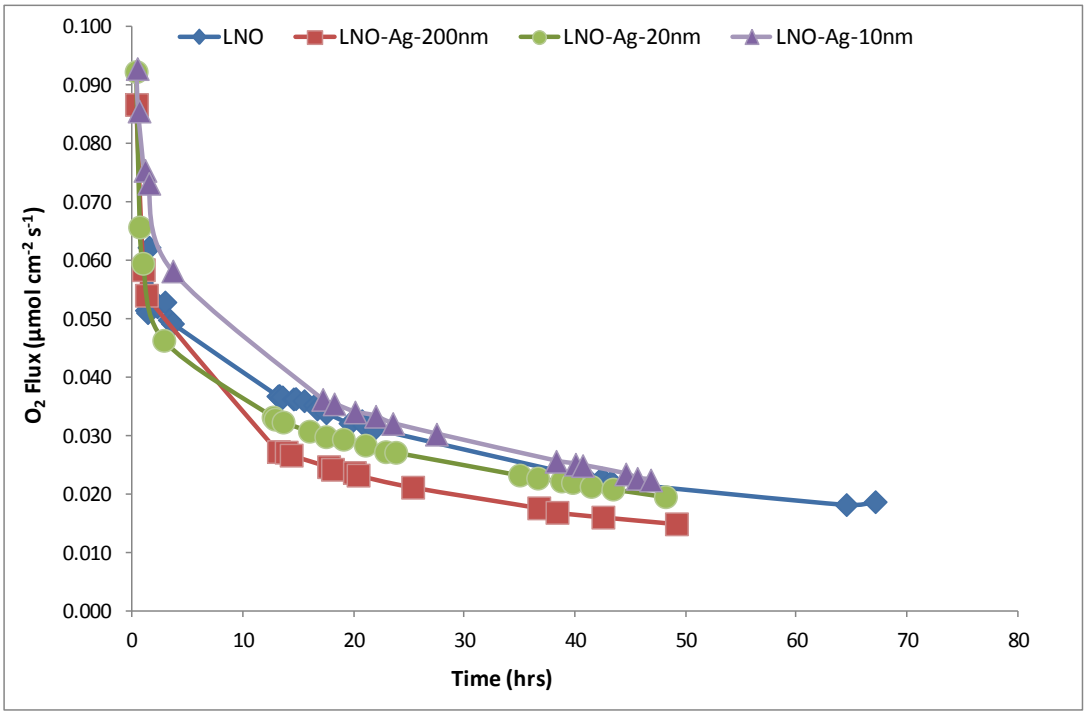

Figure 37: Oxygen permeability of the LNO membranes coated with silver layer of different thicknesses [Air: 20ml/min, He: 30ml/min].

From Figure 37 it can be seen that the oxygen permeation flux for the LNO membranes sputtered with silver decreased as compared to the pure LNO membrane. The LNO membrane coated with a silver layer of thickness 200nm showed a decrease of about 28% in the permeation flux. However, this decrease in the flux values became less as the thickness of the silver coating decreased. The membrane coated with a silver layer of 10nm showed almost the same flux as the pure LNO membrane.

These results were in contradiction with our previous findings where the silver layer was acting as an activation layer at the surface, thus enhancing the permeation. So, in order to investigate this behavior we did the SEM analysis of the membrane surface after the permeation test. From the SEM images of the membrane surface shown in Figure 38 we can see a uniform distribution of some particles of the size of about 10µm on the membrane surface. In order to check the composition of these particles we performed the EDX analysis and found that these particles were of silver. The EDX analysis for these particles is shown in Figure 39. This could explain the decrease in the permeation flux. The silver coating that was done using silver paste was porous whereas the silver coating done with the ion sputtering machine was quite dense, so at high temperature this dense silver layer broke into small particles of silver metal distributed all over the membrane. The particle size was around 10µm which was large enough to block the oxygen from reaching the membrane surface. These particles covered a large area of the membrane surface and therefore the effective surface area of the membrane for permeation was reduced. As a result there was decrease in the flux. As the thickness of the coating reduced the particle size also decreased covering less area and thus there was less decrease in the flux values.

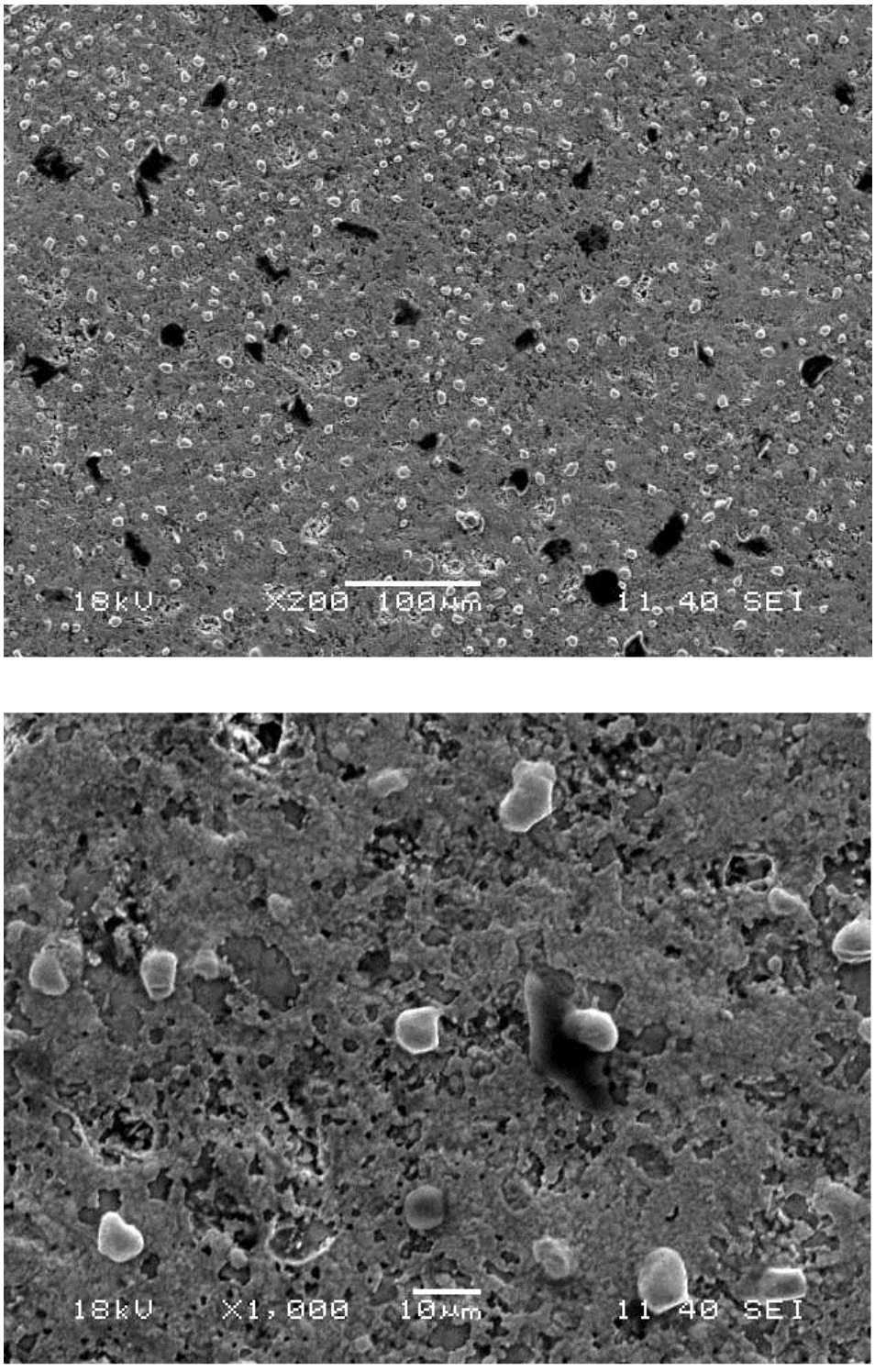

Figure 38: SEM analysis of the LNO membrane coated with 200nm thick silver layer

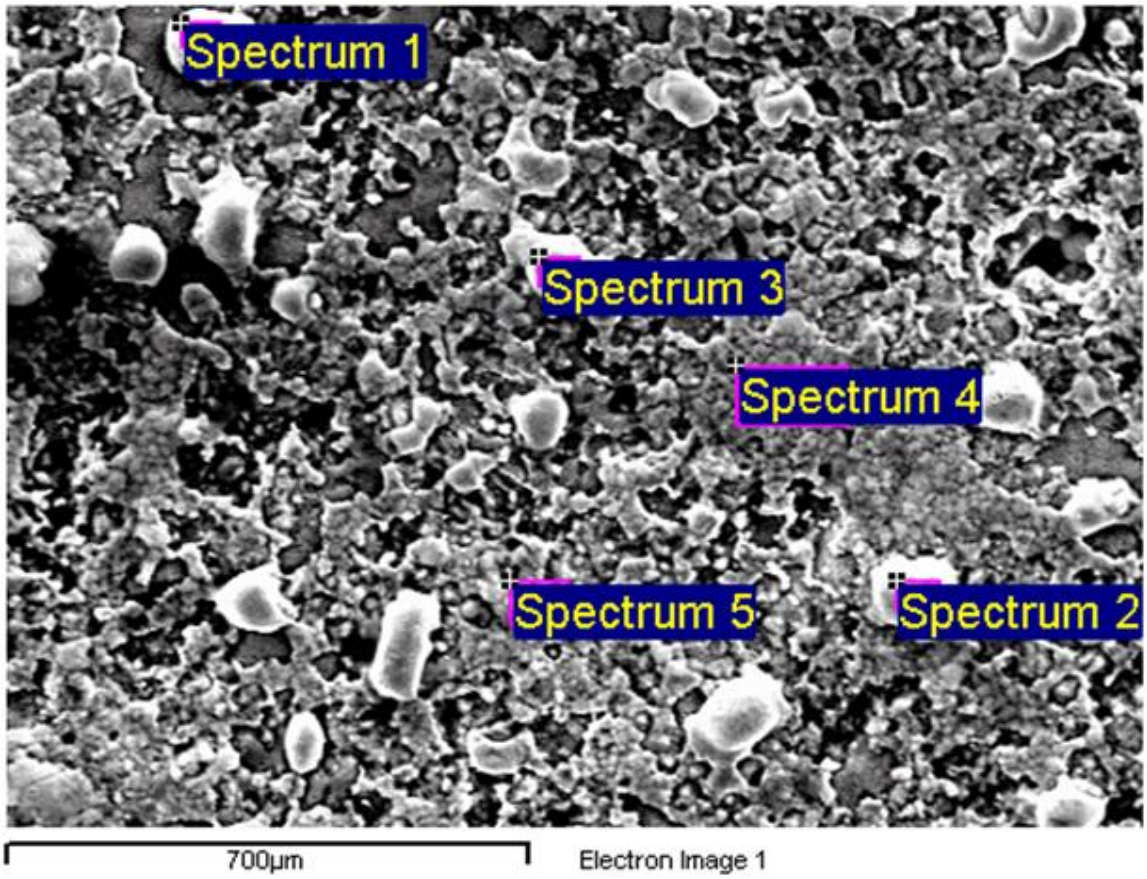

Spectrum	O	Ni	Ag	La	Total
Spectrum 1	0.00	0.00	99.14	0.86	100.00
Spectrum 2	0.00	0.00	99.20	0.80	100.00
Spectrum 3	0.00	0.00	100.00	0.00	100.00
Spectrum 4	0.00	3.46	91.22	5.32	100.00
Spectrum 5	27.60	1.69	67.22	3.49	100.00

Figure 39: EDX analysis of the particles on the membrane surface

4.3 Doping of the La_2NiO_4 (LNO) Membrane

4.3.1 LNO Membrane doped with 20% iron ($La_2Ni_{0.8}Fe_{0.2}O_4$)

The $La_2Ni_{0.8}Fe_{0.2}O_4$ (LNF) powder was also prepared using the sol-gel method and the membrane was prepared under the same conditions as the LNO membrane. The membrane was tested for oxygen permeability and the results of the experiment are shown in Figure 40.

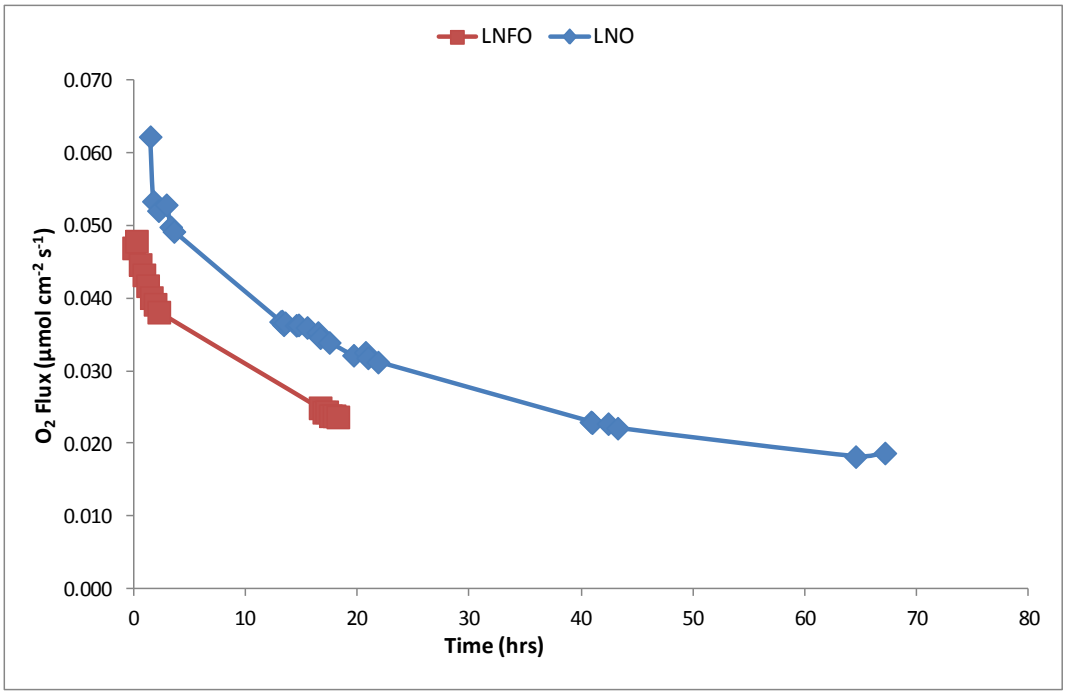

Figure 40: Oxygen permeability of the $La_2Ni_{0.8}Fe_{0.2}O_4$ membrane [Air: 20ml/min, He: 30ml/min].

It was observed that there was a decrease of about 25% in the permeation flux of the membrane with the incorporation of iron. Cheng Li et. al. [39] prepared some dense supported membranes of $La_2Ni_{0.8}Fe_{0.2}O_4$ and La_2NiO_4 and observed an increase of about

3 to 4 times in the flux for the $La_2Ni_{0.8}Fe_{0.2}O_4$ supported membranes. This shows that the doping of LNO with iron enhanced the surface activity of the membrane. However, from our results we found that doping of iron decreased the permeability. Hence, it can be said that iron does not contribute to the bulk diffusion of the oxygen ions. Klande et. al. [48] also observed a lower value of permeation flux for the $La_2Ni_{0.9}Fe_{0.1}O_4$ membrane as compared to the LNO membrane. Kharton et.al. [62] found that the incorporation of iron promoted hole localization and decreased conductivity. Tsipis et. al. [63] stated that the doping of iron for nickel increased the oxygen ion mobility only at temperatures above 900°C.

4.3.2 Doping of the LNO Membrane with cobalt

La_2NiO_4 was doped with different concentrations of cobalt to form the $La_2Ni_{1-x}Co_xO_4$ (x= 0.05, 0.1, 0.2, 0.25, 0.3, 0.5, 0.8) perovskite powders. The $La_2Ni_{1-x}Co_xO_4$ membranes were prepared under the same conditions as the LNO membrane. The XRD and the SEM analysis were conducted to see the structure development of the membranes. The EDX analysis was also performed to confirm the stoichiometric distribution of elements in the membrane. The SEM and EDX analysis of the $La_2Ni_{0.75}Co_{0.25}O_4$ membrane are shown as an example in Figure 41 and Figure 42 respectively. The SEM images showed the development of a dense structure sufficient enough for doing the permeation test while the EDX analysis confirmed the homogeneous distribution of the elements. The grain size of the $La_2Ni_{0.75}Co_{0.25}O_4$ membrane was large as compared to that of LNO membrane.

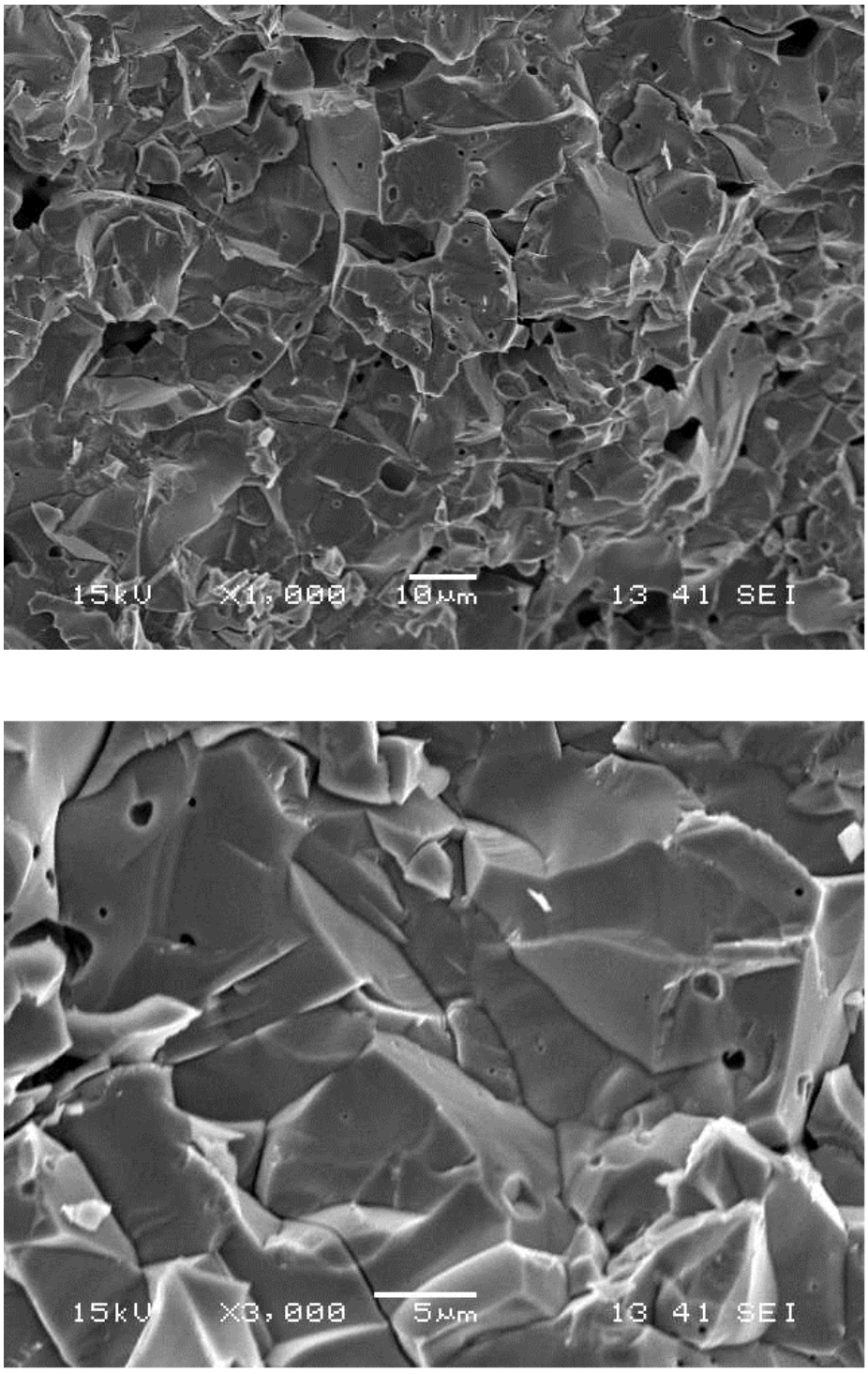

Figure 41: SEM images of the $La_2Ni_{0.75}Co_{0.25}O_4$ membrane

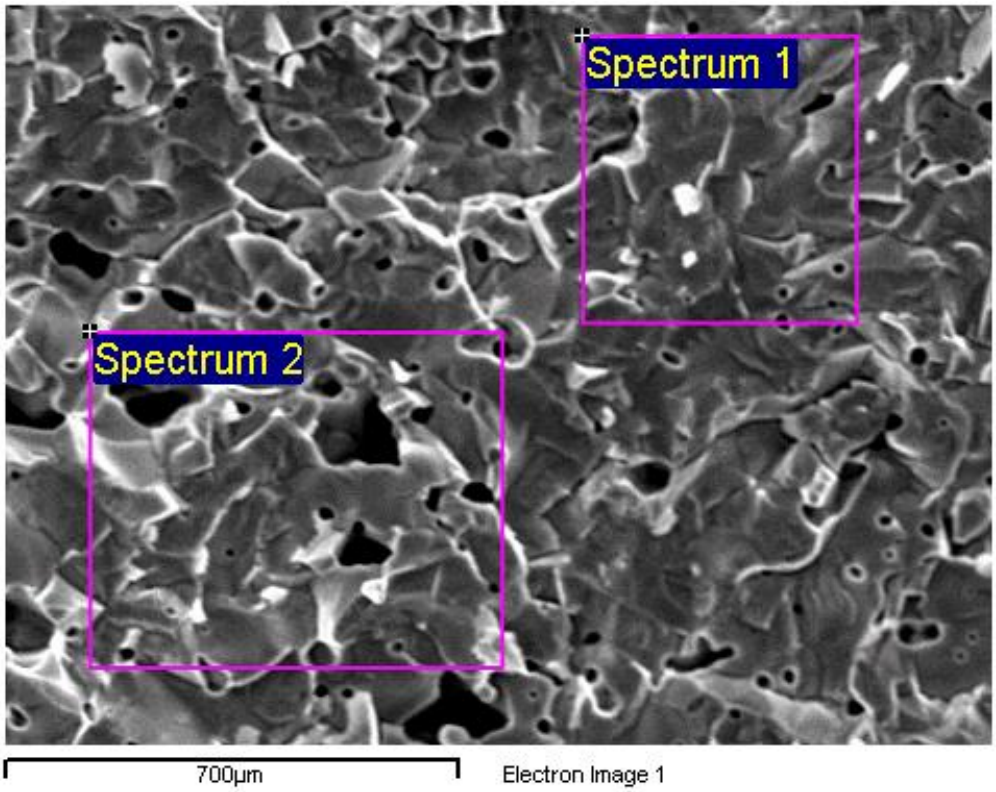

Spectrum	O	Co	Ni	La	Total
Spectrum 1	48.78	4.51	12.67	34.04	100.00
Spectrum 2	46.42	3.93	12.92	36.73	100.00
Mean	47.60	4.22	12.80	35.39	100.00
Std. deviation	1.67	0.41	0.18	1.90	
Max.	48.78	4.51	12.92	36.73	
Min.	46.42	3.93	12.67	34.04	

Figure 42: EDX analysis of the $La_2Ni_{0.75}Co_{0.25}O_4$ membrane

After the characterization the oxygen permeability for each of these membranes was tested. The permeation test was done with respect to time and the experimental conditions were kept the same as before. The combined experimental results for all the cobalt doped membranes are shown in Figure 43.

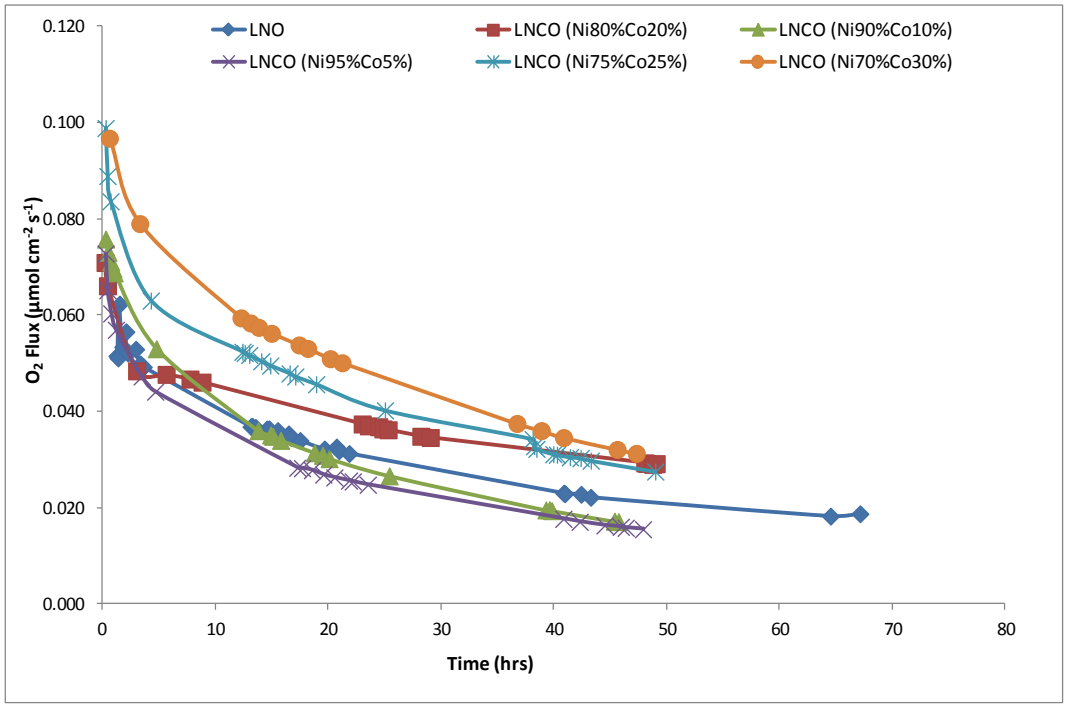

Figure 43: Oxygen permeability of the $La_2Ni_{1-x}Co_xO_4$ (x=0, 0.05, 0.1, 0.2, 0.25, 0.3) membranes [Air: 20ml/min, He: 30ml/min].

It can be seen from Figure 43 that there was not much effect on the flux for 5% or 10% substitution of cobalt. Infact, a slight decrease in the flux was observed after 10 to 15 hours of starting the test. For the membrane doped with 20% cobalt ($La_2Ni_{0.80}Co_{0.20}O_4$), we found an increase of about 25% in the flux values. The permeation flux was further enhanced by increasing the cobalt concentration to 25% and 30%. For the

$La_2Ni_{0.75}Co_{0.25}O_4$ membrane and the $La_2Ni_{0.70}Co_{0.30}O_4$ membrane the maximum value of flux obtained was about 0.1 µmol $cm^{-2}s^{-1}$. In the region where the flux was relatively stable (almost after 20hours) we achieved a value of 0.051 µmol $cm^{-2}s^{-1}$ for the $La_2Ni_{0.70}Co_{0.30}O_4$ membrane which was about 1.5 times higher than the flux for LNO membrane around the same time. As the concentration of cobalt was further increased we found that there was a good amount of leakage in the system i.e. we also obtained good quantities of nitrogen along with oxygen. This is why the oxygen permeability graphs for $La_2Ni_{0.5}Co_{0.5}O_4$ and $La_2Ni_{0.2}Co_{0.8}O_4$ were not reported here.

So, we can say that the incorporation of cobalt in the La_2NiO_4 structure has increased the oxygen permeability of the membrane upto certain limit and after that with further incorporation of cobalt the permeation decreased and the leakage increased. The increase in the leakage observed in the GC with the increase of cobalt concentration is shown in Figure 44. The reason could be understood from the XRD analysis of the membranes shown in Figure 45. It can be seen from the XRD's of the membranes that with the increase in the cobalt concentration the K_2NiF_4 structure is getting reduced. For the $La_2Ni_{0.2}Co_{0.8}O_4$ membrane the K_2NiF_4 structure is almost lost. We know that it is this structure that is responsible for the selective permeation of the oxygen ions and since this structure is lost, so the permeation is also reduced.

Similar findings were obtained by P. Haworth et. al. [26] when they substituted yttrium in place of iron in BSCF-5582. They observed that there was improvement in the oxygen permeability only upto a certain concentration of yttrium. Beyond this concentration the XRD of the membrane showed the disappearance of the perovskite structure. In another study, Tatsumi Ishihara et. al. [64] tried to improve the conductivity of oxide ions of

$La_{0.8}Sr_{0.2}Ga_{0.8}Mg_{0.2}O_3$ (LSGM) perovskites membranes by doping it with certain transition metals like Fe, Co, Ni, Cu, Mn. Among all the transition metal elements doped they found that cobalt is the most effective for increasing the electrical conductivity.

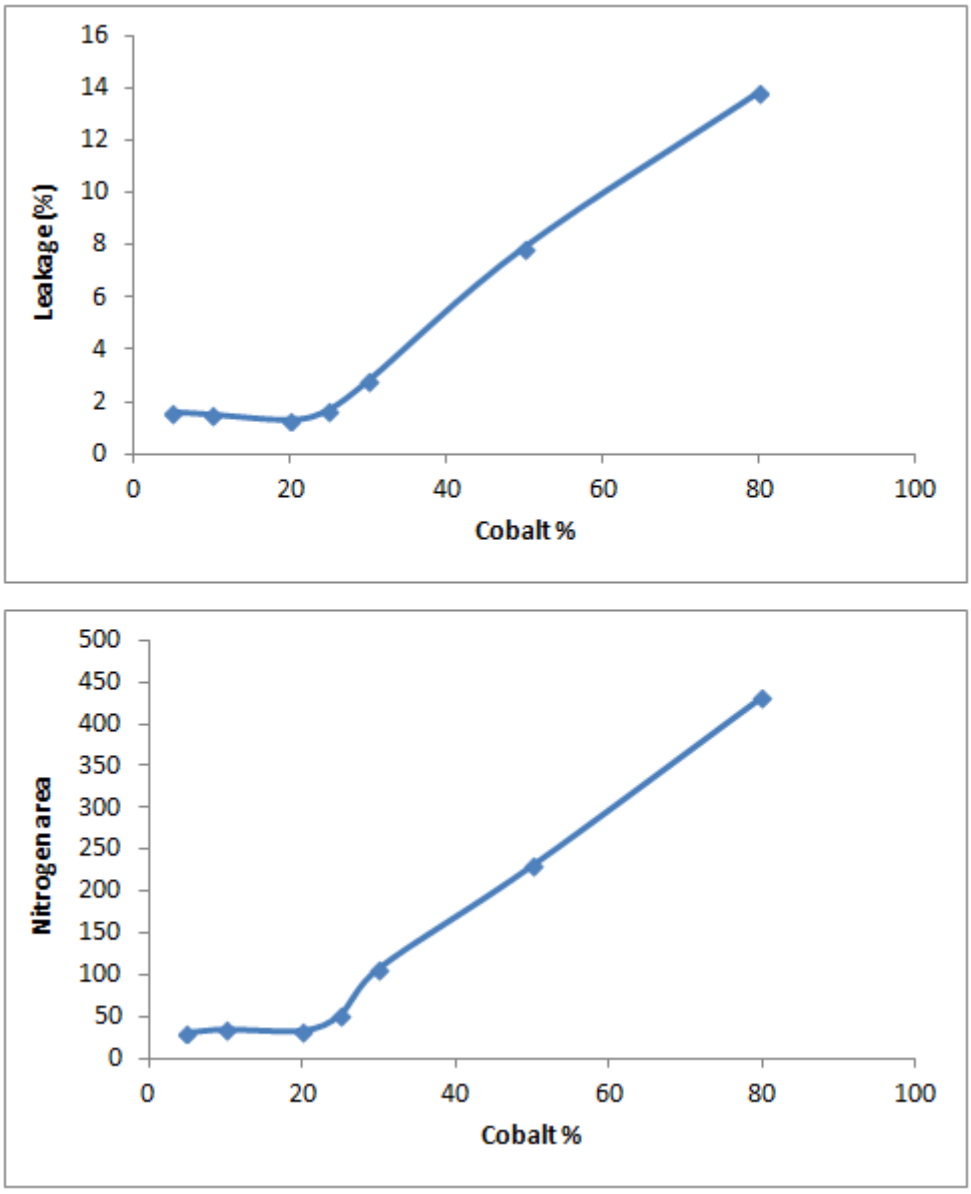

Figure 44: Leakage observed in the GC with respect to cobalt concentration

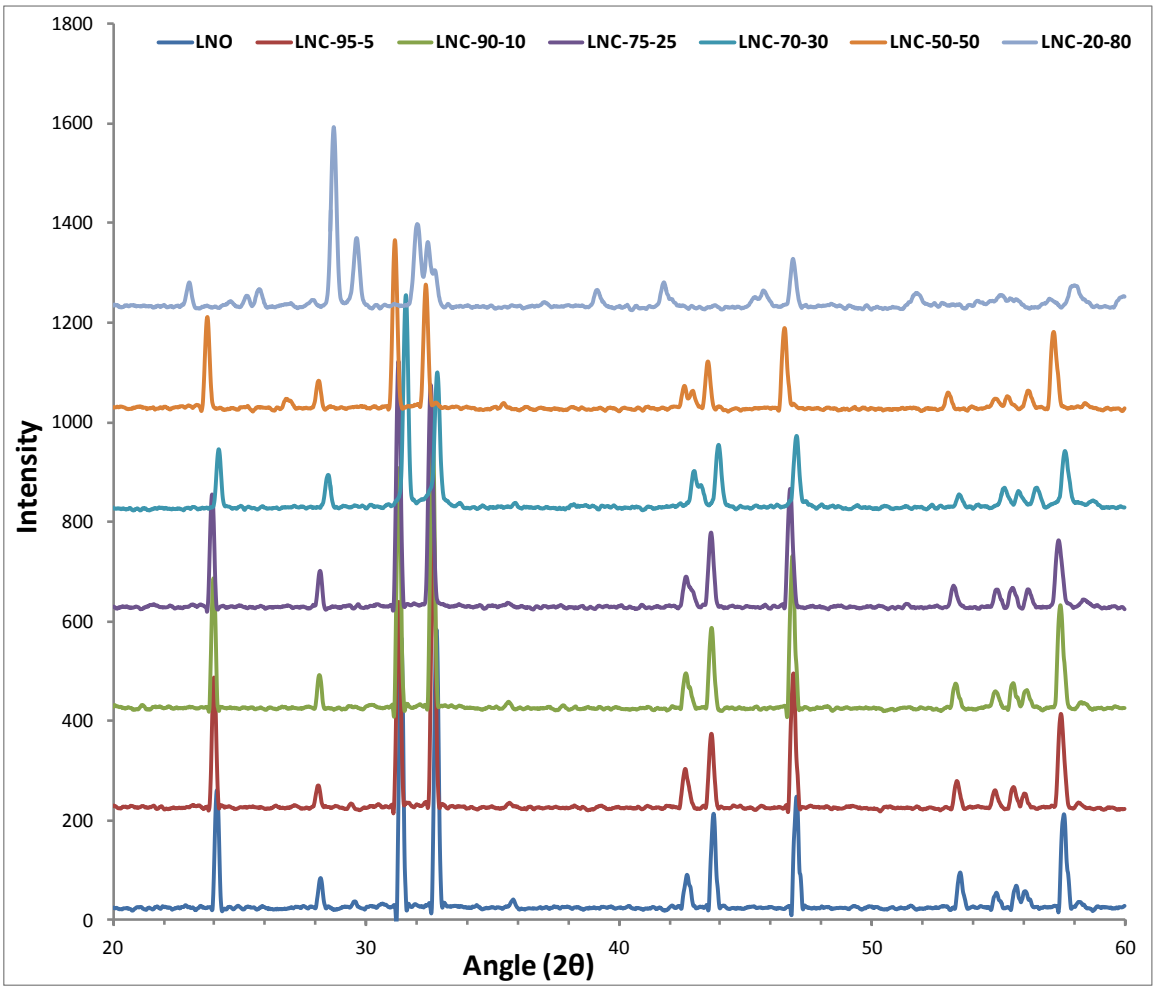

Figure 45: XRD analysis of the $La_2Ni_{1-x}Co_xO_4$ membranes

The $La_2Ni_{0.80}Co_{0.20}O_4$ membrane was coated with porous silver paste to see that whether this silver layer is also acting as a catalyst for the $La_2Ni_{0.80}Co_{0.20}O_4$ membrane. The permeation results are shown in Figure 46.

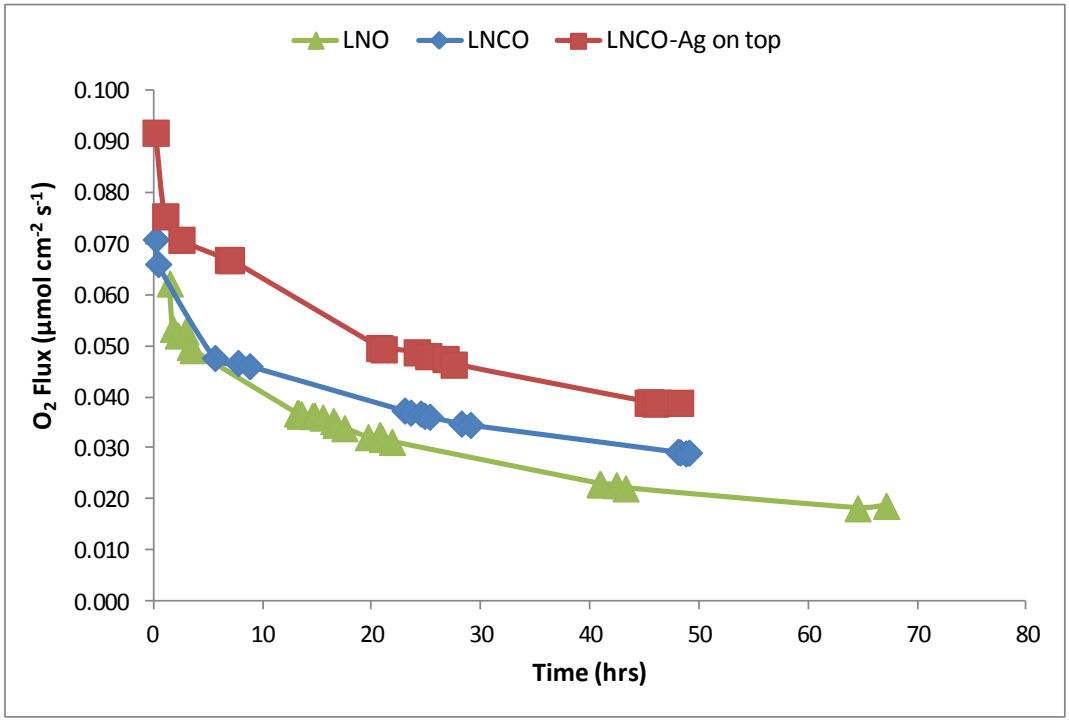

Figure 46: Oxygen Permeability of the $La_2Ni_{0.8}Co_{0.2}O_4$ membrane coated with silver paste [Air: 20ml/min, He: 30ml/min].

It was observed that the silver coating also enhanced the surface reactions for the $La_2Ni_{0.80}Co_{0.20}O_4$ membrane. An increase of about 30% in the permeation flux was observed as compared to the pure $La_2Ni_{0.80}Co_{0.20}O_4$ membrane, whereas as compared to the LNO membrane this increase was about 50%. So, it can be seen that the cobalt incorporation improves the bulk diffusion in the membrane whereas the silver coating enhances the surface reactions.

CHAPTER 5

CONCLUSIONS

La_2NiO_4 membranes were prepared via sol gel process and the oxygen permeability of these membranes was studied. The desired K_2NiF_4 structure was obtained for the membranes. A good sealing was obtained as the leakage for almost all experiments was less than 2%.

5.1 Pure La_2NiO_4 (LNO) Membrane

Three types of oxygen permeability measurements were carried out on the LNO membrane. In the first case the oxygen permeability of the LNO membrane was measured with different ratios of oxygen and nitrogen in the feed gas and the results showed that the oxygen permeation flux was linearly proportional to the oxygen concentration on the feed side. The permeation flux for the LNO membrane was found to be surface limited. In the second case the oxygen permeability of the LNO membrane was measured with respect to temperature and it was observed that the permeability increased with rise in temperature. A maximum oxygen flux of 0.064 µmol $cm^{-2}s^{-1}$ (0.099ml min^{-1} cm^{-2}) was obtained at temperature of 800°C. The flux value increased by more than 2 times for a temperature increase of 100°C i.e. from 700°C to 800°C. The activation energy for the LNO membrane was found to be 0.67eV. For the third case a long term stability test was performed on the LNO membrane at 700°C so as to analyze the stability of the permeation flux with time. It was observed that the flux decreased

sharply at the starting and after sometime it stabilized. The value of flux decreased from 0.062 µmol $cm^{-2}s^{-1}$ at the starting to 0.019 µmol $cm^{-2}s^{-1}$ after 70 hours i.e. a decrease of almost 70%. The main reason for this decrease was found to be the spreading of the glass sealing on the membrane which made a good portion of the membrane ineffective by blocking the membrane surface. The LNO membrane prepared by SPS showed a decrease in the permeation value as the desired K_2NiF_4 structure was not obtained after SPS. So, it can be said that SPS is not a suitable technique for these types of membranes.

5.2 La_2NiO_4 (LNO) Membrane coated with silver

The LNO membrane was coated with silver on the feed side. The silver coating was done in two ways: (a) by coating the membrane with silver paste and (b) by using an ion sputter machine with a silver target. For the LNO membrane coated with silver paste on the feed side, the maximum flux obtained was around 0.08 µmol $cm^{-2}s^{-1}$. An increase of about 35% to 40% in the flux values was observed for the silver coated LNO membrane as compared to the pure LNO membrane. So, it can be said that the silver acted as a catalyst for the reactions occurring on the membrane surface and thus it is improving the rate of interfacial oxygen exchange on the feed side. Since, the rate of oxygen transfer for the LNO membrane was surface limited so it can be said that this increase in the flux value was mainly due to the improvement in the interfacial oxygen exchange. However, coating the membrane with silver paste on both sides did not show any further improvement in the value of permeation flux. The silver coating did not improve the oxygen exchange on the permeate side. In case of the membranes coated with silver by using an ion sputtering instrument a decrease in the flux value was observed as compared

to the pure LNO membrane. The flux value decreased further with increase in the thickness of the silver coating. This was because at high temperature this dense silver coating disintegrated into small particles of silver distributed all over the membrane which reduced the effective surface area of the membrane exposed for permeation.

5.3 Doping of the La_2NiO_4 (LNO) Membrane

The LNO membrane was doped with 20% iron to form the $La_2Ni_{0.8}Fe_{0.2}O_4$ membrane and a decrease of about 25% in the permeation flux was observed for this membrane as compared to the pure LNO membrane.

La_2NiO_4 was also doped with different concentrations of cobalt to form the $La_2Ni_{1-x}Co_xO_4$ (x= 0.05, 0.1, 0.2, 0.25, 0.3, 0.5, 0.8) membranes. The XRD analysis showed the development of the required K_2NiF_4 structure. For the membrane doped with 20% cobalt ($La_2Ni_{0.80}Co_{0.20}O_4$), we found an increase of about 25% in the flux values. The permeation flux was further enhanced by increasing the cobalt concentration to 25% and 30%. For the $La_2Ni_{0.75}Co_{0.25}O_4$ membrane and the $La_2Ni_{0.70}Co_{0.30}O_4$ membrane the maximum value of flux obtained was about 0.1 μmol $cm^{-2}s^{-1}$. An increase in the leakage was observed with further increase in the cobalt content. So, it can be said that the optimum quantity of cobalt which gives the maximum value of flux is around 30% as beyond this concentration there was decrease in the permeation flux and a good amount of leakage was also observed.

CHAPTER 6

FUTURE WORK

The future work includes the following:

1. The membrane that we obtained was not completely dense. So, in order to obtain a fully dense membrane other processes like Hot Isostatic Pressing (HIP) can be considered for future work. HIP could be an effective process as in HIP the material is subjected to both elevated temperature and isostatic pressure simultaneously.
2. The silver coating on the surface was found to enhance the permeation owing to its catalytic activity on the surface. Therefore, the membrane can be coated with similar other materials that would enhance the surface exchange.
3. Multi-layer membranes are another alternative to increase the permeation flux as we have seen in the literature. So, multi-layer membranes can be prepared using layers of the same material of different thicknesses and density or using different materials where one material forms the porous base and the other materials are deposited as dense layers on the base.
4. Due to the limitation of the glass sealing we were not able to test the permeability at higher temperatures. The glass used to react with the membrane at these high values of temperature. So, different alternatives like silver or gold rings can be used for sealing the system as these materials have high melting points, so we can

measure the permeability of the membranes at higher temperatures without affecting the membrane.

5. As discussed in the literature, hollow fiber membranes increase the permeation flux to a considerable extent. So, hollow fiber LNO membranes can be prepared to increase the permeability. Further, modifications can be done on the surface of these membranes to enhance the permeation.

References

[1] L. Sun and M. Wang, “Global Warming and Global Dioxide Emission: An Empirical Study,” *Journal of Environmental Management*, vol. 46, no. 4, pp. 327–343, Apr. 1996.

[2] E. Technology, “FOR CO 2 CAPTURE AND STORAGE.”

[3] H. Herzog and D. A. N. Golomb, “Carbon Capture and Storage from Fossil Fuel Use,” vol. 1, pp. 277–287, 2004.

[4] C. Guizard, “Nanophase ceramic ion transport membranes for oxygen separation and gas stream enrichment,” *Membrane Science and Technology*, pp. 435–471, 2000.

[5] K. Li, *Ceramic Membranes forSeparation and Reaction*.

[6] A. Thursfield and I. S. Metcalfe, “The use of dense mixed ionic and electronic conducting membranes for chemical production,” *Journal of Materials Chemistry*, vol. 14, no. 16, p. 2475, 2004.

[7] S. Stølen, E. Bakken, and C. E. Mohn, “Oxygen-deficient perovskites: linking structure, energetics and ion transport.,” *Physical chemistry chemical physics : PCCP*, vol. 8, no. 4, pp. 429–47, Jan. 2006.

[8] T. Ishihara, “Perovskite Oxide for Solid Oxide Fuel Cells,” 2009.

[9] G. A. S. J. Skinner, “ORIGINA L PA PER Recent developments in Ruddlesden – Popper nickelate systems for solid oxide fuel cell cathodes,” pp. 538–546, 2006.

[10] M. Al Daroukh, V. V Vashook, H. Ullmann, F. Tietz, and I. A. Raj, “Oxides of the AMO 3 and A 2 MO 4 -type : structural stability , electrical conductivity and thermal expansion,” vol. 158, pp. 141–150, 2003.

[11] P. Cousin and R. a. Ross, “Preparation of mixed oxides: a review,” *Materials Science and Engineering: A*, vol. 130, no. 1, pp. 119–125, Nov. 1990.

[12] X. Qi, Y. S. Lin, and S. L. Swartz, “Electric Transport and Oxygen Permeation Properties of Lanthanum Cobaltite Membranes Synthesized by Different Methods,” *Industrial & Engineering Chemistry Research*, vol. 39, no. 3, pp. 646–653, Mar. 2000.

[13] S. Liu, X. Tan, K. Li, and R. Hughes, “Synthesis of strontium cerates-based perovskite ceramics via water-soluble complex precursor routes,” *Ceramics International*, vol. 28, no. 3, pp. 327–335, Jan. 2002.

[14] Z. Wu, W. Zhou, W. Jin, and N. Xu, “Effect of pH on synthesis and properties of perovskite oxide via a citrate process,” *AIChE Journal*, vol. 52, no. 2, pp. 769–776, Feb. 2006.

[15] "Correlation between oxygen transport properties and microstructure in La0.5Sr0.5FeO3−δ” .

[16] “Investigation of phase structure, sintering, and permeability of perovskite-type Ba0.5Sr0.5Co0.8Fe0.2O3−δ membranes” .

[17] H. J. M. Bouwmeester and A. J. Burggraaf, “Dense ceramic membranes for oxygen separation,” 1996.

[18] S. Li, W. Jin, N. Xu, and J. Shi, “Synthesis and oxygen permeation properties of,” vol. 124, pp. 161–170, 1999.

[19] W. K. Hong and G. M. Choi, “Oxygen permeation of BSCF membrane with varying thickness and surface coating,” *Journal of Membrane Science*, vol. 346, no. 2, pp. 353–360, Jan. 2010.

[20] Z. Shao, W. Yang, Y. Cong, and H. Dong, “Investigation of the permeation behavior and stability of,” *Journal of*, vol. 172, pp. 177–188, 2000.

[21] “Properties and performance of BaxSr1−xCo0.8Fe0.2O3−δ materials for oxygen transport membranes.pdf.” .

[22] Z. Shao, H. Dong, G. Xiong, and Y. Cong, “Performance of a mixed-conducting ceramic membrane reactor with high oxygen permeability for methane conversion,” *Journal of Membrane*, vol. 183, pp. 181–192, 2001.

[23] X. Tan, “BSCF ceramic hollow fiber membranes for oxygen permeation,” vol. 52, no. 10, 2006.

[24] J. Caro, H. H. Wang, C. Tablet, a. Kleinert, a. Feldhoff, T. Schiestel, M. Kilgus, P. Kölsch, and S. Werth, “Evaluation of perovskites in hollow fibre and disk geometry in catalytic membrane reactors and in oxygen separators,” *Catalysis Today*, vol. 118, no. 1–2, pp. 128–135, Oct. 2006.

[25] “Ultrahigh oxygen permeation flux through supported Ba0.5Sr0.5Co0.8Fe0.2O3−ı membranes.”

[26] P. Haworth, S. Smart, J. Glasscock, and J. C. Diniz da Costa, “Yttrium doped BSCF membranes for oxygen separation,” *Separation and Purification Technology*, vol. 81, no. 1, pp. 88–93, Sep. 2011.

[27] “Influence of CO2 on the oxygen permeation performance and the microstructure of perovskite-type (Ba0.5Sr0.5)(Co0.8Fe0.2)O3−δ membranes.pdf.”

[28] J. H. Park and J. P. Kim, “Oxygen permeation and stability of Ba0. 5Sr0. 5Co0. 8Fe0. 2O3− δ membrane according to trace elements and oxygen partial pressure in synthetic air,” *Energy Procedia*, 2009.

[29] J. Yi and M. Schroeder, “High temperature degradation of Ba0.5Sr0.5Co0.8Fe0.2O3−δ membranes in atmospheres containing concentrated carbon dioxide,” *Journal of Membrane Science*, vol. 378, no. 1–2, pp. 163–170, Aug. 2011.

[30] K. Foy, “Comparison of ion transport membranes,” *Proc. 4th Annual Conference on Carbon*, pp. 1–11, 2005.

[31] A. Petric and P. Huang, “Evaluation of La – Sr – Co – Fe – O perovskites for solid oxide fuel cells and gas separation membranes,” *Solid State Ionics*, vol. 135, pp. 719–725, 2000.

[32] Y. Zeng and Y. Lin, “Perovskite-type ceramic membrane: synthesis, oxygen permeation and membrane reactor performance for oxidative coupling of methane,” *Journal of membrane science*, vol. 150, 1998.

[33] J. Park, “Oxygen permeability and structural stability of La 0.6 Sr 0.4 Co 0.2 Fe 0.8 O 3− δ membrane,” *Korean Journal of Chemical Engineering*, 2007.

[34] P. Zeng, R. Ran, Z. Chen, H. Gu, and Z. Shao, “Significant effects of sintering temperature on the performance of La0. 6Sr0. 4Co0. 2Fe0. 8O3- oxygen selective membranes,” *Journal of Membrane*, 2007.

[35] S. Li, W. Jin, P. Huang, N. Xu, J. Shi, M. Z. Hu, and E. A. Payzant, “Comparison of Oxygen Permeability and Stability of Perovskite Type La 0 . 2 A 0 . 8 Co 0 . 2 Fe 0 . 8 O 3-δ (A) Sr , Ba , Ca) Membranes,” pp. 2963–2972, 1999.

[36] X. Tan, Z. Wang, and H. Liu, “Enhancement of oxygen permeation through La0. 6Sr0. 4Co0. 2Fe0. 8O3− ı hollow fibre membranes by surface modifications,” *Journal of Membrane Science*, 2008.

[37] S.-Y. Jeon, M.-B. Choi, H.-N. Im, J.-H. Hwang, and S.-J. Song, “Oxygen ionic conductivity of La2NiO4+δ via interstitial oxygen defect,” *Journal of Physics and Chemistry of Solids*, vol. 73, no. 5, pp. 656–660, May 2012.

[38] D. C. Zhu, X. Y. Xu, S. J. Feng, W. Liu, and C. S. Chen, "La2NiO4 tubular membrane reactor for conversion of methane to syngas," *Catalysis Today*, vol. 82, no. 1–4, pp. 151–156, Jul. 2003.

[39] C. Li, G. Yu, and N. Yang, "Supported dense oxygen permeating membrane of mixed conductor La2Ni0.8Fe0.2O4+δ prepared by sol–gel method," *Separation and Purification Technology*, vol. 32, no. 1–3, pp. 335–339, Jul. 2003.

[40] V. V. Vashook, I. I. Yushkevich, L. V. Kokhanovsky, L. V. Makhnach, S. P. Tolochko, I. F. Kononyuk, H. Ullmann, and H. Altenburg, "Composition and conductivity of some nickelates," *Solid State Ionics*, vol. 119, no. 1–4, pp. 23–30, Apr. 1999.

[41] J. M. Bassat, P. Odier, A. Villesuzanne, C. Marin, and M. Pouchard, "Anisotropic ionic transport properties in La 2 NiO 4 + d single crystals," vol. 167, pp. 341–347, 2004.

[42] V. V Vashook, N. E. Trofimenko, H. Ullmann, and L. V Makhnach, "Oxygen nonstoichiometry and some transport properties of," vol. 131, pp. 329–336, 2000.

[43] C. Li, T. Hu, H. Zhang, Y. Chen, J. Jin, and N. Yang, "Preparation and characterization of supported dense oxygen permeating membrane of mixed conductor La 2 NiO 4 + δ," vol. 226, pp. 1–7, 2003.

[44] K. Wiik, S. Aasland, H. L. Hansen, and I. L. Tangen, "Oxygen permeation in the system SrFeO 3Àx – SrCoO 3Ày," vol. 153, pp. 675–680, 2002.

[45] P. Odier, Y. Nigara, and M. Sayer, "Phase Relations in the La-Ni-0 System : Influence and Stoichiometry on the Structure of La2Ni04 of Temperature," vol. 40, pp. 32–40, 1985.

[46] S. J. Skinner and J. A. Kilner, "Oxygen diffusion and surface exchange in La 22x Sr x NiO 41 d," vol. 135, pp. 709–712, 2000.

[47] A. a. Yaremchenko, V. V. Kharton, M. V. Patrakeev, and J. R. Frade, "p-Type electronic conductivity, oxygen permeability and stability of La2Ni0.9Co0.1O4+δElectronic supplementary infromation (ESI) available: further experimental data for the oxygen permeability, total conductivity and Seebeck coefficient of La2Ni0.9Co0.1O," *Journal of Materials Chemistry*, vol. 13, no. 5, pp. 1136–1144, Apr. 2003.

[48] T. Klande, "Effect of doping, microstructure, and CO2 on La2NiO4+δ-based oxygen-transporting materials." 2011.

[49] N. Cebasek, T. Norby, and Z. Li, “Kinetic Decomposition of a La2NiO4+ Membrane under an Oxygen Potential Gradient,” *Journal of the Electrochemical Society*, vol. 159, no. 8, pp. F461–F467, Jul. 2012.

[50] H. Kruidhof, H. J. M. Bouwmeester, R. H. E. Doorn, and A. J. Burggraaf, “Influence of order-disorder transitions on oxygen permeability through selected nonstoichiometric perovskite-type oxides,” vol. 65, pp. 816–822, 1993.

[51] S. J. Xu and W. J. Thomson, “Stability of La 0 . 6 Sr 0 . 4 Co 0 . 2 Fe 0 . 8 O 3-δ Perovskite Membranes in Reducing and Nonreducing Environments,” vol. 5885, no. 1979, pp. 1290–1299, 1998.

[52] S. Lee, S. K. Woo, K. S. Lee, and D. K. Kim, “Mechanical properties and structural stability of perovskite-type, oxygen-permeable, dense membranes,” *Desalination*, vol. 193, no. 1–3, pp. 236–243, May 2006.

[53] E. Wachsman, “Functionally gradient bilayer oxide membranes and electrolytes,” *Solid State Ionics*, vol. 152–153, pp. 657–662, Dec. 2002.

[54] X. Tan, “Oxygen permeation behavior of La0.6Sr0.4Co0.8Fe0.2O3 hollow fibre membranes.pdf.” 2012.

[55] Y.-H. Lin, Y. Liu, B.-P. Zhang, C.-W. Nan, J.-F. Li, and Z. Shen, “Electrical Transport Properties of La 2 CuO 4 Ceramics Processed by the Spark Plasma Sintering,” *Journal of the American Ceramic Society*, vol. 4008, p. 070924065850007–???, Sep. 2007.

[56] C. L. Song, Y. J. Wu, X. Q. Liu, and X. M. Chen, “Dielectric properties of La1.75Ba0.25NiO4 ceramics prepared by spark plasma sintering,” *Journal of Alloys and Compounds*, vol. 490, no. 1–2, pp. 605–608, Feb. 2010.

[57] M. S. Toprak, M. Darab, G. E. Syvertsen, and M. Muhammed, “Synthesis of nanostructured BSCF by oxalate co-precipitation – As potential cathode material for solid oxide fuels cells,” *International Journal of Hydrogen Energy*, vol. 35, no. 17, pp. 9448–9454, Sep. 2010.

[58] S. A. Nedilko and V. A. Drozd, “Solid solutions in Eu ž La / – Sr – V ž Ti , Cr , Nb , Mo / – O systems with K 2 NiF 4 -type structure,” no. July, pp. 340–344, 2001.

[59] S. Li, W. Jin, P. Huang, N. Xu, J. Shi, M. Z. Hu, and E. A. Payzant, “Membrane for Oxygen Permeation,” vol. 45, no. 2, 1999.

[60] “Synthesis, characterization and oxygen permeability of LSCF (6428) membrane and coating on dense substrate.”

[61] W. Jin, S. Li, P. Huang, N. Xu, and J. Shi, “Preparation of an asymmetric perovskite-type membrane and its oxygen permeability,” vol. 185, pp. 237–243, 2001.

[62] V. V. Kharton, E. V. Tsipis, E. N. Naumovich, a. Thursfield, M. V. Patrakeev, V. a. Kolotygin, J. C. Waerenborgh, and I. S. Metcalfe, “Mixed conductivity, oxygen permeability and redox behavior of K2NiF4-type La2Ni0.9Fe0.1O4+δ,” *Journal of Solid State Chemistry*, vol. 181, no. 6, pp. 1425–1433, Jun. 2008.

[63] E. Tsipis, “Oxygen nonstoichiometry and ionic transport in La2Ni(Fe)O4 + δ,” *Solid State Ionics*, vol. 179, no. 1–6, pp. 57–60, Mar. 2008.

[64] T. Ishihara, T. Akbay, H. Furutani, and Y. Takita, “Improved oxide ion conductivity of Co doped,” vol. 115, pp. 585–591, 1998.

Vitae

Name	:Zeeshan Alam
Nationality	:Indian
Date of Birth	:7/30/1987
Email	:zeeshanalam123@gmail.com
Address	:Aligarh, India
Academic Background	: **B.Tech in Mechanical Engineering** Zakir Husain College of Engineering and Technology Aligarh Muslim University, Aligarh, India **M.S. in Materials and Manufacturing** King Fahd University of Petroleum and Minerals Dhahran, Saudi Arabia